Deltares

Modeling the hydrodynamics and salinity of the Pontchartrain Basin

MSc Thesis Report

Sanne van den Heuvel

Deltares

Title
Modeling the hydrodynamics and salinity of the Pontchartrain Basin

Client
TU Delft
Deltares
Royal Haskoning

Pages
126

Keywords
Pontchartrain Basin, Violet Diversion, Lake Borgne, Lake Pontchartrain, Mississippi River, tidal propagation, salinity, Delft3D

Summary
In 2005 Hurricane Katrina flooded 80% of the city of New Orleans. On the short term levees are rebuild and heightened. On the long term barriers are build and wetlands are restored. For this last purpose the Violet Diversion is planned to freshen the Biloxi Marsh and Lake Borgne. This goal of this study is to model a dynamic salinity equilibrium for the Pontchartrain Basin. Lessons learned from this study can be a start for the modeling of the Violet Diversion and the impacts on the salinity (gradients) in the Pontchartrain Basin. The Delft3D model is calibrated for tidal propagation. When modeling salinity it is recommended to simulate in 3D as gravitational circulation occurs. For future modeling nontidal water level elevations and currents need to be added to the boundary conditions of the current domain. Therefore it is recommended to increase the model domain Gulfwards and westward to capture the entire Mississippi River Birdfoot.

References
See Chapter 9

Version	Date	Author	Initials	Review	Initials	Approval	Initials
1.0	aug. 2010	S. van den Heuvel		Ir. J.G. Boon		Ir. T. Schilperoort	
				Ir. M. van Ormondt			

State
final

Modeling the hydrodynamics and salinity of the Pontchartrain Basin

Final Report
MSc-thesis
Sanne van den Heuvel

Delft University of Technology
Faculty of Civil Engineering and Geosciences
Department of Hydraulic Engineering

Graduation committee:

Prof. dr. ir. M.J.F. Stive	Delft University of Technology
Ir. R.J. Labeur	Delft University of Technology
Dr. ir. B.C. van Prooijen	Delft University of Technology
Ir. J.G. Boon	Deltares
Ir. M. van Ormondt	Deltares
M. van Ledden PhD MBA	Royal Haskoning

Preface

Delft, August 23, 2010

This report is written in the framework of the MSc Thesis for the Master Hydraulic Engineering, specialization Coastal Engineering, at the faculty of Civil Engineering and Geosciences at the Technical University Delft. I performed my graduation thesis for the Dutch consultant Royal Haskoning and the research institute Deltares. They made it possible for me to spend part of my graduation time in New Orleans to study the area and gather more data. One day a week I worked at the U.S. Army Corps at four days a week I worked at the University of New Orleans (UNO) at the Department of Earth and Environmental Sciences. In the Netherlands I spent most of my time at the department of Coast and Sea (Zee- en Kustsystemen).

The three months in New Orleans showed me a part of the U.S.A. I never had imagined seeing. It is a lively city with a big cultural heritage. The jazz music, the food and the Saints, I all got to love. Although much of the mess that Hurricane Katrina left was not visible anymore, the impact can still be found. Either with a lady at the bar sharing her experience, that she sat on the rooftop for several days while help was on the way, or with families in the St. Bernardpolder who were recommended to evacuate for Hurricane Ike, but most of all in the work of the U.S. Army Corps. Being able to see the construction of the IHNC barrier and all engineers working on the Hurricane Protection System was a unique experience.

I would like to thank Royal Haskoning and Deltares for giving me the opportunity to experience New Orleans. Especially Mathijs van Ledden, for the good reception and arrangements in New Orleans, as well as all the opportunities to see as much of the engineering world as possible. For all his enthusiasm and support I could fortunately return a favor as “Black Piet”. To all the Haskoning employees in New Orleans that taught me about the different aspects of the Hurricane Risk Reduction System and showed me “the places to be” I am grateful as well.

I thank Nancy Powell for inviting me one day a week at the office, and Bob Turner for getting me into the IHNC Storm Surge Barrier tour. Tim Jarquin gave me a tour at the Violet Siphon and the St. Bernardpolder, which was a great contribution to my understanding of the area. At UNO I thank Ioannis Georgiou for his support to my graduation thesis. Although time was scarce, Ioannis made time to help me with my modeling and my insight in the Pontchartrain Basin. I even joined a fieldwork.

There are also some people in the Netherlands to thank. First of all, Johan Boon and Maarten van Ormondt of Deltares for their guidance towards graduation. Also Marcel Stive, Robert Jan Labeur and Bram van Prooijen, who were always accessible for good advice. My fellow graduate students at Deltares, with whom I shared many laughs and frustration, I wish them good luck on their graduation. Last but certainly not least, I thank my friends and family for all the advice and support. Furthermore I am grateful for the pleasure of sharing my New Orleans experience with two friends.

In the past period I have learned a lot about hydraulic engineering, New Orleans and myself. I hope this study will help New Orleans become safer against storm surges and I certainly hope to be back soon.

Sanne van den Heuvel

Contents

List of Tables

List of Figures

1 Summary

The area of New Orleans was hit by Hurricane Katrina in August 2005. A large part of the city got flooded due to bad design, construction and maintenance of the levee system. In order to increase the level of protection of the city, the levees are heightened and strengthened in the framework of the Hurricane and Storm Damage and Risk Reduction System (HSDRRS). On the long term the restoration of coastal wetlands is also part of the program.

Since the 1930's wetland erosion in coastal Louisiana has been recorded. The main cause of the erosion is the canalization of the Mississippi River, land subsidence and sea level rise, and salt water intrusion by alteration of drainage patterns. One way of initiating wetland restoration is the construction of diversions. The Violet Diversion is the largest diversion planned in the Pontchartrain Basin. Water from the Mississippi River is diverted into Lake Borgne and the Biloxi marsh in order to decrease salinities in those target areas.

In order to get more insight in the impact of the diversion on salinity (gradients), hydrodynamic and salinity modeling of the Pontchartrain Basin is desired. Due to lack of data and time, model calibration on salinity was not accomplished. The goal of this study is to model a dynamic equilibrium of yearly averaged salinity in the Pontchartrain Basin. The lessons learned from this study can be a start for subsequent modeling efforts of the Violet Diversion.

In Delft3D-FLOW a grid was set-up to model tidal propagation in Lake Borgne. The grid consists of a little less than 53,000 nodes. The initial bathymetry and roughness are taken from the ADCIRC SL15 model. The model is forced with the amplitudes and phases of the ten most important tidal constituents. In order to calibrate the model, the tidal channels are enlarged and the bottom friction is decreased. The necessity of these changes was already proven by the application of the harmonic method on the Pontchartrain Basin, as well as the moderate results of previous model studies. The model is calibrated on tidal amplitudes (accuracy within 10%) and fluxes through the tidal passes (accuracy within 1%). Phases were considered less important.

Salinity was implemented by simulating initial salinities and river discharges on top of the tide. Comparing 2D with 3D simulations, gravitational circulation occurs in the 3D modeling. This causes an increased salt water intrusion from the Gulf of Mexico towards Lake Borgne and the Biloxi Marsh. However, the salinities in this target area are too low in the dynamic equilibrium situation. This is explained by the underestimation of transport by tides and Mississippi River discharge towards Lake Borgne. Previous model studies proved that circulation around the continental shelf cannot be neglected for tidal transport. Also, the Mississippi River discharge can flow around the Birdfoot. Due to the choice of the model domain, that flow cannot occur in this study.

Using the tide-calibrated model for salinity studies, it is recommended to model in 3D to simulate the gravitational circulation. Nontidal water level elevations and currents should be included in the boundary conditions. This can be achieved by enhancing the model domain to capture a larger part of the Gulf of Mexico and the Mississippi Birdfoot. Then the flow around the Birdfoot can also be simulated. Wind should also be added to the hydrodynamic simulations. The measured salinities and the target salinities show seasonal variation. Therefore future modeling should strive for real-time simulation by forcing the model with time-series. The diversion flow can then be varied per month or season.

2 Introduction

2.1 Background

Most of the area near New Orleans is situated below Mean Sea Level (MSL). The area exists mainly of marshes and small communities located on the sedimentary deposits of the Mississippi River. The main sources of income are tourism, cargo handling, oil production and refinement and fisheries. Almost every year the area is hit by tropical storms, typically during the months June till November.

In 2005 Hurricane Katrina caused a disaster in New Orleans. The hurricane made landfall near the southern tip of the Mississippi Birdfoot at August 29 and continued towards the state of Mississippi. It caused a storm surge that breached the levees (dikes) at the eastern side of New Orleans. Due to the storm surge and the heavy rainfall, the water level in Lake Pontchartrain rose. This caused more levee breaches, at the northern side of the city. About 80% of the city got flooded, see Figure 2.1. One month later, hurricane Rita reflooded part of the area.

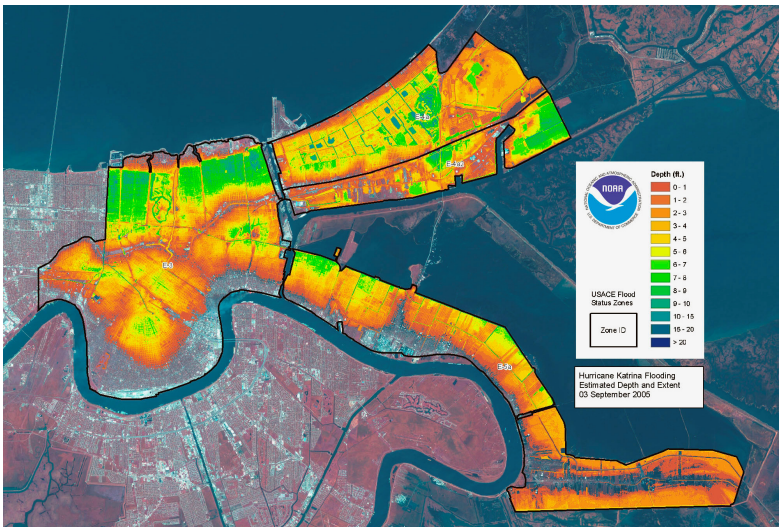

Figure 2.1 Hurricane Katrina flooding, estimated depth and extent (NOAA News, 2010)

The failure of the levees can be accredited to design flaws, according to research of the American Society of Civil Engineers (ASCE, 2007). According to this report, the two major causes of the levee failures were insufficient safety margins in soil strength and overtopping. After the flooding, the U.S. Congress assigned 14.45 billion dollars to the U.S. Army Corps of Engineers (USACE) to increase the strength of the Hurricane and Storm Damage and Risk Reduction System (HSDRRS) of New Orleans. Among others, this includes heightening and strengthening of the levees and construction of closure structures (MVN USACE, 2009). The improved protection system should provide a 100-year level of protection to the city of New Orleans and should take effect at the start of the 2011 hurricane season. More information about projects that are of interest for this research can be found in Chapter 4 and 6.

According to the Louisiana Coastal Protection and Restoration Authority (LACPR, 2007), wetlands form a natural buffer against hurricane and storm surges. Every two miles of wetland south of New Orleans, reduces a storm surge by half a foot (S. Blumenthal, 2010).

Due to several natural and man-induced reasons, the wetlands in coastal Louisiana have been eroding since the 1930's, see Figure 2.2. Therefore, the natural protection of New Orleans has been decreasing ever since. If no measures are taken, New Orleans and the surrounding cities will become more and more vulnerable to future extreme events. Land loss and increased change of flooding will drive wildlife as well as human communities away to higher areas. Another negative impact of the wetland erosion is the decreased protection of navigational and energy infrastructure.

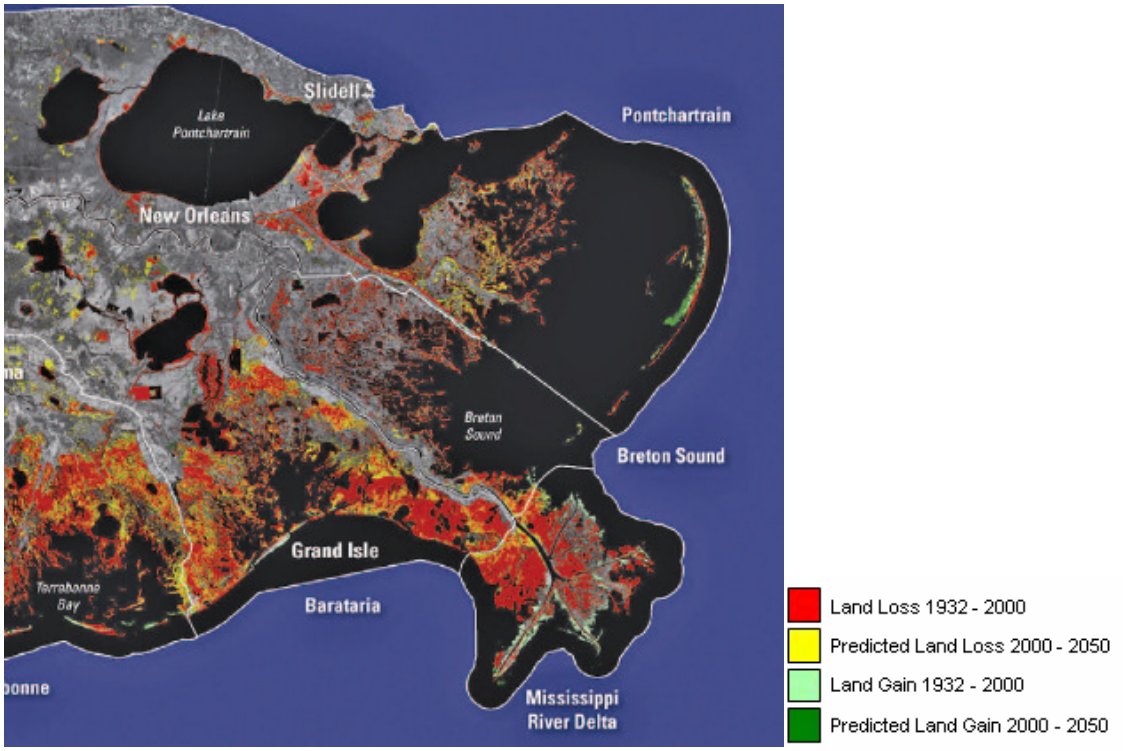

Figure 2.2 Previous and future land loss and land gain in the Mississippi Delta (LACPR, 2007)

In order to have natural protection in the future, coastal restoration needs to be taken on. The multiple lines of defense strategy of the U.S. Army Corps of Engineers combines structural measures with coastal restoration in order to reach an increased protection against storm surges for the New Orleans area. Several alternatives to achieve coastal restoration are river diversions, marsh creation, shoreline restoration and stabilization and ridge restoration.

The goal of diversions is to reduce salinity and introduce sediments. The direct link between wetland erosion and increased salinity has never been proven directly, but several researchers (Chatry et al., 1983) consider the increased salinity in several Louisiana estuarine waters as one of the causes of the habitat degradation. The Violet Diversion, part of USACE's coastal restoration program, is expected to have the largest impact on salinity gradients of all diversions planned in the Pontchartrain Basin (USACE, 2009a). The Pontchartrain Basin covers all water east of the Mississippi River Delta indicated in Figure 2.2. Water from the Mississippi River will be diverted into Lake Borgne, see Figure 2.3. With this effort the salinity in Lake Borgne and the Biloxi Marsh will be reduced.

Figure 2.3 Map depicting the 2006 proposal to expand the Mississippi River freshwater diversion at Violet, LA (LPBF, 2006)

In order for the Violet Diversion to be most effective, more insight in the hydrodynamics of the area is required. To investigate the impact of the diversion on salinities and salinity gradients in Lake Borgne and the Biloxi Marsh, a salinity model has been set up in Delft3D-FLOW. This is a hydrodynamic model which solves the unsteady flow equations in either two or three dimensions. Salinity as well as density driven currents can be added to the flow simulations.

2.2 Research goal

The goal of this study is to make a start in modeling the hydrodynamics and the salinity in Lake Borgne and the Biloxi Marsh. This is done by simulating the dynamic equilibrium using a hydrodynamic model. The dynamic equilibrium consists of a yearly averaged salinity forced by rivers, which moves back and forth by the tidal motion. The results of this study will provide more insight in the physics of the Pontchartrain Basin, and will focus on some particulars of salinity modeling in the Pontchartrain Basin. This study can be considered as the first step towards modeling the Violet Diversion and its impacts on the salinity (gradients) in Lake Borgne and the Biloxi Marsh.

2.3 Approach

A literature study was performed to gain all data necessary for modeling tides and salinities in the Pontchartrain Basin. Before setting up the model, these data are analyzed to provide insight in the appropriate schematization of the area and important parameters. This effort results in assumptions and restriction for the model. This literature study also resulted in information about previous model studies for this area. These studies can help to gain insight in important parameters and restrictions of certain model settings.

The model is calibrated for water levels and tidal fluxes. A detailed model calibration for salinity was not feasible with the data and time available. The model performance with respect to salinity simulations is investigated. For this purpose, the hydrodynamics are the input for a tracer analyses in a water quality model. With this insight, the hydrodynamic model is used to model the closure of the MRGO and study the relative impact of the Violet Diversion on salinity gradients.

2.4 Report overview

The next chapter deals with the background of the coastal erosion. The causes and rates of erosion will be discussed. The background of the targets set by the U.S. Army Corps are treated as well. Based on this information assumptions are formulized. The project area is treated in more detail.

After this chapter a distinction will be made between modeling of tides and salinity. First the data analysis and model calibration for tidal propagation is treated. After this is completed successfully, the report moves on to the salinity data and model performance with respect to salinity.

Chapter 4 contains the results of the literature study for tidal propagation. The collected data are analyzed as a first step towards modeling the area with Delft3D-FLOW. The analysis will provide more insight in the schematization of the area and important parameters. In this chapter previous model studies of the Pontchartrain Basin are elaborated as well. The model set-up and calibration for water levels and tidal fluxes can be found in chapter 5.

After the calibration for tidal propagation is completed, the focus shifts towards salinity. Chapter 6 contains the results of the literature study for salinity. The data are analyzed and previous model studies are investigated. Chapter 7 will explain the process of the modeling salinities in the Pontchartrain Basin with the hydrodynamic model developed in Chapter 5. It also contains the modeling results of the Violet Diversion, which gives insight in the relative impact of the diversion on salinity gradients in the Pontchartrain Basin.

Chapter 8 contains the conclusions of this model study and recommendations for future modeling efforts of the Pontchartrain Basin.

3 Project description

As explained in the previous chapter, coastal erosion has a large impact on Louisiana and is by some parties appointed as one of the reasons why Hurricane Katrina could do so much damage. The background and causes of the coastal erosion are treated in this section. In order to reverse the degradation of the wetlands, diversions of the Mississippi River are planned. The targets salinities for these diversions are called the Chatry salinity targets. The background of these targets and their impact on the model studies in this study are explained below. The section concludes with a description of the model area.

3.1 Background of coastal erosion

Since the 1930's land loss of coastal Louisiana is registered. Since then, approximately 4900 km^2 of land is lost to the sea. The state accounts for 30% of the total coastal marsh loss in the US. Between 1990 and 2000 the wetland loss was approximately 62 km^2 per year. It is estimated that the next 50 years another 1300 km^2 of land will be lost (Barras et al., 2003). This means the erosion rate decreases to approximately 26 km^2 per year. The reason for the decrease is the rapid coastal erosion in the period 1956 to 1978. After this period, the wetland loss and shoreline erosion rates kept on declining. Extrapolation of these data, combined with the increasing efforts of coastal restoration and marsh creation projects and beneficial use of dredged materials in the wetlands, explains the lower land loss rate. Figure 2.2 illustrates the areas of land loss and land gain, over the last 70 years and until 2050.

In 2005 hurricane Katrina made landfall near the southern tip of the Mississippi Birdfoot. Shortly after, hurricane Rita passed by. The U.S. Geological Survey (USGS) estimated that the two hurricanes together caused another 562 km^2 of land loss (Barras, 2006).

Due to the land loss, the natural protection against storm surges diminishes. If no measures are taken, New Orleans and the surrounding cities will become more and more vulnerable for future extreme events. Besides these problems and the decreased protection of navigational and energy infrastructure, the wetland erosion also causes several ecological problems. Nutrients, carried by the river water, will flow into the Gulf of Mexico since it is no longer filtered by the marshes. Due to the high concentrations of nutrients in the northern Gulf of Mexico, water quality becomes an issue e.g. in terms of increased algae growth. Another environmental issue is the degradation of swamp forest biology by salt water intrusion and hydrological modifications. The wetland erosion causes salt water intrusion, which limits the oyster growth.

3.2 Causes of Louisiana's coastal erosion

There are several natural and man-induced causes that can explain the coastal land loss. Sediment shortage is one of the main causes (Walker et al., 1987; Temple et al., 1988; Demas et al., 2009). Due to a shortage in river supply and compaction, the wetlands are drowning and are not able to keep up with sea level rise. This leads to inundation. Salt water intrusion is another main cause for wetland erosion (Evers et al., 1992). Both causes, the negative sediment budget and the increased salinity, are elaborated below.

A shortage of sediment in the area is mainly caused by canalization of the Mississippi River. In the 18^{th} century French settlers started to build levees around the Mississippi River in order to protect the city of New Orleans from river floodings. Later, the Mississippi River started to gain importance as a shipping route.

The canalization of the Mississippi River causes the sediment carried by the river, to be deposited at deep waters in the Gulf of Mexico. Therefore, the wetlands in Barataria Basin and Breton Sound Basin have no natural supply of river sediment anymore.

Over time, the wetlands are subsiding. This is partly due to natural compaction, which is accelerated along the natural levees. But also man-induced subsidence as a result of urbanization and ground water withdrawal plays a big role. Next to subsidence, the area is also affected by sea level rise. Sediment input might be necessary for the wetland area to keep up with these processes.

Canal modification of hydrological flows in the wetlands causes altered drainage patterns. The canals cause salt water intrusion as well as shortening of the residence time of fresh water in the marshes. Spoil banks were made out of the dredged material. These are not strong enough to prevent erosion by boat wakes. At the same time, the spoil banks prevent fresh water from reaches the marshes. Estimates about the wetland erosion caused by canal modification vary, from 25 to 90%, but are significant (P.H. Templet and K.J. Meyer-Arendt, 1988).

Besides the canal modification, sea level rise and erosion of the wetlands causes salt water intrusion. The salinity in the Pontchartrain Basin might also be increased due to a decrease in fresh water inflow from the Mississippi River, tributary rivers and other rivers that discharge in the area.

Several researchers have reported this increase in salinity in Louisiana's coastal waters (Wiseman, 1990). Wiseman studied salinity trends using two historical data sets. One dataset has been collected by the Louisiana Department of Wildlife and Fisheries (LDWF), the other by USACE. Record lengths vary per station, but are all in the period between 1955 and 1985. Most data are near-surface measurements, therefore no conclusion can be drawn with respect to vertical stratification. However, the processes of overbank flooding and groundwater flow in the root zone can explain the large impact of surface salinities on marsh health. Although there is no spatial pattern, many stations showed a significant trend in salinity.

As can be seen in Figure 3.1, all but one station east of the Mississippi River show a positive trend in monthly mean salinity. For monthly salinity variance and maxima, an equal positive trend can be seen. This means that the salinity in the area east of the Birdfoot increases.

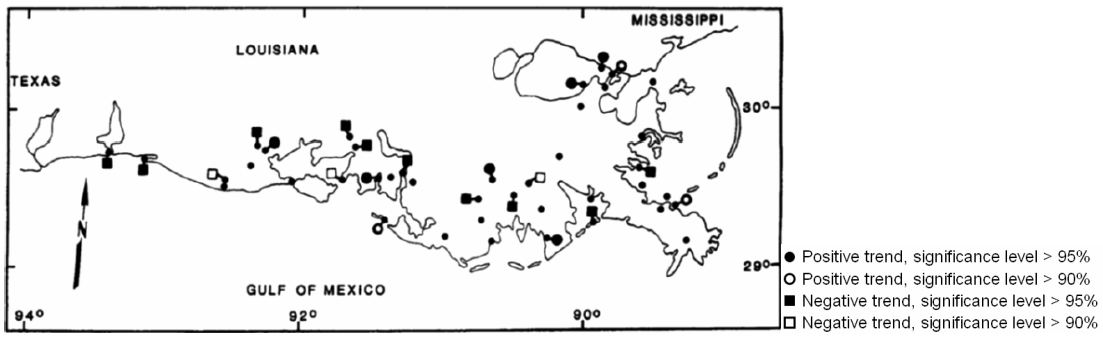

Figure 3.1 Stations where the monthly mean salinities exhibited a statistically significant trend (Wiseman et al., 1990)

The increase in salinity has a large impact on the coastal landscape. Wetlands can be classified based on their salinity tolerance. Four marsh types (fresh, intermediate, brackish and saline) are subdivided over salinities ranging from 0.1 parts per thousand (ppt) to over 16 ppt, (USACE, 2009a). As salinities increase to values higher than the ideal range for a certain marsh type, the vegetation will start to change to a more salt-tolerant type. This leads to wetland degradation in many cases, as the salinity increases too fast for the wetlands to keep up. With this transition process, where other types of vegetation will start to grow, the area is more vulnerable to inundation by hurricanes and storm surges. Figure 3.2 shows the marsh types as established by USGS (2006) after the 2005 hurricanes Katrina and Rita.

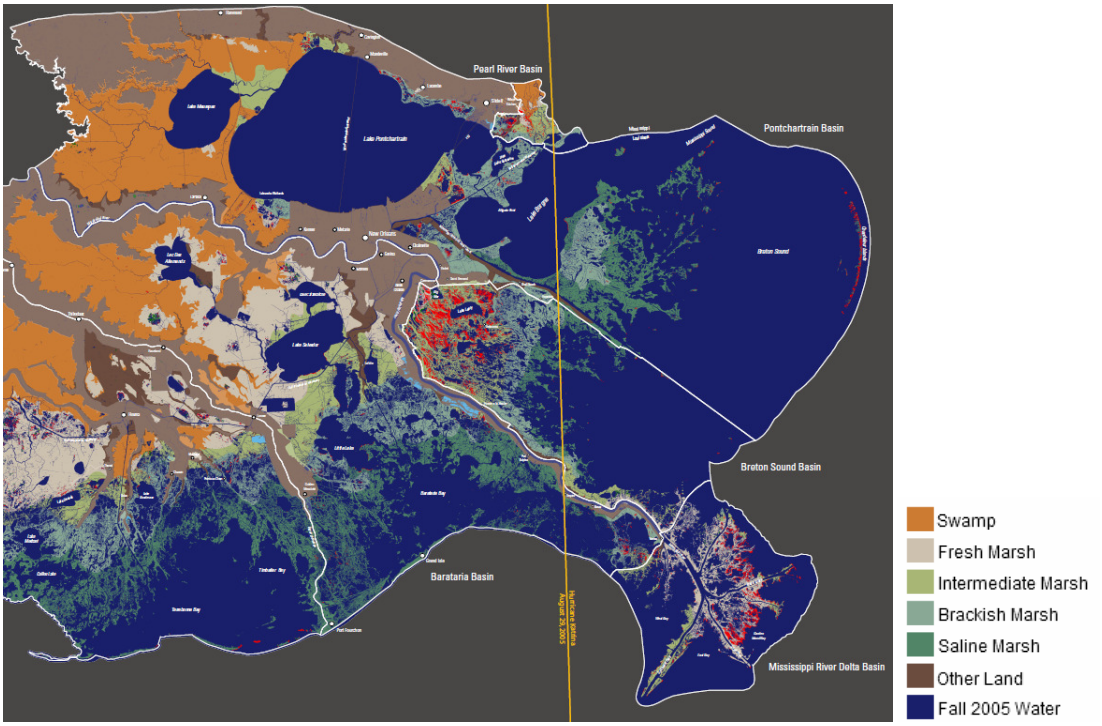

Figure 3.2 Marsh communities after the 2005 hurricanes (USGS, 2006)

Although it has never been proven directly that an increase in salinity results in wetland erosion, the researches discussed in this paragraph show a strong agreement between salinity increase and erosion of wetlands. Since a direct proof lacks, it is also not known what would be the ideal salinity for wetland restoration in the Pontchartrain Basin. In order to have tangible targets for restoration projects the U.S. Army Corps uses the salinity targets for oyster growth, the so-called Chatry salinity targets. It is assumed that when the salinity targets are achieved 40% of the time, salinity gradients are attained that are comparable to historic conditions (1971 – 1981) when the wetlands were healthier. The Chatry salinity targets and their background are elaborated in the following section.

3.3 Salinity target of Violet Diversion

After several researchers observed increasing salinity and decreasing oyster seed grounds, Chatry (1983) performed a research to formulate the optimum annual salinity regime for oyster production on Louisiana seed grounds. The state's prime seed grounds are located between the Mississippi River and the MRGO, see Figure 3.6, bounded by Breton Sound. Chatry gathered salinity, spatfall and seed oyster production data at several stations from April 1971 till September 1981. The spatfall was expressed in setting intensities per cm^2 of oyster larvae.

Oysters of 26 till 75 mm in height were defined as seed oysters. These oysters are between 7 and 14 months old. Therefore, production data should be compared to salinity and spatfall data of the previous year.

In the dataset, there were eight years with good seed oyster production (> 20 oysters/m^2). Among all analyzed stations, the salinities showed remarkable similarities in those eight years. The optimum salinity regime is defined as the monthly mean salinity of each station in those eight years of good oyster production.

By using the data of several stations in the years of good oyster seed production, a mean salinity with a wider range can be determined of each month. Figure 3.3 shows these values. Although a large salinity range is allowed, there seems to be a seasonal change in salinity. During the months April and May lower salinities (below 8 ppt) are preferred. During the rest of the year, salinities between 12 and 18 ppt are desirable.

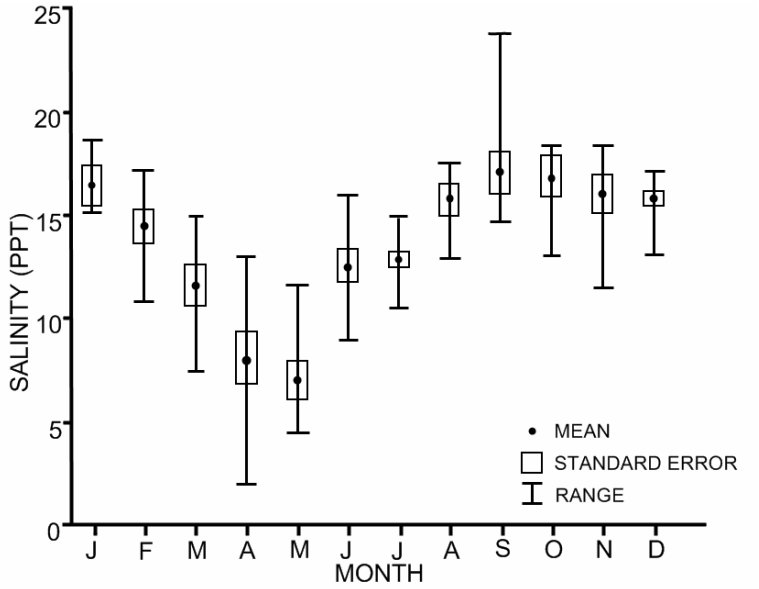

Figure 3.3 Optimum salinities as defined by Chatry (Chatry et al, 1983)

As was established in the previous section, salinity is important for the coastal landscape and the wetland erosion. Per vegetation type (fresh, intermediate, brackish and saline) a desired salinity range can be identified for preservation. However, it has never been established what the ideal or desired marsh layout is for the Biloxi Marsh or any other marsh in Louisiana. In order to be able to quantify the effects of a project, targets are desirable. Therefore, the U.S. Army Corps has adopted these Chatry salinity targets for several projects. In the years analyzed in the Chatry study, the Louisiana wetlands were in better shape then they are in now.

The Chatry salinity targets were already used for the design of the Bonnet Carré Spillway, upstream of the city of New Orleans (McAnally and Berger, 1997) The Bonnet Carré Spillway discharges water from the Mississippi River into Lake Pontchartrain when the river's water level reaches a critical stage. Since these target salinities were not achieved with the Bonnet Carré Spillway, they remain the targets for the Violet Diversion (Georgiou et al., 2007). According to USACE, the Chatry targets should be met 40% of the time. From Figure 3.4 it can be seen that the salinities in the outer stations of the Biloxi Marsh are occasionally lower than the target salinities, but not more than 40% of the time.

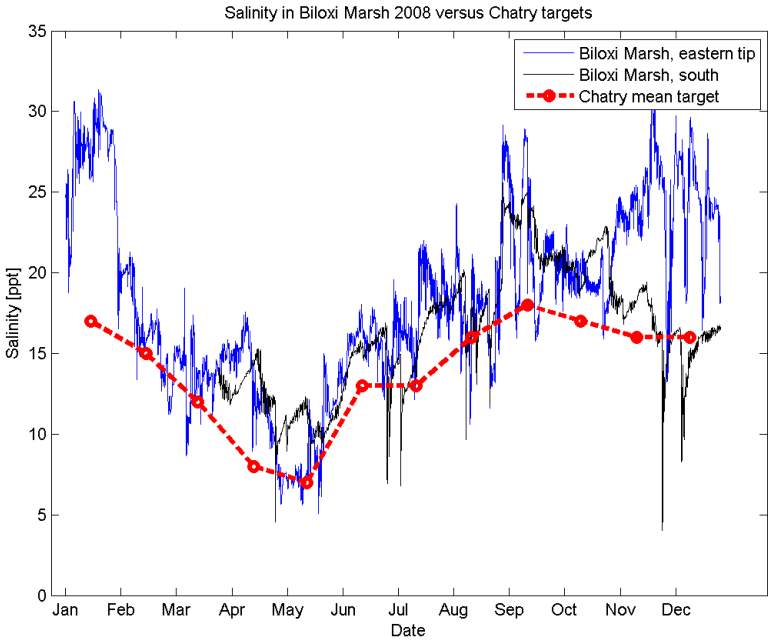

Figure 3.4 Chatry salinity targets compared to the 2008 salinities in the target area (Biloxi Marsh)

The Lake Pontchartrain Basin Foundation (LPBF, 2006b) uses the 1990-1932 wetland layout as a target for their projects because since then the 'dramatic loss of wetlands' started to change the landscape. Figure 3.5 shows the baseline condition of 1932 as reconstructed by LPBF. The blue dotted lines are a visualization of the Chatry salinity targets. It can be seen that the Chatry salinity targets show resemblance to the baseline vegetation. West of the left blue line, the proposed Palmisano line, the salinity is always below 15 ppt. This is Lake Pontchartrain, Lake Borgne and part of the Biloxi Marsh. The right line, the proposed Ford line, indicates the area where the mean salinity should be 15 ppt. This line is situated just Gulfwards of the Biloxi Marsh. If these targets are satisfied, the Biloxi Marsh would become a mix of brackish and intermediate marsh.

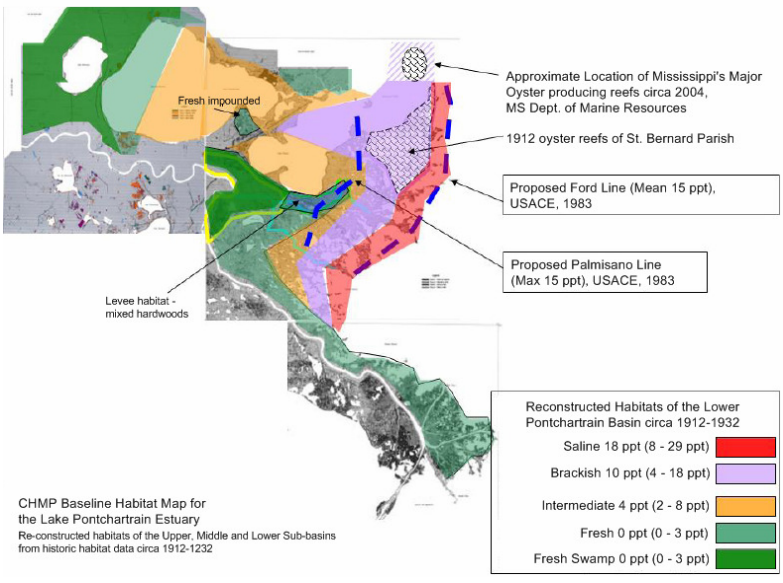

Figure 3.5 Isohalines after the Chatry salinity optimum (LPBF, 2006)

3.4 Project area

The project area area covers the Pontchartrain Basin. This is the area east of New Orleans and the Mississippi River as shown in Figure 3.6. The Pontchartrain Basin covers Lake Maurepas and Lake Pontchartrain, Lake Borgne and the Biloxi Marsh and Breton and Chandeleur Sound. The rivers that discharge into these lakes and coastal zones, will be taken into account for the salinity balance. The ridges of Chandeleur Sound and Breton Sound mark the offshore bound of the project area. This makes that the boundaries of the project area are sufficiently far away from the area of interest, which is Lake Borgne and the Biloxi Marsh.

Figure 3.6 Project area: Pontchartrain Basin (Google Earth, 2009)

In Figure 3.7 some important channels near the area of interest are marked. Lake Pontchartrain is linked to Lake Borgne by three channels: the Rigolets, the Chef Menteur and the Inner Harbor Navigational Canal (IHNC) through the Gulf Intracoastal Waterway (GIWW). The construction of the IHNC was completed in 1923, while the GIWW was completed in the early 1930's (Sikora and Kjerfve, 1985). The Mississippi River Gulf Outlet (MRGO) used to be a direct connection between the GIWW and the Gulf of Mexico since 1963, but on 20 July 2009 a rock dam was constructed at Bayou La Loutre (USACE, 2010), see paragraph 3.1.1.

Figure 3.7 Area of interest

Violet is located in the Central Wetlands Area (CWA), west of Lake Borgne, see Figure 3.8. At Violet, a siphon is located. At sufficiently high water levels in the Mississippi River water is diverted into the CWA. The fresh water input into the area is an attempt to offset salinity intrusion from the MRGO (DNR, 1992). Via the Violet Canal the water reaches the CWA. The fresh water leaves through the Bayou Dupre gate into the MRGO.

The Violet siphon was built in 1979 and operated several years. Due to a lack of money, it only functioned for a few years until 1992 when it was restored. Due to the small flow compared to the influence of the MRGO and siltation of the Violet Canal, the project was de-authorized in 2000. In 2003 the siphon was reopened again. The peak capacity of the siphon is 8.5 m/s, which is far too small to benefit the marshes at the other site of the MRGO (LPBF, 2006b).

For the Violet Diversion, the same location will be used. The siphon will be replaced by a structure capable of diverting larger discharges. Since it is foreseen that the CWA and the Bayou Dupre Gate do not have the capacity to store and drain the increased amounts of water, a second gate at Bayou Bienvenue will be used.

Figure 3.8 Central Wetlands Area (CWA) (Google Earth, 2009)

3.5 Modeling assumptions and restrictions

Based on the research goal formulated in the first chapter and the information on the Chatry salinity targets and the project area, modeling assumptions are formulized.

The first step in modeling the salinities in the Pontchartrain Basin using Delft3D is to calibrate the model for tidal elevations and fluxes. For the tidal elevations stations throughout the model area are used. The tidal fluxes are analyzed in the passes between Lake Pontchartrain and Lake Borgne. Phases are considered less important for this study, as the water level elevations and fluxes are an indication of the water exchange between Lake Borgne and the Gulf of Mexico on one side, and Lake Pontchartrain on the other side. A possible phase difference between measurements and model results are not of importance when modeling a yearly averaged dynamic equilibrium.

The next step is to incorporate salinities. This is done by forcing the model with river discharges. Wind will not be taken into account. The goal of the study is to simulate a dynamic salinity equilibrium. After the dynamic equilibrium is reached, the closure of the MRGO and the Violet Diversion are added to the simulation to study their relative impact on salinities and salinity gradients.

The Chatry salinity targets for the Violet Diversion are formulated per month and show seasonal variations. The months April and May are the only months with a target below 12 ppt. With these yearly averaged simulations the monthly variations in discharges cannot be simulated, therefore the Chatry targets cannot be reproduced with this model effort. A dynamic equilibrium can only give insight in the relative impact of the Diversion on salinity gradients. Therefore only the position of the 15 ppt isohaline in the simulations will be compared to the desired position as indicated in Figure 3.5. Studying the effects of the Violet Diversion on salinity (gradients) in the Pontchartrain Basin and how often the Chatry salinity targets are met, can be done in a subsequent study.

The Mississippi River water that is diverted at Violet reaches the MRGO via the Violet Canal. This canal runs through the CWA. Since the salinities in the CWA are not of interest for this study, and modeling the CWA would require a high grid resolution, the diverted discharge will be introduced into the model area at the Bayou Dupre Gate. This restriction will lead to a limited number of cells in the CWA, which reduces the modeling time.

In this study the impact of sea level rise on wetland salinities with or without Violet Diversion will not be taken into account. Increased sea level rise will lead to an increase of salt water intrusion. Increased salinities are therefore expected. It is recommended to study the effects of sea level rise on the impact of the Violet Diversion in future modeling efforts.

3.6 Conclusions

This chapter described the wetland erosion in coastal Louisiana. Since the 1930's, coastal erosion has been registered. The erosion rate is estimated to be around 62 km^2 per year; currently the erosion rate is 26 km^2. The erosion leads to a decreased natural buffer against storm surges.

There are several causes for the degradation and erosion of the wetlands. Canalization of the Mississippi River caused a shortage in sediment supply to the subsiding wetlands in order for them to keep up with sea level rise. Together with artificial canals in the wetlands, this leads to increased salinity.

The construction of the Violet Diversion is one of the projects in the wetland restoration program. This diversion, downstream of New Orleans, will divert fresh water from the Mississippi River into Lake Borgne and the Biloxi Marsh. This will lead to lower salinities in the project area.

Salinity targets were formalized to decrease the salinity in wetlands for better oyster growth. Due to lack of knowledge about the ideal salinity gradients in the Pontchartrain Basin for ecosystem restoration, the Chatry targets are adopted by the U.S. Army Corps as salinity targets for wetland restoration that should be met 40% of the time. Since this model effort aims to simulate a yearly averaged situation, the monthly variations cannot be modeled. Therefore only the position of the 15 ppt isohaline will be studied.

The first step in the model study is to calibrate the model for tidal elevations and fluxes. Thereafter the salinity is modeled, using the rivers as an additional forcing. After a dynamic equilibrium is reached, the Violet Diversion is added to the simulation. The diverted water will be introduced into the model at the Bayou Dupre Gate, thereby modeling of the CWA is avoided. Sea level rise and its impacts on salinities in the project area are not taken into account in this study.

4 Data analysis for tidal propagation

After establishing the research goal and the project description in the previous chapters, data are collected. In this chapter only the data with respect to tidal propagation will be treated. Since the model study with respect to salinity is a different process and a step following tidal calibration, the gathered salinity data and model results will be treated later on.

In the first section the collected data are summed up. Section 2 will deal with the analysis of these data. A simple model will be used to provide more insight in the physics of the system and important parameters. The conclusions from this analysis will be used for the model calibration. Before the actual calibration, previous model study will be studied to get more insight in valuable parameters and points of particular interest when modeling this area. These models and their performance will be treated in the last section of this chapter.

4.1 Gathered data

The hydrodynamics in the project area will be forced by tides and wind. River discharges will be taken into account when analyzing the salinity. The hydrodynamics caused by hurricanes will not be taken into account in this project and will therefore not be treated in this chapter.

4.1.1 Bathymetry

The Pontchartrain Basin is located at the northern Gulf Coast. The Gulf of Mexico is an ocean basin, which is considered part of the Atlantic Ocean. It is connected to the Atlantic Ocean at the Yucatán Channel and the Strait of Florida. The Gulf of Mexico is approximately 1500 kilometer wide and has a surface area of approximately 1.6 million km^2. The deepest location is located in the trough called Sigsbee Deep, with a depth of 4384 meter (Wikipedia, 2010).

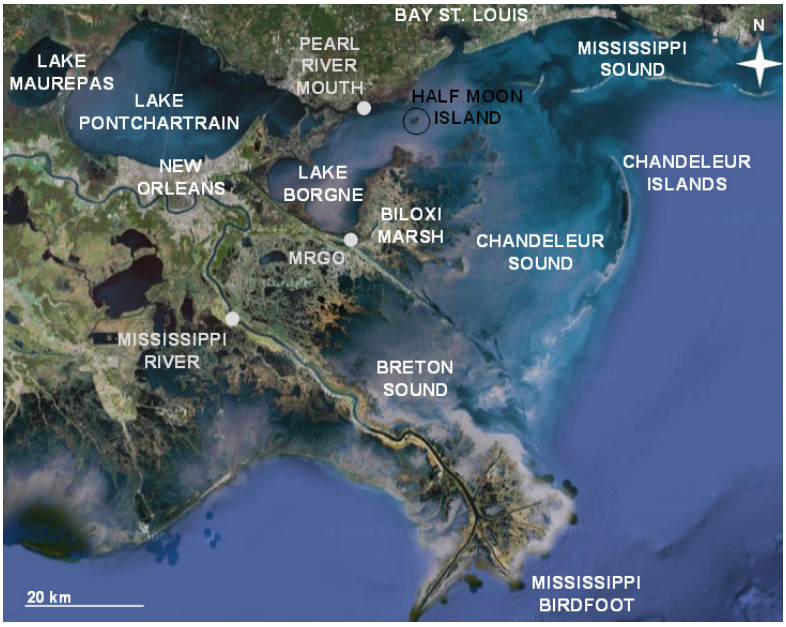

Figure 4.1 Project area

The Mississippi River Gulf Outlet (MRGO) used to be a connection between the Gulf of Mexico and Lake Borgne. Construction of the channel was completed in 1968 to provide a shorter shipping route to New Orleans. It stretched from the Inner Harbor Navigational Canal (IHNC) to the 38-feet depth contour (11.6 meters depth) in the Gulf, see Figure 4.1.

The bottom width of the MRGO after construction was 152 meter. Hurricane Katrina caused shoaling of the MRGO in 2005. The U.S. Congress decided that it was not worthwhile to maintain the channel. After de-authorization of the MRGO, closure of the MRGO was completed in July 2009, 460 meter south of Bayou La Loutre (USACE, 2010). A rock dam of 450 meter wide (bottom) was constructed to a level of 2.5 meter above reference level (NAVD88, see paragraph 3.1.2), see Figure 4.2.

Figure 4.2 Rock dam as closure of the Mississippi River Gulf Outlet (MRGO) at Bayou La Loutre

Lake Borgne has a surface area of 730 km^2, with an average depth of 3.0 meter (Gulfbase.org, 2010). Via three channels Lake Borgne is connected to Lake Pontchartrain. Lake Pontchartrain is oval shaped with a width of 64 km. The north-south distance is 39 km. The lake has a surface area of 1,630 km^2 and an average depth of 3.7 meter. The characteristics of the Gulf of Mexico and Lake Borgne and Lake Pontchartrain are summarized in Table 4.1.

Table 4.1 Characteristics of water bodies in project area

Area	Parameter	Value
Gulf of Mexico	Width	1,500 km
	Surface area	1.6 x 10^6 km^2
	Depth, max	4,384 m
Lake Borgne	Width (east-west)	34 km
	Length (north-south)	30 km
	Surface area	730 km^2
	Depth, average	3.0 m
Lake Pontchartrain	Width (east-west)	64 km
	Length (north-south)	39 km
	Surface area	1,630 km
	Depth, average	3.7 m

The Rigolets and the Chef Menteur Pass are natural passes between Lake Borgne and Lake Pontchartrain. The third pass, the Inner Harbor Navigational Canal (IHNC), was completed in 1923. For dimensions of the three tidal passes, see Table 4.2. The ratio of tidal prism between the three tidal channels is 60% for the Rigolets, 30% for the Chef Menteur Pass and 10% for the IHNC (Sikora and Kjerfve, 1985). The area in between the channels, that separate Lake Borgne and Lake Pontchartrain, is swamp, see Figure 4.3. The left photo shows the fresh and intermediate marsh, taken in northward direction between the Rigolets and the Chef Menteur pass. The right photo gives an impression of the cypress swamp, taken east of the Rigolets. These land bridges are a storage area for water, flow velocities are low.

Table 4.2 Dimensions of the passes between Lake Borgne and Lake Pontchartrain according to Haralampides (Georgiou et al., 2007)

	Total length (l) [km]	Average depth (d) [m]	Cross-sectional area (A) [m^2]
The Rigolets	14.5	8.0	7,500
Chef Menteur	11.3	13.0	2,422
IHNC	30.0	7.5	2,924

Figure 4.3 The land bridge between Lake Borgne and Lake Pontchartrain. Left: fresh and intermediate marsh; right: cypress swamp.

The bathymetry that is used for this model study originates from the ADCIRC SL15 model (Bunya et al., 2010). The model domain consists of a part of the Atlantic Ocean, the Caribbean Sea and the Gulf of Mexico, see Figure 4.4.

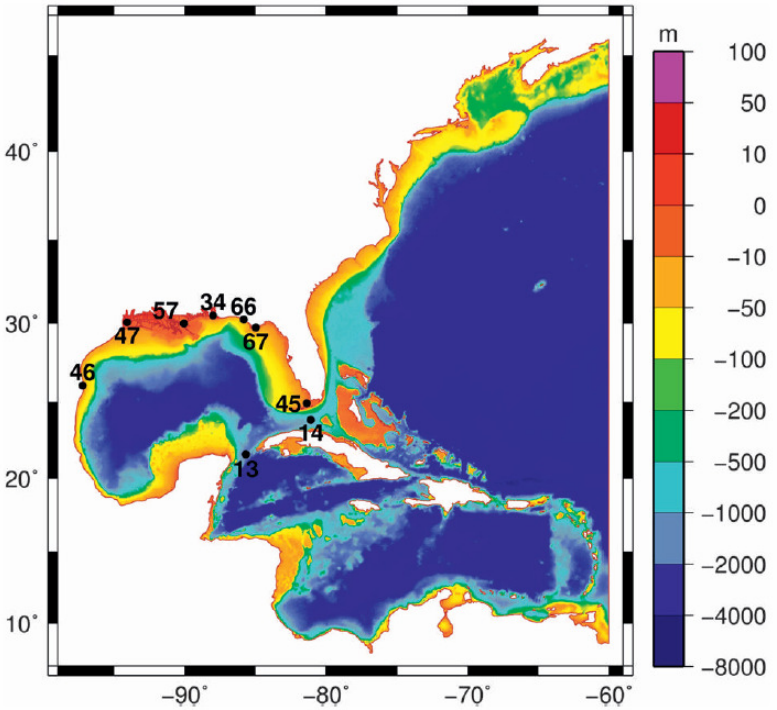

Figure 4.4 ADCIRC SL15 model domain with bathymetry in meters (Bunya et al., 2010)

For this study only the data covering the project area are used. For the Gulf of Mexico three sources are used: NOAA's bathymetric sounding database, the Digital Nautical Chart database and the 5-minute gridded elevations/bathymetry for the world (ETOPO5) database. For the floodplain topography the Atlas and the Mississippi Coastal Analysis Lidar Projects are used. When no data were available in the wetlands a height of 0.80m was applied for marshland and -0.40m for water, conform the Louisiana Gap Analysis Project (LA-GAP). Data along the Mississippi and Louisiana coastline are mostly dated prior to Hurricane Katrina in August 2005. However, the land bridge and channels between Lake Borgne and Lake Pontchartrain are post-Katrina data, as well as the Chandeleur Islands (USGS; U.S. Geological Survey) and the islands at Mississippi Sound (USACE), except for Half Moon Island, Deer Island and Singing River Island (all MARIS; Mississippi Automated Resource Information System 2006).

Table 4.3 shows the dimensions of the tidal passes in the SL15 bathymetry. The depth is comparable to the depth set by Haralampides, but the cross-sectional area of the Chef Menteur and the IHNC are considerably smaller in the SL15 bathymetry.

Table 4.3 Dimensions of the passes between Lake Borgne and Lake Pontchartrain in the SL15 bathymetry

	Total length (l) [km]	**Average depth (d) [m]**	**Cross-sectional area (A) [m^2]**
The Rigolets	14.5	13.0	7,800
Chef Menteur	11.3	14.0	1,160
IHNC	30.0	7.5	1,070

4.1.2 Reference level

Along the Louisiana coastline, depth can be expressed relative to several reference levels. Since later on in this report different reference levels will be used, they will explained here. The most important reference levels for the data collected for this project is NAVD88 and the tidal datums (e.g. MSL, MLLW).

NAVD88 is short for the North American Vertical Datum of 1988. It replaced the National Geodetic Vertical Datum of 1929 (NGVD29), also known as the Sea Level Datum of 1929, since that system was outdated. The primary tidal benchmark of NAVD88 is located at Father Point/Rimouski, Quebec, Canada. The new datum was published in 1990, except for areas with known crustal motion. The Lower Mississippi Valley in Louisiana undergoes subsidence due to crustal motion. The benchmark elevations that were published in 1992 are not fit for use anymore. Errors up to 6 cm can occur (USACE FAQS, 2010).

For conversion between vertical datums the program VDatum (VDatum, 2010) is used. This program is developed by NOAA. In order to convert NAVD88 to tidal datums, GEOID transformation grids are required. The latest version is the GEOID09 (NOAA GEOID, 2010). For each update of the hybrid geoid, the bench marks in Louisiana are updated for subsidence. The nearest project area of VDatum to the Pontchartrain Basin is 'Louisiana, Mobile Bay, Version 01'.

The difference between Local Mean Sea Level (LMSL) and NAVD88 is 0.27 meter. This means that when bathymetry is given relative to NAVD88, the water level has to be increased by 0.27 meter in order to use Mean Sea Level (MSL) as reference level.

4.1.3 Tide

First the tidal propagation from the Atlantic Ocean into the Gulf of Mexico and towards the project area will be treated. After the global characteristics of the tide in the project area is described, measurements are collected and summed up for several stations.

The tide enters the Gulf of Mexico through the Yucatán Channel and the Strait of Florida. Besides this, there is another exchange of water between the Gulf of Mexico and the Atlantic Ocean. The so-called Loop Current, a warm ocean current, enters the Gulf through the Yucatán Channel and leaves the Gulf through the Strait of Florida. The current turns clockwise in the Gulf (Hofmann and Worley, 1986).

For several locations along the Florida Peninsula and in the Gulf of Mexico, see Figure 4.5, the tidal predictions from NOAA are plotted for two days in Figure 4.6. From Mayport to Virginia Key there is a large decrease in amplitude.

Figure 4.5 Locations for comparison of tidal predictions (Google Earth, 2009)

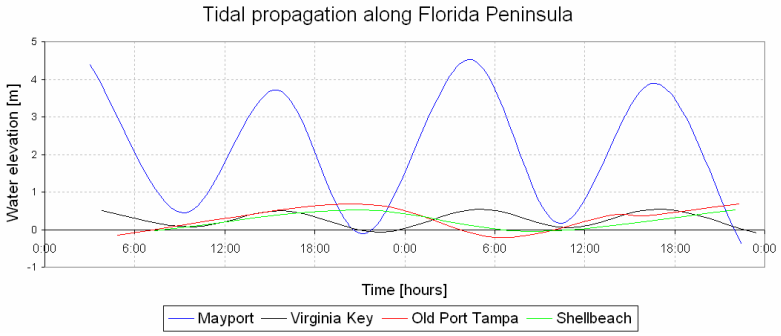

Figure 4.6 Tidal prediction along Florida Peninsula; first high or low water from February 23 2010 (NOAA Tides and Currents, 2010)

Looking at the period of the tide, Mayport and Virginia Key are semi-diurnal, while in the Gulf of Mexico the diurnal tidal components dominate. This is due to the location of the amphidromic points (Westerink et al., 1994). The diurnal components O1 and K1 have an amphidromic point near the Bahamas and off the coast of Honduras, while the semi-diurnal components M2 and N2 have an amphidromic point near the middle of the Gulf of Mexico. This can be seen in Figure 4.7.

The phase of the tides propagates counterclockwise around the amphidromic points (Yanagi and Takao, 1998).

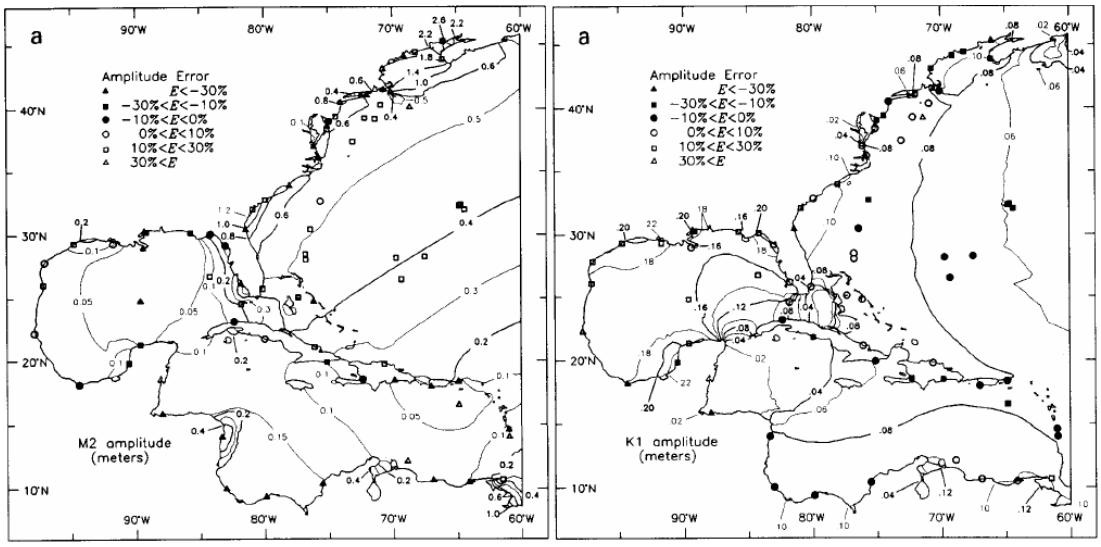

Figure 4.7 Amplitudes in the Gulf of Mexico for components M2 and K1 (Westerink et al., 1994)

The low waters in the Gulf occur more simultaneously (within 6 hours) than the high waters (within 9 hours). It is suggested by several researchers (Zetler and Hansen, 1970) that the tide in the Gulf of Mexico is co-oscillating with the tide in the Atlantic Ocean but opposite in phase. The tide enters the Gulf through the Florida Strait and leaves through the Yucatán Channel five to six hours later. From NOAA measurements and tidal analysis it follows that O1 and K1 are the main tidal constituents in the Gulf of Mexico.

The tide propagates into the project area via Mississippi Sound and the tidal pass between Mississippi Sound and the Biloxi marsh into Lake Borgne, see Figure 4.1. Lake Borgne has a diurnal tide with a mean range (MHW-MLW) of 0.44 meter (NOAA Tides and Currents, 2010, Shell Beach). The phase lag between the southern tip of the Birdfoot to Shell Beach is 5 hours. Through the three passes the tide propagates into Lake Pontchartrain. The phase difference between Lake Borgne and Lake Pontchartrain is 5½ hours, see Figure 4.8.

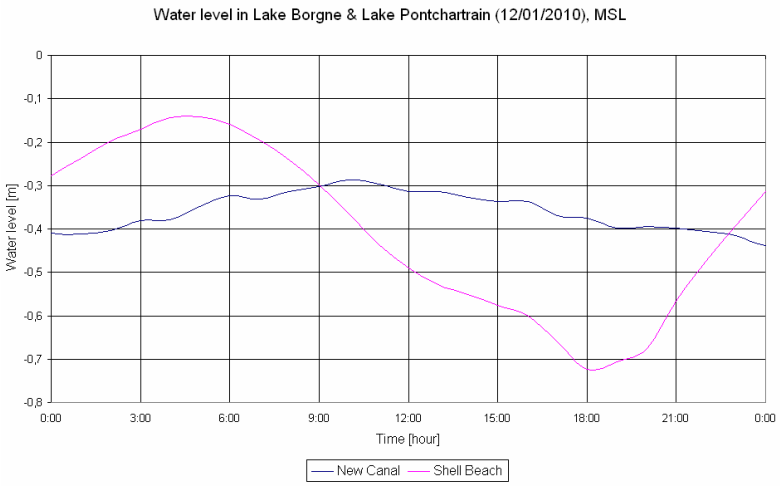

Figure 4.8 Phase difference between Lake Borgne (Shell Beach station) and Lake Pontchartrain (New Canal station) (NOAA Tides and Currents, 2010)

With a tidal prism of 1.56 x 10^8 m^3 (Sikora and Kjerfve, 1985), the tidal range in Lake Pontchartrain is 0.15 meter (NOAA Tides and Currents, 2010). The estimated flushing time of the lake is 60 days (Sikora and Kjerfve, 1985). The mean flow velocity due to tidal forcing is 0.002 m/s. Flow velocities increase towards the IHNC and the Rigolets to values of approximately 0.1 m/s and 0.18 m/s respectively (LSU, 2006/2007).

The National Oceanic and Atmospheric Administration (NOAA) performs daily water level measurements for several locations in the Pontchartrain Basin and nearby. There are several other institutes measuring water levels in the project area, like US Geological Survey (USGS) and the U.S. Army Corps of Engineers (Rivergages.com, 2010). Due to the length and continuation of the records, these data were not all as reliable as the NOAA. Since NOAA has a sufficient number of gages, only these data are used.

Table 4.4 gives the locations in latitude and longitude that are used in the calibration process, see Figure 4.9. Along the Mississippi coastline, information at the stations of Pascagoula, Bay Waveland and Gulfport Harbor are collected. For tidal information at the Mississippi Birdfoot the station of Southwest Pass is used. In Lake Borgne and Lake Pontchartrain the stations at Shell Beach respectively at New Canal are analyzed. For mean and daily tidal range see Table 4.5.

Table 4.4 Locations of NOAA stations used for the calibration process (NOAA Tides and Currents, 2010)

Location	Institute	Station ID	Longitude	Latitude
Dock E, Port of Pascagoula	NOAA	8741041	-88.5008	30.3356
Pilots Station East, SW Pass, LA	NOAA	8760922	-89.4011	28.9192
Gulfport Harbor	NOAA	8745557	-89.0692	30.3517
Bay Waveland Yacht Club	NOAA	8747437	-89.3181	30.3181
Shell Beach	NOAA	8761305	-89.6675	29.8667
New Canal (West End)	NOAA	8761927	-90.1022	30.0183

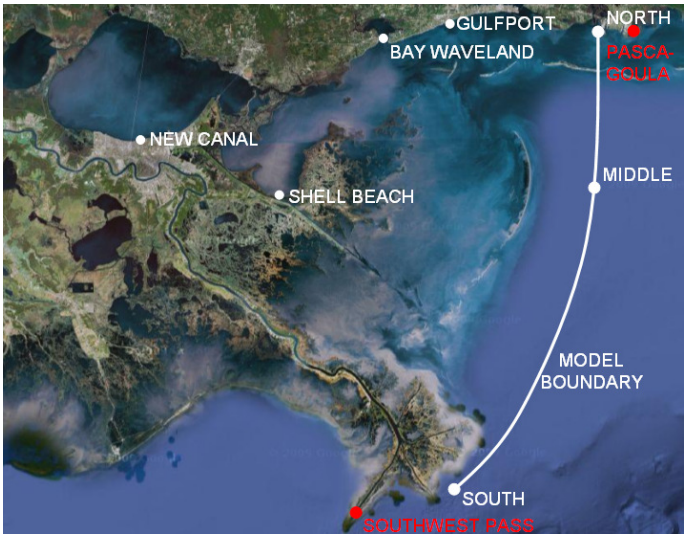

Figure 4.9 Location of NOAA station used for the calibration process (Google Earth, 2009)

Table 4.5 Tidal datums with respect to Mean Sea Level (MSL) (NOAA Tides and Currents, 2010)

	Southwest Pass	Pascagoula	Gulfport Harbor	Bay Waveland	Shell Beach	New Canal
Mean Higher-High Water (MHHW)	0.181	0.239	0.261	0.262	0.212	0.076
Mean High Water (MHW)	0.177	0.212	0.232	0.231	0.199	0.076
Mean Low Water (MLW)	-0.180	-0.205	-0.242	-0.233	-0.213	-0.075
Mean Lower-Low Water (MLLW)	-0.841	-0.233	-0.268	-0.265	-0.229	-0.075
Mean range [m]	0.357	0.417	0.474	0.464	0.412	0.151
Great diurnal range [m]	0.365	0.471	0.529	0.527	0.441	0.151

The measured water levels can be decomposed into information about tidal constituents: period, phase and amplitude. The phase is given as the phase lag of the observed tidal constituent relative to the theoretical equilibrium tide, either in GMT or local time (NOAA Tides and Currents, 2010). The tidal constituents at abovementioned stations are summarized in Table 4.6, Table 4.7 and Table 4.8.

Table 4.6 Measured tidal constituents at either side of the model boundary (NOAA Tides and Currents, 2010)

Tidal constituent	Speed [°/hr]	Southwest Pass		Pascagoula	
		Amplitude [m]	Phase [°]	Amplitude [m]	Phase [°]
K1	15.04	0.133	21	0.170	35
O1	13.94	0.132	12	0.149	28
P1	14.96	0.043	21	0.056	34
Q1	13.40	0.033	358	0.029	24
M2	28.98	0.017	123	0.027	130
S2	30.00	0.013	106	0.023	154
MF	1.10	0.000	0	0.000	0
N2	28.44	0.005	142	0.014	102
K2	30.08	0.003	91	0.006	156

Table 4.7Measured tidal constituents along Mississippi coastline (NOAA Tides and Currents, 2010)

Tidal constituent	Speed [°/hr]	Gulfport Harbor		Bay Waveland	
		Amplitude [m]	Phase [°]	Amplitude [m]	Phase [°]
K1	15.04	0.172	41.0	0.174	63.7
O1	13.94	0.157	32.0	0.167	49.6
P1	14.96	0.043	43.6	0.049	63.6
Q1	13.40	0.037	10.0	0.037	35.2
M2	28.98	0.035	169.6	0.031	213.2
S2	30.00	0.026	185.3	0.026	225.0
MF	1.10	0.000	0.0	0.009	106.0
N2	28.44	0.006	211.4	0.007	240.1
K2	30.08	0.010	154.1	0.013	210.5

Table 4.8Measured tidal constituents in Lake Borgne and Lake Pontchartrain

Tidal constituent	Speed [°/hr]	Shell Beach		New Canal	
		Amplitude [m]	Phase [°]	Amplitude [m]	Phase [°]
K1	15.04	0.138	98.2	0.034	181.5
O1	13.94	0.128	82.9	0.037	177.5
P1	14.96	0.042	95.5	0.011	181.2
Q1	13.40	0.026	76.9	0.007	175.5
M2	28.98	0.024	286.9	0.001	288.8
S2	30.00	0.019	329.5	0.004	16.4
MF	1.10	0.000	0.0	0.000	0.0
N2	28.44	0.007	338.3	0.001	58.2
K2	30.08	0.014	305.0	0.001	23.5

4.2 Preliminary analysis of model data

The gathered data are analyzed in this section. This analysis will be useful in the model calibration phase. For both lakes important parameters are determined. Then the harmonic analysis is applied for Lake Pontchartrain. Schematizing all channels and lakes as line elements, the tidal amplitudes and phases in Lake Borgne and Lake Pontchartrain can be calculated. This exercise gives an insight in the model data and the dependency of the outcome on several parameters. The theoretical background of the schematization can be found in Appendix A and Battjes (2002).

4.2.1 Schematization of project area

Figure 4.10 shows the schematization of the project area. The tide in the Gulf of Mexico propagates to Lake Borgne. The tide reaches the lake through the MRGO. Near Half Moon Island the tide that propagates east of the Biloxi Marsh also reaches Lake Borgne. Over time a tidal channel has eroded south of the island, while north of it a smaller portion of the tidal transport takes place. From Lake Borgne, the tide then propagates into Lake Pontchartrain via the three tidal passes: the Rigolets, the Chef Menteur Pass and the IHNC.

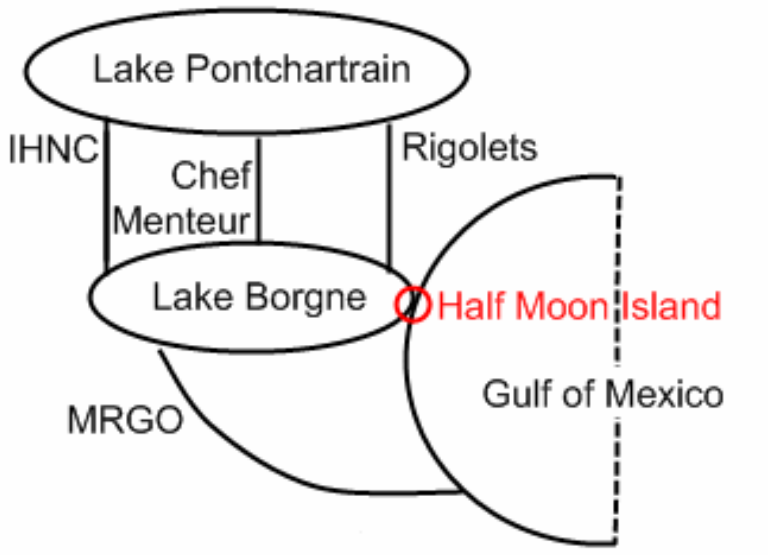

Figure 4.10 Schematization of area

For each lake the relevance of friction over local inertia can be determined by applying (5.1). Not for all parameters values are known yet. Therefore estimations are used: $\hat{U}$ is estimated to be 0.7 m/s, d_s is 3.0 m (see Table 4.1), C is estimated to be 65 $m^{1/2}/s$ and T is taken to be 24 hours. This leads to a value of 7.27 x 10^{-5} rad/s for ω and c_f is 0.0023. This leads to a ratio of σ = 7.4.

$$\sigma = c_f \frac{\hat{U}}{\omega \cdot d_s} \tag{5.1}$$

$$c_f = \frac{g}{C^2} \tag{5.2}$$

$$\omega = \frac{2\pi}{T} \tag{5.3}$$

where
c_f = friction coefficient [-], see (5.2)
$\hat{U}$ = amplitude of tidal velocity [m/s]
ω = tidal frequency [rad/s], see (5.3)
d_s = average depth [m]
g = 9.81 m^2/s; gravitational acceleration [m^2/s]
C = Chezy coefficient [$m^{1/2}/s$]
T = 86400 s; period of tide [s]

If $\sigma << 1$, friction plays no important role. If $\sigma >> 1$, friction is dominant over local inertia. It is concluded that friction is dominant in Lake Borgne. If the amplitude of the flow velocity is estimated too high, the dominance of friction will decrease. The ratio σ will reduce to one if the amplitude of the velocity is 0.1 m/s. Since this is a very low velocity, it can be concluded that friction cannot be neglected in Lake Borgne.

The same can be done for Lake Pontchartrain. Values used are based on data gathered earlier this chapter; $c_f = 0.0023$; $\hat{U} = 0.05 m/s$; $\omega = 7.27 \cdot 10^{-5} rad/s$; $d_s = 3.7 m$.
Then the ratio is $\sigma = 0.43$. This means that in Lake Pontchartrain local inertia dominates over friction.

From Figure 4.11 the tidal propagation through the area can be analyzed. The amplitude decreases and the phase lag increases when continuing into the project area towards Lake Pontchartrain.

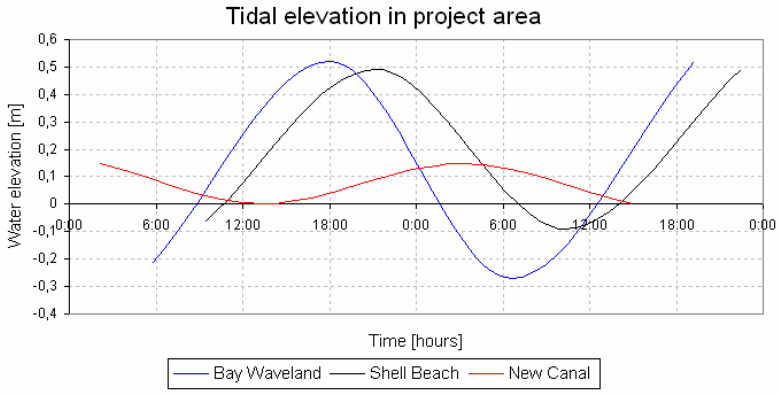

Figure 4.11 Tidal elevation in project area

The storage approximation considers a lake connected to the sea by a small opening or a channel. For the storage approximation to be a correct schematization, there are two conditions to be met. These are met simultaneously:

1. The length of the lake is much smaller than the tidal wave length.
2. The entire surface area of the lake oscillates simultaneously to the tidal forcing, which means that there is no phase difference over the lake.

Looking at Lake Borgne first, it is connected to the Gulf of Mexico by both a channel (the MRGO) and a small opening near Half Moon Island. To see if the first conditions is met for Lake Borgne, the length of the tidal wave is calculated using (5.4) and (5.5).

$$L = c \cdot T \tag{5.4}$$

$$c = \sqrt{g \cdot d_s} \tag{5.5}$$

where
L= tidal wave length [m]
c = tidal propagation velocity [m/s]

The velocity of the tidal propagation is 5.42 m/s and the wave length is 469 km. As the length of Lake Borgne (34 km, see Table 4.1) is much smaller than the tidal wave length, it is allowed to schematize the lake as a storage basin. This means the water level in the entire lake rises and falls at the same time. Except for Shell Beach there are no NOAA stations in Lake Borgne, therefore it cannot be visualized that the phase difference along the Lake Borgne shore is negligible.

From Lake Borgne the tide propagates to Lake Pontchartrain via the three tidal passes. For Lake Pontchartrain the same check is done to see if the lake can be schematized as a storage basin. The tidal propagation is 6.02 m/s. Again the tidal wave length of 513 km is much larger than the length of the lake (64 km, see Table 4.1), and Lake Pontchartrain can also be schematized according to the storage approximation. This is confirmed in Figure 4.12, where the water levels at different locations in Lake Pontchartrain (Figure 4.13) are shown. The phase difference along the shoreline of Lake Pontchartrain is very small. This means the water level in the lake rises and falls at the same time in the entire lake. Since both requirements are met, the storage consideration can also be applied for Lake Pontchartrain.

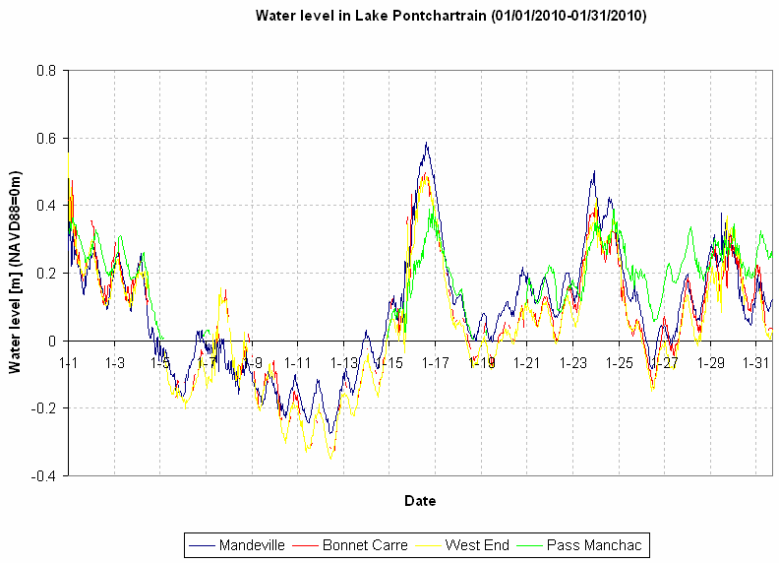

Figure 4.12 Tide in Lake Pontchartrain (Rivergages.com, 2010)

Figure 4.13 Locations of water level comparison (Google Earth, 2009)

Knowing that in both lakes the water level rises and falls at the same time, the schematization for the harmonic method can be set up. The schematization considers the propagation of the tide through prismatic channel sections, each with different geometries. It is assumed that the tidal water level elevation is small compared to the total water depth and that the channel geometry does not change with the tidal elevation. The sections covering the lakes are assumed to be so small that there is no phase difference over a section. This way the storage consideration is also met in the harmonic method.

Each channel is a separate section, as well as the lakes, see Figure 4.14. In Table 4.9 the sections and node numbers are linked to the channels and lakes. An iteration follows to calculate the water levels in all sections. For more information about this schematization, see Appendix A.

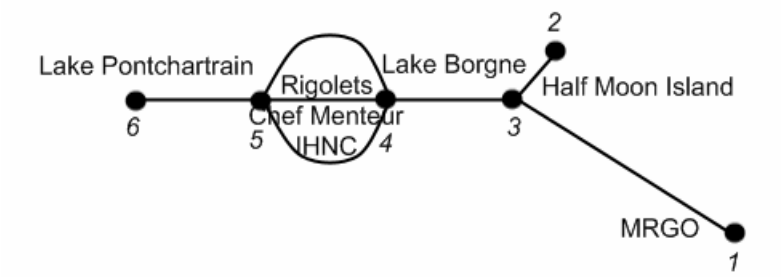

Figure 4.14 Schematization of Pontchartrain Basin for application of the harmonic method

Table 4.9 Schematization of Pontchartrain Basin for application of the harmonic method

Section	Element	Node begin	Node end
1	Mississippi River Gulf Outlet (MRGO)	1	3
2	Opening near Half Moon Island	2	3
3	Lake Borgne	3	4
4	Rigolets	4	5
5	Chef Menteur	4	5
6	IHNC	4	5
7	Lake Pontchartrain	5	6

For the schematization the data collected by Haralampides (Georgiou et al., 2007) are used, as well as the channel and lake characteristics in the ADCIRC SL15 bathymetry. For the schematization of the tidal propagation around Half Moon Island, the geometry of the tidal channel south of the island is estimated from the ADCIRC SL15 bathymetry. The area north of Half Moon Island is not taken into account. It can be analyzed whether each of the channels is well represented in the SL15 bathymetry, or what changes have to be made to gain the correct fluxes and water levels in respectively the channels and the lakes. The friction factor c_f is estimated to be 0.0023 for all sections.

4.2.2 Results of harmonic method

Figure 4.15 shows the outcomes of the harmonic method for tidal propagation in Lake Borgne and Lake Pontchartrain using the channel characteristics of Haralampides (Georgiou et al., 2007) respectively the SL15 bathymetry. In both cases, the tidal amplitudes are too small, especially in Lake Pontchartrain for the ADCIRC SL15 data. For the Haralampides dataset the phase in Lake Borgne is too small, while the phase lag in Lake Pontchartrain is too large. The phases in Lake Borgne for the ADCIRC SL15 data show a better match.

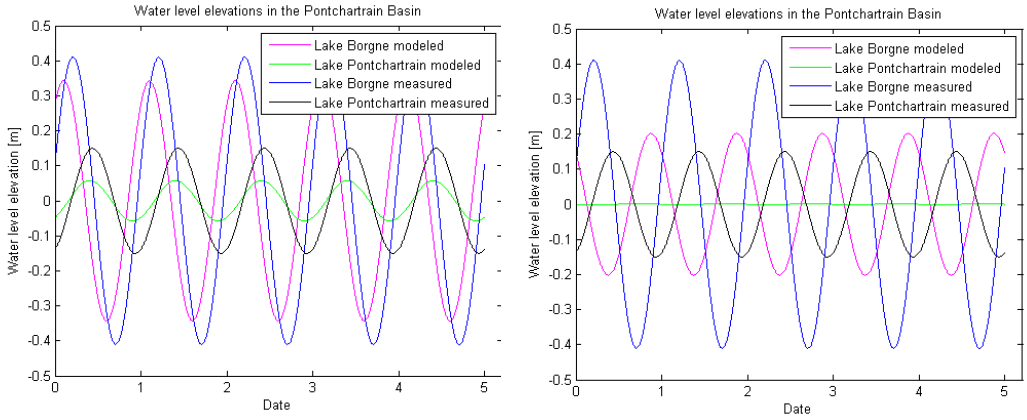

Figure 4.15 Calculated water level elevations in Lake Borgne and Lake Pontchartrain using the harmonic method (modeled) versus NOAA measurements (measured) using the channel characteristics of Haralampides (left) and the ADCIRC SL15 bathymetry (right)

The small calculated amplitude is caused by low fluxes. This can be explained by small cross-sectional areas of the channels. This explanation is supported by the fact that the calculations with Haralampides' characteristics perform better than the SL15 bathymetry. It was previously established that the cross-sectional area of the former were larger than those in the SL15 bathymetry. Next to increasing the cross-sectional areas, the channel roughness could be decreased.

For a sensitivity check of the system, the depth as established by Haralampides is increased by 50%, which also means an increase in cross-sectional area by 50%. The roughness coefficient c_f is subsequently decreased by 50%, which means the bottom will be smoother. The results in Table 4.10 illustrate that the Lake Borgne is most sensitive to changes in friction, while Lake Pontchartrain is more sensitive to changes in the cross-sectional area. This is consistent with the ratios of friction over inertia for both lakes, calculated in Section 4.2.1.

Table 4.10 Sensitivities of tidal amplitudes in Lake Borgne and Lake Pontchartrain to changes in depth and friction

	Haralampides	d + 50%		c_f + 50%	
	Amplitude [m]	Amplitude [m]	Change	Amplitude [m]	Change
Lake Borgne	0.202	0.347	+72%	0.378	+87%
Lake Pontchartrain	0.006	0.105	+50%	0.077	+35%

The next step in this analysis is to reproduce the measured water level elevations in Lake Borgne and Lake Pontchartrain by changing the cross-sectional and the friction coefficient. The starting point is the channel characteristics of Haralampides. Table 4.11 gives the adjusted values for the depth and the friction coefficient. With these values the amplitudes in Lake Borgne and Lake Pontchartrain are reproduced with an accuracy of 1%. Phases are harder to model. High water in Lake Borgne occur almost simultaneously with the high waters

Table 4.11 Adjusted depth and friction coefficients to reproduce the measured tidal amplitudes using the harmonic method

Section	Element	Depth d [m]	Friction coefficient c_f [-]
1	Mississippi River Gulf Outlet (MRGO)	12	0.0014
2	Opening near Half Moon Island	12	0.0010
3	Lake Borgne	3.7	0.0011
4	Rigolets	13	0.0013
5	Chef Menteur	13	0.0013
6	IHNC	8	0.0012
7	Lake Pontchartrain	3.7	0.0023

As can be seen from Figure 4.16, the calculated water levels are equal to the measured water levels (within 1%), but they are out of phase. In Lake Borgne high waters occur earlier in the schematization than in the measurements, while the calculated phase difference between Lake Borgne and Lake Pontchartrain is larger than measured. When comparing Figure 4.16 to Figure 4.15 it is concluded that the phases did not change much in the process of reproducing the amplitudes.

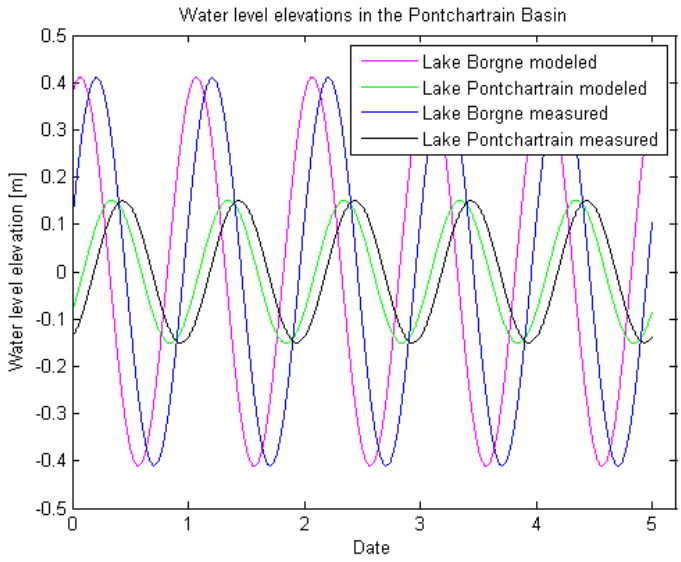

Figure 4.16 Calculated water level elevations in Lake Borgne and Lake Pontchartrain using the harmonic method (modeled) versus NOAA measurements (measured) using the adjusted depth and friction coefficients

4.2.3 Conclusions

A first insight in the tidal propagation of the Pontchartrain Basin is gained by schematizing all channels and lakes as line elements and applying the harmonic method. The channel characteristics given by Haralampides (Georgiou et al., 2007) as well as the channel representation in de ADCIRC SL15 bathymetry are too small to convey the right amount of water to Lake Pontchartrain. Changing the cross-sectional area has the largest impact on water levels in Lake Borgne, while decreasing the channel roughness has more impact on water levels in Lake Pontchartrain. Table 4.11 contains the best-fit values. With these channel characteristics the calculated water level elevation in Lake Pontchartrain are equal to the measured elevations.

4.3 Previous model studies

Now that the data are analyzed, a first impression of the physics of the system is clear. In addition, a better feeling of the sensitivity of the system to certain terms (e.g. friction, inertia) and parameters (e.g. roughness) has been achieved. The next step is to analyze previous model studies of the Pontchartrain Basin to study the strengths and weaknesses of other model studies and which parameters can be used.

There have been several studies to model the hydrodynamics of the Pontchartrain Basin. Different models have been used for these studies. Five important studies are discussed below for model set-up and results. The goal of this section is to give an insight in what sort of models are already used to model the Pontchartrain Basin and how they performed. Some important parameters for this model study are mentioned in detail. For those models that also studied salinity, only the results on tidal propagation will be treated here. For information on performance of salinity modeling, reference is made to Chapter 6.

First, the ADCIRC model will be discussed. It was used to study the influence of pass modification on tidal propagation in the Pontchartrain Basin. The ADCIRC model was also used for the simulation of storm surges caused by Hurricanes Katrina and Rita. The second model discussed here, FVCOM, was used to study the influence of diversions on salinity in the Pontchartrain Basin. For construction of the IHNC storm surge barrier, the RMA2 model was used to study changes in flow velocities. The last model discussed here is the ADH model. This was used to study the impact of measures in the HSDRRS program on the larval fish transport in the MRGO and GIWW.

4.3.1 ADCIRC model

The Advanced Circulation Model (ADCIRC) is a finite element model for hydrodynamic simulations.

4.3.1.1 Modeling of tidal propagation

The first application of the ADCIRC model discussed here, is the modeling of tidal propagation in the Pontchartrain basin to study the influence of modification of the tidal passes and navigation channels for hurricane storm surge protection (Jacobsen, 2007). The ADCIRC SL15 model is depth averaged and was applied using a mesh of 2.1 million nodes with a minimum spacing of 60 meter. The open boundary runs from Mississippi Sound to near the mouth of the Mississippi River, across the Chandeleur Sound, see Figure 4.17. Landward the mesh extends to Lake Pontchartrain and Lake Maurepas. The SL15 bathymetry, see Section 4.1.1, was used for this study. The Manning's roughness value varies from 0.02 to 0.2 in the model. Along the pass banks the Manning value was slightly modified, for better results.

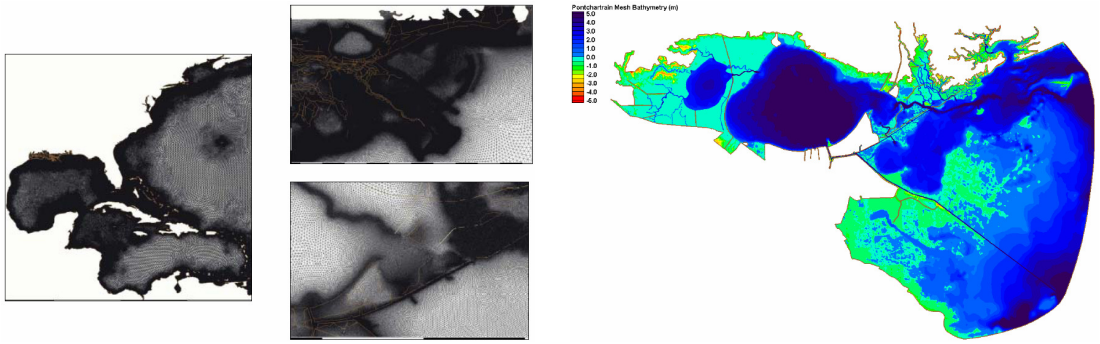

Figure 4.17 ADCIRC SL15 mesh of the Gulf of Mexico and Caribbean (left), Pontchartrain Basin (middle) and bathymetry of the Pontchartrain study (Jacobsen, 2007)

The model was forced only by astronomical tidal elevations at the open boundary, derived for each node using an ADCIRC tidal database. The mean water level (MWL) is set to 0.36 meters, which would correspond to a summer, steric adjusted regional level, consistent with the bathymetric datum. The time step for the simulations is 2 seconds. Initially the eddy viscosity was set to 50 m^2/s, which was later modified for better model results. All important parameters are summed up in Table 4.12.

Table 4.12 ADCIRC modeling characteristics (tidal propagation in Pontchartrain Basin)

ADCIRC	**Tidal propagation in Pontchartrain Basin after pass modification**
Grid type	unstructured
Number of layers	1; depth averaged
Nodes	2.1×10^6
Maximum resolution	60 m
Bathymetry sources	ADCIRC SL15
Roughness	Manning (0.02-0.2)
MWL	0.36 m
Time step	2 s
Eddy viscosity	50 m^2/s
Forcing	Astronomical tidal elevations
Modeled parameters	Tidal amplitudes

The ADCIRC results differed at least 33% from the observed tidal amplitudes at 10 of the 30 compared gages, see Figure 4.18. The model performs best for the amplitudes near the boundary and in Lake Pontchartrain. Phases have not been compared in this study. The moderate performance of the ADCIRC model can be explained by the original set-up of the larger model. The ADCIRC SL15 model was developed for simulation of hurricane storm surges.

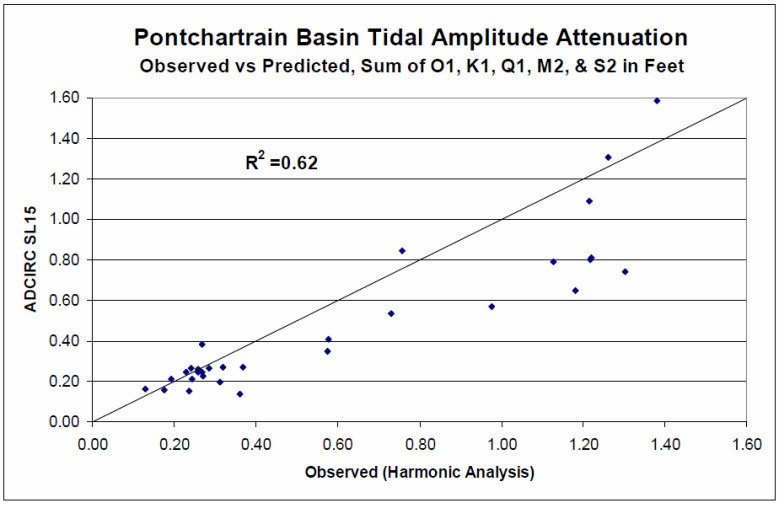

Figure 4.18 Results ADCIRC SL15 model (Jacobsen, 2007)

4.3.1.2 *Storm surge modeling*

A separate model study (Bunya et al., 2010) was conducted using the ADCIRC SL15 mesh. The goal of the study was to reproduce the storm surges of Hurricanes Katrina and Rita. The model was validated separately for riverine flows, tides, wind waves and hurricane storm surges. Only riverine flows and tides were validated for no storm conditions.

The deepwater wind wave model WAM was used to generate wave fields and directional spectra. It is assumed that wind waves are locally generated in the Gulf of Mexico, almost no wave action enters the Gulf via the Yucatan Channel or the Florida Strait. The WAM model domain covers the entire Gulf with a 0.05° [5560 meters] grid resolution. The nearshore wind wave model STWAVE transforms the waves from the WAM model to the shore. The grid resolution is 200 meter. All wave and wind data were imported into the ADCIRC model. The ADCIRC model computed the surface water elevations and currents.

The grid is based on the EC2001 astronomical tide model that covered the U.S. East coast and the Gulf of Mexico and the S08 storm surge model for southern Louisiana. The model domain covers the entire Gulf of Mexico, the western North Atlantic Ocean and the Caribbean Sea, see Figure 4.19 (left). The size of the model is based on the intention to cover all dynamics that occur during the exchange of water between the Gulf and the Atlantic Ocean. The part from Beaumont, Texas, to Mobile Bay, Alabama, has an increased grid resolution to better solve the storm surges in Louisiana and Mississippi and its lateral spreading, see Figure 4.19 (right).

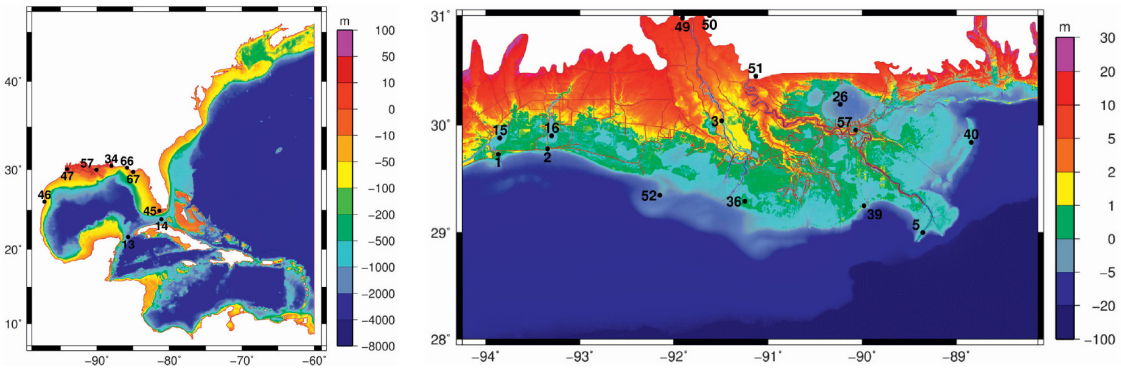

Figure 4.19 SL15 model domain (left) and detail of Louisiana and Mississippi domain (Bunya et al., 2009)

The maximum grid size is 24 kilometer in the Atlantic Ocean. The cell size decreases in the Gulf to a minimum of 50 meter. The maximum resolution is needed for resolving wave radiation stresses and currents along the Mississippi and Louisiana coast, around barrier islands and around Lake Pontchartrain. The unstructured grid contains 2,409,635 nodes. The different sources for the SL15 bathymetry are described in detail in Section 4.1.1. and by Bunya et al. (2009).

Initial water levels were raised by 0.134 meter to accommodate for NAVD88 in stead of LMSL. Additional increases were calculated for Hurricanes Katrina and Rita to account for the annual fluctuations in sea level due to thermal expansion of the upper Gulf layers.

The roughness was expressed in Manning coefficients varying from 0.02 to 0.20, see Figure 4.20. It was based on land cover definitions from the USGS LA-GAP for Louisiana, USGS MS-GAP for Mississippi and the USGS National Land Cover Data (NLCD) for Texas and Alabama. Lateral eddy viscosity varied for water (5m^2/s) and land (50 m^2/s). The model characteristics are summed up in Table 4.13.

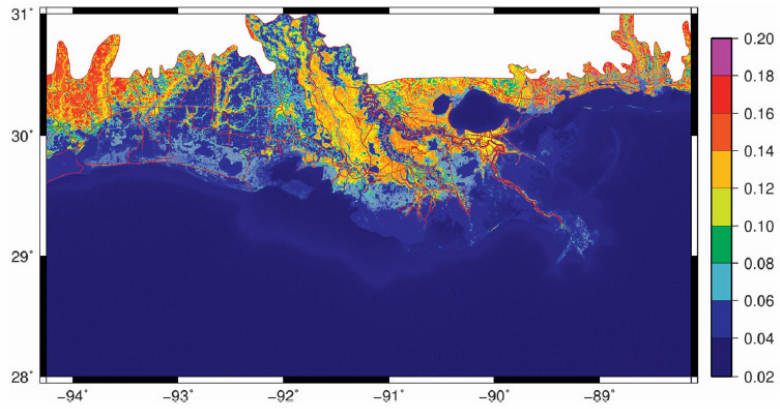

Figure 4.20 Detail of applied values for Manning roughness along Louisiana coast (Bunya et al., 2009)

Table 4.13 ADCIRC modeling characteristics (storm surge model for Louisiana and Mississippi coast)

ADCIRC	**Hurricane Katrina and Rita storm surge modeling**
Grid type	unstructured
Number of layers	1; depth averaged
Nodes	2.4 x 10^6
Maximum resolution	50 m (Louisiana and Mississippi coast)
Minimum resolution	24 km (open boundary at Atlantic Ocean)
Bathymetry sources	ADCIRC SL15
Roughness	Manning (0.02-0.20)
MWL	0.134 m
Time step	1 s
Eddy viscosity	50 m^2/s (water); 5 m^2/s (land)
Forcing	Tidal constituents, wind waves, river discharges, hurricane surges
Modeled parameters	Tidal amplitudes and phases

For tidal propagation the constituents O1, K1, Q1, M2, N2, S2 and K2 are used. The constituents are used to force the boundary in the Atlantic Ocean. NOAA tidal measurements are used for validating the model. In Louisiana the stations Southwest Pass, Grand Isle, New Canal and East Bank are used, see Figure 4.21. In Mississippi and Alabama the stations of Pascagoula, Gulfport Harbor and Bay Waveland are used amongst others. A 60-day time series was used to analyze the constituents.

Figure 4.21 Location of gages used in ADCIRC storm surge modeling (Google Earth, 2009)

In Figure 4.22 the model performance with respect to tidal amplitudes and phases are visualized. All amplitudes are within 0.05 m of the measurements (outer band). The phases fall very near to the 20° band (outer band). Only the K2 constituent shows large deviations in modeled phase.

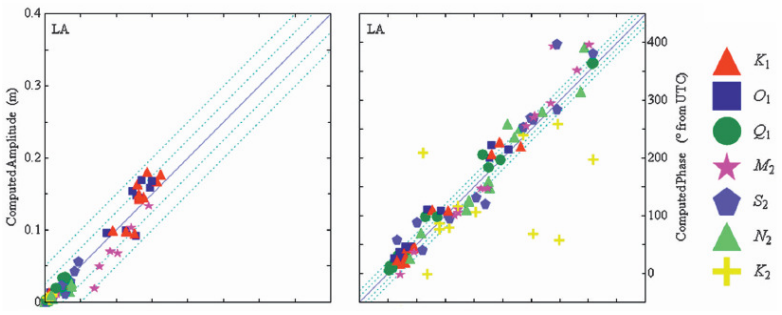

Figure 4.22 ADCIRC SL15 model performance on tidal amplitudes and phases in Louisiana

4.3.2 FVCOM model

Another study of the Pontchartrain basin was made using the Finite Volume Coastal Ocean Model (FVCOM) (Georgiou et al., 2007). This is a prognostic, unstructured-grid, finite-volume, free-surface, 3D primitive equation coastal ocean circulation model (SMAST/UMASSD, 2004). The purpose of the study was to investigate several diversions for modification of the salinities in the Pontchartrain Basin.

The mesh consists of 6893 nodes in the horizontal plane and has a spatial resolution varying from 75 to 100 meter in the MRGO and the tidal passes to 300 to 3000 meter at the open boundary at Mississippi, Chandeleur and Breton Sound, see Figure 4.23. The model was applied in 3D for the modeling of salinity, using three vertical layers. In a later stadium eleven layers will be used.

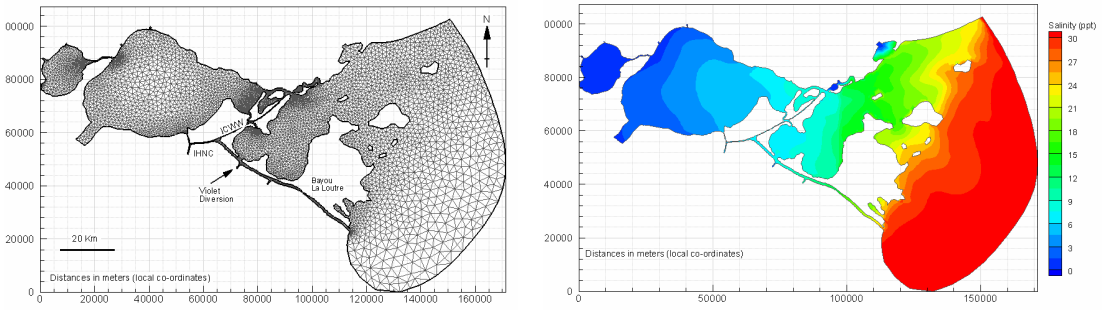

Figure 4.23 Model domain (left) and initial salinity (right) of the FVCOM model (Georgiou et al., 2007)

The bathymetry is a combination of data from the National Oceanic and Atmospheric Administration (NOAA) National Ocean Service (NOS) surveys and 1996 US Geological Survey data. For Chandeleur and Breton Sound, data from the ADCIRC SL15v3 grid were used. The model was forced by a tidal signal, consisting of four astronomical components. The initial elevation was equal to mean sea level (MSL). The model characteristics are summed up in Table 4.14. Water levels and fluxes were compared to measurements taken in 1997.

Table 4.14 FVCOM modeling characteristics

FVCOM	**Impact of diversions on salinity in Pontchartrain Basin**
Grid type	unstructured
Number of layers	3
Nodes per layer	6893
Total number of elements	12780
Maximum resolution	75 -100 m (MRGO, tidal passes)
Minimum resolution	300 - 3000 m (open boundary near Chandeleur Islands)
Bathymetry sources	NOAA, NOS, USGS, ADCIRC SL15v3
MWL	MSL
Forcing	Astronomical components, river discharges (monthly mean)
Modeled parameters	Tidal elevations, tidal fluxes, salinity

The calibration process focused on tidal elevations throughout the model area and tidal flows through the passes between Lake Borgne and Lake Pontchartrain. After calibration the modeled fluxes in the tidal passes between Lake Borgne and Lake Pontchartrain are within 5% of the observed fluxes, see
Table 4.15. In the table the maximum occurring flows during the tidal cycle are given, which are averaged for flood and ebb. The second line in the table indicates the error of the ADCP measurements, which is less or equal to 4% of the total flow. From Table 4.16 it can be derived that the difference in modeled and observed tidal amplitude is smaller than 10%, except for in the Rigolets Pass. The phase difference is largest at Pass Manchac (between Lake Pontchartrain and Lake Maurepas, Figure 3.6) where the model leads 3 hours on the measurements.

Table 4.15 Simulated and observed flows for August 1997, FVCOM study (Georgiou et al., 2007)

	Flows in [m^3/s]	IHNC	Chef Menteur Pass	Pass Manchac	Rigolets	Total
Observed	Flood/ebb	368	2407	991	5097	8863
	Error (+/- 4%)	*15*	*96*	*40*	*204*	*355*
Simulated	Flood/ebb	439	2322	1034	4955	8764
	Difference	*71*	*85*	*42*	*142*	*99*

Table 4.16 Simulated and observed tidal ranges and phases for spring tide, FVCOM study (Georgiou et al., 2007)

		Lake Pontchartrain	Rigolets Pass	Half Moon Island	Pass Manchac
Observed	Range [m]	0.17	0.31	0.65	0.16
	Phase [hours]	24	25	25	26
Simulated	Range [m]	0.16	0.43	0.66	0.15
	Phase [hours]	23	23	24	23

4.3.3 RMA2 model

For the design and construction of the IHNC barrier the RMA2 model was used to investigate the flow velocities in the channels near the barrier, under typical flow conditions (AECOM, 2009). The RMA2 model is a two dimensional, depth averaged finite element numerical model. The model predicts surface elevations and horizontal velocities. The model domain reaches from Lake Pontchartrain to Chandeleur Sound, and does not include the Chandeleur Island. The mesh consists of 13,330 nodes and the resolution varies from 3050 to 3.05 meter, see Figure 4.24.

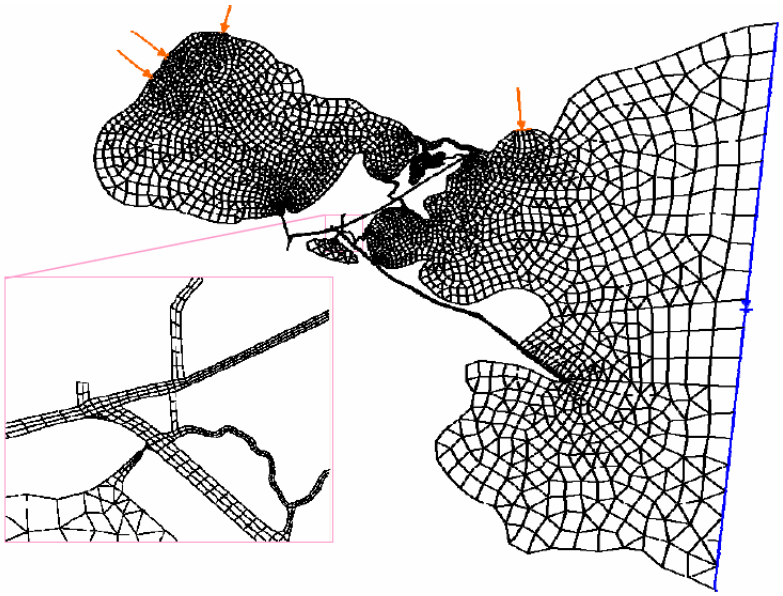

Figure 4.24 Model domain with computational mesh for modeling of flow velocities near the IHNC storm surge barrier. Zoom-in is the location of the barrier (AECOM, 2009)

The bathymetry consists of data of USACE surveys, NOS soundings and NOAA nautical charts. For parts of the IHNC, Bayou Bienvenue, MRGO and GIWW multibeam data were available from November 2008. The model was forced with freshwater inflow, tide and wind.

The freshwater inflow into the model consists of the rivers discharging into Lake Pontchartrain. The rivers discharging into Lake Maurepas were added to the model at the location of Pass Manchac (were the Lake Pontchartrain en Lake Maurepas are connected). The tidal input is a time series of tidal elevation at Gulfport Harbor.

Model calibration was done adjusting the friction and the eddy viscosity to obtain the best results for water levels, velocities and fluxes. The best results were achieved using a Manning roughness coefficient of 0.015, which is a typical value for concrete lined channels or the minimum value for a clean straight dredged channel (Brater, 1996). Varying the Manning coefficient with depth had no significant effect on model predictions. The initial value for the eddy viscosity of 48 [Pa.s] was not adjusted since the model performance with adjusted roughness was good enough. For the important model characteristics, see Table 4.17. For comparison of the water level, T-tide (Pawlowicz et al., 2002) was used. Water levels and tidal fluxes were compared to measurements in December 2008 and January 2009.

Table 4.17 RMA2 modeling characteristics

RMA2	**Flow velocities in IHNC near storm surge barrier**
Grid type	unstructured
Number of layers	1; depth averaged
Nodes	13,330
Maximum resolution	3.05 m (tidal passes)
Minimum resolution	3050 m (open boundary at Chandeleur Sound)
Bathymetry sources	USACE, NOS, NOAA
Roughness	Manning (0.015 everywhere)
Eddy viscosity	48 m^2/s
Forcing	Tidal constituents, wind, river discharges
Modeled parameters	Tidal amplitude, tidal fluxes

In the area of interest for this study (Lake Borgne and connected channels), the amplitudes are within 10% of the measurements and phases within 10 degrees. At the Gulf side of the MRGO the predicted phase differs almost 40 degrees from the measurements. In Lake Pontchartrain the model does not perform as well as in the area of interest. Predicted amplitudes are 16% (constituent O1) and 22% (constituent K1) larger than the measurement with a phase lag of 19 respectively 6 degrees, see Table 4.18. A different tidal boundary consisting of tidal constituents was extracted from a larger model to see whether the point in the MRGO would have a better fit with measurements, but this did not appear to be the case. Velocities in the model were compared to measurements taken during the 1 month simulation period. The values match relatively well, with no bias for over- or underprediction by the model, see Figure 4.25 and Figure 4.26. Only in the GIWW there was a phase shift during the calibration period, but not before or after this period. Flux measurements were performed during 2 days at four to six locations. The flux and its phase did not coincide for every location at every time, but considering the model before and after the dates of the measurements, this appeared not be trends in the model. Validation of the model was done using velocity measurements from five datasets in 2008. The model predictions match well with the observed data in trends and values. Only in the GIWW there is a phase difference between model and measurements, similar to the calibration phase.

Table 4.18 Measured vs. predicted dominant tidal constituents summary, RMA2 study (AECOM, 2009)

Location	O1 Amplitude [m]			O1 Phase [°]		
	Measured	Predicted	Error [%]	Measured	Predicted	Error [%]
CM1	0.12	0.12	-4.9	98.82	97.38	-1.44
CM2	0.12	0.13	2.4	97.61	95.85	-1.76
CM4	0.12	0.11	-7.7	97.10	93.83	-3.27
WL1	0.12	0.13	10.3	91.84	88.50	-3.34
WL3	0.12	0.13	7.3	70.81	71.88	1.07
WL4	0.13	0.12	-9.1	46.15	85.22	39.07
Chef Menteur	0.06	0.06	-5.0	54.11	58.88	4.77
Lakefront	0.02	0.02	16.7	121.12	140.03	18.97
Location	**K1 Amplitude [m]**			**K1 Amplitude [m]**		
	Measured	**Predicted**	**Error [%]**	**Measured**	**Predicted**	**Error [%]**
CM1	0.17	0.16	-3.6	111.19	106.89	-4.30
CM2	0.17	0.17	3.6	110.04	105.51	-4.53
CM4	0.17	0.17	-1.8	108.32	104.50	-3.82
WL1	0.17	0.20	15.8	102.42	99.34	-3.08
WL3	0.18	0.20	10.2	79.74	81.96	2.22
WL4	0.19	0.18	-3.3	59.17	96.15	36.98
Chef Menteur	0.07	0.07	4.4	124.42	122.80	-1.62
Lakefront	0.03	0.03	22.2	207.55	213.97	6.42

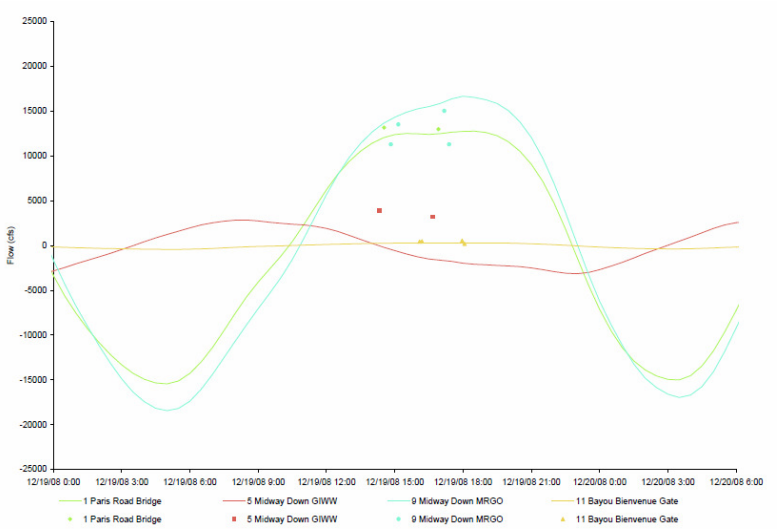

Figure 4.25 Measured and predicted flux (December 2008 ADCP survey), RMA2 study [e]

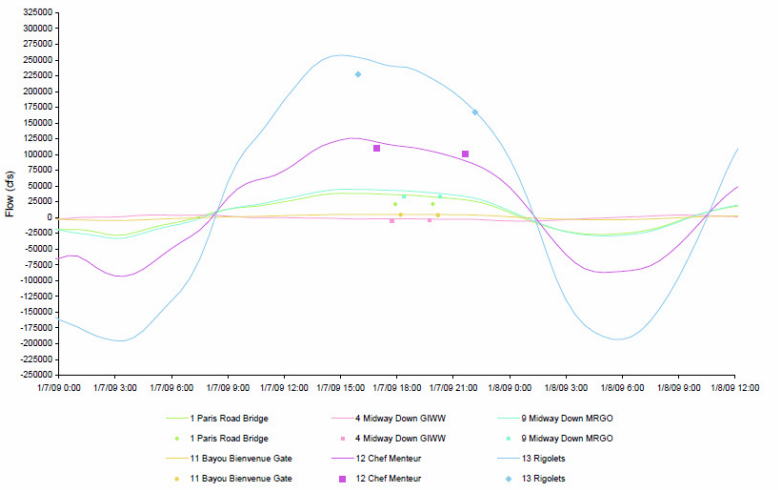

Figure 4.26 Measured and predicted flux measurements (AECOM January ADCP surveys), RMA2 study [e]

4.3.4 ADH model

ERDC (USACE Engineering Research and Development) used an existing model in order to study the impact of measures in the proposed hurricane and storm damage risk reduction (HSDRRS) on the larval fish transport in the MRGO and the GIWW (CHL ERDC, 2009). The tool used is called Adaptive Hydraulics (ADH). Only the 2D shallow water equations are used for this purpose. An ADH model was already developed and calibrated for HPO (USACE Hurricane Protection Office) to study the navigational effects in the GIWW for the IHNC barrier. The mesh includes Lake Maurepas and Lake Pontchartrain on one side and the Chandeleur Islands on the other side, see Figure 4.27. The mesh runs along the MRGO and the Mississippi River. The mesh was adapted for this study.

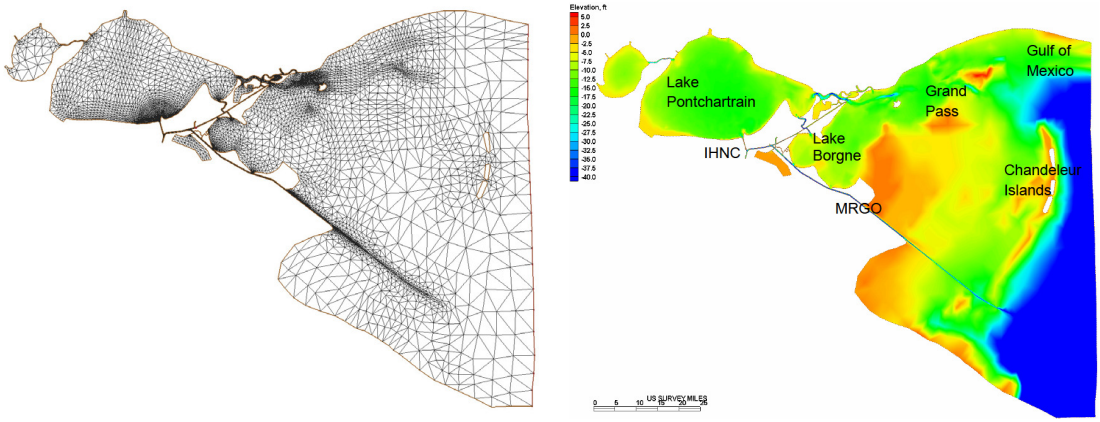

Figure 4.27 Model domain and bathymetry for the ADH model to study the larval fish transport in the MRGO (CHL ERDC, 2009)

The bathymetry was updated by measurements in the IHNC, GIWW, Bayou Bienvenue and northern MRGO. The roughness is expressed in Manning's roughness parameters. Any changes in roughness effects due to the water depth are calculated using an estimated roughness height. The model is forced by time series of river inflow, tide and wind between August 2007 and October 2008. The tidal forcing consists of tidal constituents and a non-predicted signal. The non-predicted signal is the difference between the observed water levels and the predicted tidal constituents. The data at Gulfport and Southwest Pass are linearly interpolated over the boundary.

Model validation was performed for surface elevations in Lake Borgne, Lake Pontchartrain and the channels, and for velocities and fluxes in the MRGO, IHNC and GIWW. The modeling characteristics that are described in the larval fish transport study and a previous study of the IHNC barrier with the ADH model (Martin et al., 2009), are given in Table 4.19.

Table 4.19 ADH modeling characteristics

ADH	**Larval fish transport near IHNC storm surge barrier**
Grid type	unstructured
Number of layers	1; depth averaged
Bathymetry sources	ERDC-CHL
Forcing	Tidal constituents, wind waves, river discharges, hurricane surges
Modeled parameters	Tidal amplitudes, river discharges, flow velocities

The tidal boundary appeared to be dominant over the river discharges. Water levels produced by the model showed a good match with the measurements. Comparison of the amplitudes of the tidal constituents showed a match within 20%, see
Table 4.20. Discharges in the model show a good magnitude and direction of the flow on several locations within the area of interest. Discharges in the IHNC near Seabrook deviate no more than 20% from measurements. Modeled flows in the MRGO and the GIWW show a small phase error. Among others, the model performance is limited by the use of only one wind station (at Lakefront Airport) and the simple representation of marshes in the model.

Table 4.20 Tidal constituents amplitude comparison, ADH study (CHL ERDC, 2009)

Con stitu ent	**Grand Pass**			**Paris Road**			**Chef Menteur**			**West End**		
	Field	Model	Error [%]	Field	Model	Error [%]	Field	Model	Error [%]	Field	Model	Error [%]
M2	0.095	0.084	-12.07	0.062	0.049	-21.17	0.042	0.035	-17.78	0.007	0.008	9.52
S2	0.123	0.101	-17.27	0.044	0.020	-47.55	0.037	0.020	-45.97	0.007	0.002	-67.77
N2	0.039	0.020	-47.86	0.011	0.008	-32.27	0.011	0.007	-39.33	0.003	0.001	-60.15
K2	0.055	0.053	-3.53	0.043	0.028	-35.27	0.034	0.034	1.35	0.005	0.005	3.16
O1	0.536	0.580	8.23	0.440	0.421	-4.43	0.349	0.393	12.55	0.131	0.118	-10.06
K1	0.337	0.371	10.04	0.446	0.395	-11.53	0.340	0.378	11.14	0.124	0.104	-16.49
Q1	0.126	0.127	0.54	0.084	0.078	-7.86	0.059	0.074	23.36	0.025	0.023	-4.40
M4	0.023	0.020	-12.40	0.008	0.012	49.90	0.007	0.010	39.44	0.001	0.001	-47.34
M6	0.11	0.008	-30.06	0.003	0.004	23.52	0.001	0.002	146.42	0.002	0.001	-67.48

4.3.5 Modeling of Mississippi River diversion regimes

The study of Rego et al. (2010) focuses on calibration of a 3D hydrodynamic model with sediment transport for the northern Gulf of Mexico, see Figure 4.28. The model is calibrated for tidal amplitudes and phases based on measurements and for sediment transport based on satellite observations of the river plume. The model is then used to simulate the river plume under passage of cold fronts and to simulate the effects of several diversion locations.

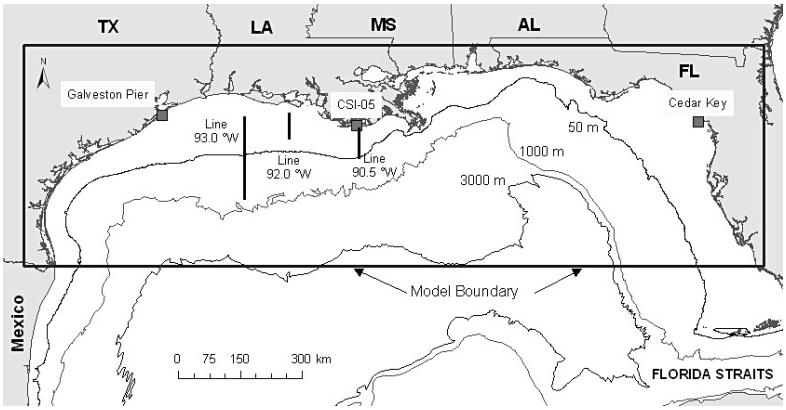

Figure 4.28 Model area (box) of H3D model by Rego et al. (2010)

The model used is called H3D which stands for Hayco three-dimensional model. The equations of motion are solved on a regular grid, with a semi-implicit scheme in time. This allows for large time steps. In the vertical direction the z-coordinate system is used which uses a variable number of layers depending on the water depth.

The grid has a constant resolution of 4 by 4 km^2. Even though the resolution does not increase near the coastline, important estuaries and barrier islands are present. The total grid has over 37,000 cells. In the vertical there are nine layers in the top 50 meter, another 9 layers from 50 to 500 meter depth, and from 500 to 3500 meter 10 layers are used. The number of layers is based on salinity profiles. The bathymetry was formed using the National Geophysical Data Center (GEODAS) database.

The model is forced by tides and wind stresses. Amplitudes and phases for 10 constituents were derived from a larger model. Temperature and salinity data at the boundary were extracted from a climatological database. The wind data are taken from four different sources and applied as spatially constant, hourly varying stress. Also relative humidity, air temperature and incident solar radiation were imposed hourly. Data of 18 gauges were used to simulate the river inflow into the model area. The data from 2002 are used for the calibration.

The model was run with a time step of 4 minutes for 365 days, assuming a spin-up time of 3 days. The model was calibrated on water levels. For all model characteristics, see Table 4.21.

Table 4.21 H3D model characteristics

H3D	**Modeling of Mississippi River Diversions**
Grid type	structured
Number of layers	28; 0 – 50 m and 50 – 500 m each 9 layers, 10 layers in 500 – 3,500 m
Nodes	37,000
Resolution	4 x 4 km^2
Bathymetry sources	GEODAS
Friction coefficient	0.003
Time step	4 min
Forcing	Tidal constituents, water temperature, wind, relative humidity, air temperature, incident solar radiation
Modeled parameters	Water levels, sediment transport

First, the water levels were calibrated using the bottom friction coefficient. With a value of 0.003, the tidal propagation is calibrated. However, large errors (25%) occur between measured and modeled tidal amplitudes and phases. This is explained by the boundary conditions. Although wind is taken into account during the modeling, and improves the model performance, the boundary consists only of tidal constituents. Information about nontidal water level elevations and currents occurring in the Gulf of Mexico are not taken into account. By adjusting the vertical diffusivity-to-viscosity ratio, the model was calibrated qualitatively for vertical mixing.

4.3.6 Conclusions

The ADCIRC-model, used for tidal propagation under pass modifications, has a tendency to underestimate tidal amplitudes. Phases were not compared. The ADCIRC application for storm surge modeling computed amplitudes within 0.05 m of the measured values for the Louisiana coast. The phases had deviations a little over 20°, except for the K2 constituent which showed larger phase difference. The FVCOM model was applied for simulation of the effects of river diversions on salinity. Tidal amplitudes, phases and the tidal fluxes in the passes were all within 10% of the measurements except for locations in the Rigolets and Pass Manchac. The RMA2 model, used for modeling flow velocities near the IHNC barrier, resulted in amplitudes and phases within 10% respectively 10º of the measurements in Lake Borgne. In Lake Pontchartrain the amplitudes were overestimated and the phases lagged. The modeled velocities showed good comparison with the measurements, except for the phase lag in the GIWW. For a study of larval fish transport in the MRGO, the ADH model was applied. The model produced tidal amplitudes within 20% of the measurements. Modeled discharges are in accordance with measurements in magnitude and direction. Only the flows in the MRGO and the GIWW show a small phase lag. The H3D model produced water levels with a deviation of 25% compared to measurements.

4.4 Recommendations for Delft3D modeling

Overall, results vary per model and study. Most studies produced tidal amplitudes, phases and velocities within 20% of the measured values. The largest errors occurred in the tidal passes, the channels of the GIWW and MRGO and in Lake Pontchartrain. The grid orientation and resolution in the channels and passes will be important for the performance of the hydrodynamic model in this study. In all studies the grid resolution increased in the channels and towards Lake Pontchartrain. Moreover, all studies used unstructured grids. With the structured grid of the Delft3D model it will be important to follow the flow pattern in the channels.

The time step in the two ADCIRC model studies was one or two seconds with a maximum resolution of 60 respectively 50 meters. Depending on the resolution in the Delft3D model, small time steps might be necessary.

Both the ADCIRC model studies and the RMA2 model used Manning coefficients to express the bottom roughness. Although the ADCIRC model studies succeed with a roughness varying from 0.02 to 0.2, the RMA2 model decreased the roughness drastically to a uniform value of 0.015. The preliminary data analysis proved that friction was important in Lake Borgne. The tidal propagation with the harmonic method showed that also in the tidal passes and Lake Pontchartrain friction played a role. Therefore, it is concluded that bottom friction plays an important role in modeling the tide in the Pontchartrain Basin and it is a good parameter for the calibration of the Delft3D model.

Varying the eddy viscosity did not result in better model performance. The best value for the eddy viscosity was approximately 50 m^2/s. This value will be used as a starting point in the calibration phase of this study.

The application of wind data from just one station was given as a limitation of the ADH model study. Wind is not taken into account in this study. Therefore it is recommended to add wind to the simulations in a following modeling effort.

From the H3D model study it was concluded that applying a boundary with only tidal constituents led to relatively large errors in water level elevations. This was explained by the lack of information about nontidal water level elevations at the boundary. As only tidal constituents are used in this study, adding nontidal forcing to the model should be a step in subsequent modeling efforts when the results of this study are not as desired.

Another limitation of the ADH model study was the simple representation of the marshes. It is important to study the flow in the marshes when calibrating the Delft3D model on tides.

5 Model calibration for tidal propagation

This chapter describes the calibration of the Delft3D model on tidal propagation in the Pontchartrain Basin. First the model set-up will be treated. The modules used for modeling tidal propagation are described shortly, followed by the construction of the grid and the considerations in this process. The considerations for input data, boundary conditions and input parameters conclude the set-up. With the default settings the model is run. The results of this run are analyzed and changes are applied in order to calibrate the model for tides. This section concludes with the performance of the calibrated run.

5.1 Model set-up

This chapter will describe the model set-up. The preliminary data analysis of the previous chapter will be of importance for the grid set-up.

5.1.1 Model description

Delft3D is a hydrodynamic model which is developed by Deltares. The model can be applied for 2D and 3D modeling of hydrodynamics, sediment transport and morphology in fluvial, estuarine and coastal environments (Deltares, 2010).

The grid is generated with the Delft3D-RGFGRID module. Using splines, a rough sketch of the grid can be made. Using spherical co-ordinates, the reference plane for the free surface level and the bathymetry follows the Earth's curvature (Deltares, 2009a). The set-up for this curvi-linear grid can be refined and adjusted to optimize the orthogonality and the smoothness in both directions.

Using Delft3D-QUICKIN the bathymetry is interpolated to the grid. Depending on the resolution of the samples compared to the grid resolution, one can choose grid cell averaging (high sample resolution) or triangular interpolation (low sample resolution).

The Delft3D-FLOW module simulates the hydrodynamics in the model area by solving the unsteady shallow water equations in two or three dimensions. The model can be used to simulate flow in shallow seas, coastal areas, estuaries, lagoons, rivers and lakes, and can include density-driven flows. Forcing of the model can consist of tides, wind and pressure gradients (barotropic or baroclinic). Source and sink terms can be included in the model by including a discharge- or withdrawal point. For more information about the equations and assumptions in Delft3D-FLOW, reference is made to (Deltares, 2009a).

5.1.2 Grid development

The results of the previous model studies prove that the channel geometry requires most attention when developing the grid. Tidal amplitudes and velocities are harder to model when moving towards Lake Pontchartrain. In all model studies this is dealt with by increased the grid resolution towards Lake Borgne and Lake Pontchartrain.

Since Delft3D uses a structured grid, local refinement and following the channel geometry need special attention. Therefore, the grid for Lake Borgne until the open boundary is developed first. Then the grid covering the tidal passes between Lake Borgne and Lake Pontchartrain is developed. Since the grid orientation and resolution of Lake Pontchartrain is least important, this grid is developed last. Eventually the grids are pasted to one, there is no nesting.

For all grids the size and resolution is a balance between resolution and model time. A high resolution is preferred in the channels and passes, but it will increase model time. Therefore the resolution decreases towards the model boundaries. All marsh areas that are not of importance for this study (near Breton Sound), or that do not carry flow (the landbridges between Lake Borgne and Lake Pontchartrain, see Chapter 4) have a low resolution or are not covered by a grid. The motivation for each separate grid is elaborated in this section.

The first grid covers the offshore area until Lake Borgne and the GIWW. The grid is oriented along the GIWW and the MRGO to capture the geometry of the channels. Especially the flow in the MRGO is important for the salinity in the area of interest, Lake Borgne and the Biloxi Marsh. The minimum cell width is here 150 meter. This means that not all the small channels in the Biloxi Marsh are captured. The cell size increases towards the area of interest to maximum 770 x 770 meter. The resolution further decreases towards the boundaries to save simulation time. For tidal propagation the cell size of maximal 1500 x 2020 meter is sufficient since it is still much smaller than the tidal wave length (approximately 500 km, see preliminary data analysis).

The layout of the Lake Borgne-grid was arranged so that the requirements of smoothness and orthogonality were met in Lake Borgne and the Biloxi marsh, the surrounding channels and the area offshore of the area of interest. In order to accomplish this, the area west of the MRGO does not fulfill the requirements everywhere.

Each tidal channel between the Lake Borgne and Lake Pontchartrain is covered by a separate grid. This way, the orientation of each channel can be captured precisely despite the channels' curvatures. If the orientation is not captured in the grid, a staircase-like flow could occur, especially in the bend of the Rigolets. The area in between the channels is not covered in the grid as it does not participate in the exchange of water between the lakes, as was established in Section 4.1.1. The number of cells along each channel is equal, in order to paste all grids together. In each channel there are six cells perpendicular to the flow direction, in order to accurately interpolate the bathymetry and solve the flow.

The grid of Lake Pontchartrain was developed last since its representation and resolution are least important. The lake acts as a storage basin of fresh water for Lake Borgne. Therefore it is more important to capture the total flux to and from Lake Pontchartrain, than the circulation in the lake. The minimal resolution in Lake Pontchartrain is 1340 x 1240 meter. Special attention was paid to the orthogonality of the grid where it is connected to the tidal passes.

After all grids were pasted to one, it was checked a last time for smoothness and orthogonality. For all cells participating in the main flow the requirements are met. The total grid consists of a little less than 53,000 nodes, see Figure 5.1.

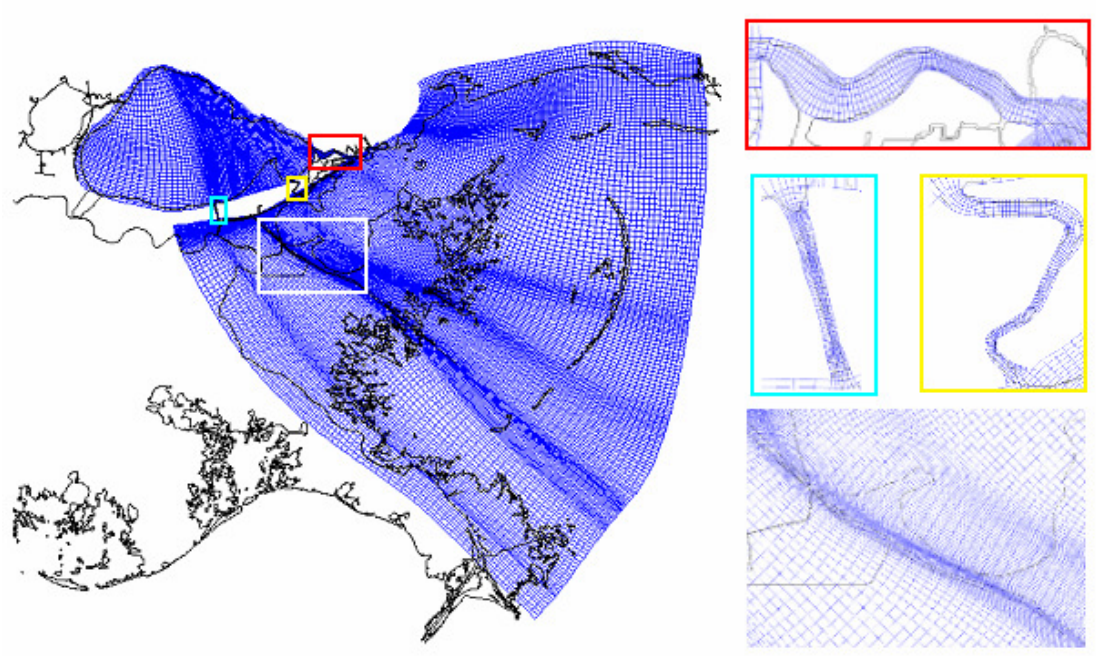

Figure 5.1 Delft3D grid

5.1.3 Input data

For the bathymetry of the model data from the ADCIRC model (ADCIRC, 2010) are used. The SL15 application has a high-resolution bathymetry for the Louisiana and Mississippi coastline. Data are gathered from different sources, resulting in a bathymetry composed of historic and more recent data. The bathymetry of ADCIRC SL15 used for this research is visualized in Figure 5.2. In the Delft3D model, the depth is specified at the grid cell corners.

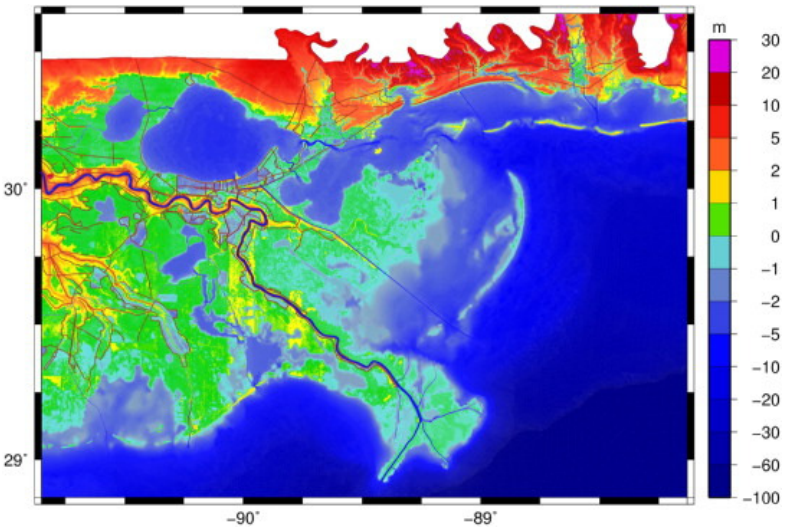

Figure 5.2 ADCIRC SL15 bathymetry (Ebersole et al., 2010)

The roughness data are also from the ADCIRC SL15 model. The roughness is expressed in a Manning value, see Figure 5.3. This is the initial roughness. The results of the preliminary data analysis and the previous model studies demonstrated that the roughness might need to be decreased. This will be addressed in the calibration process.

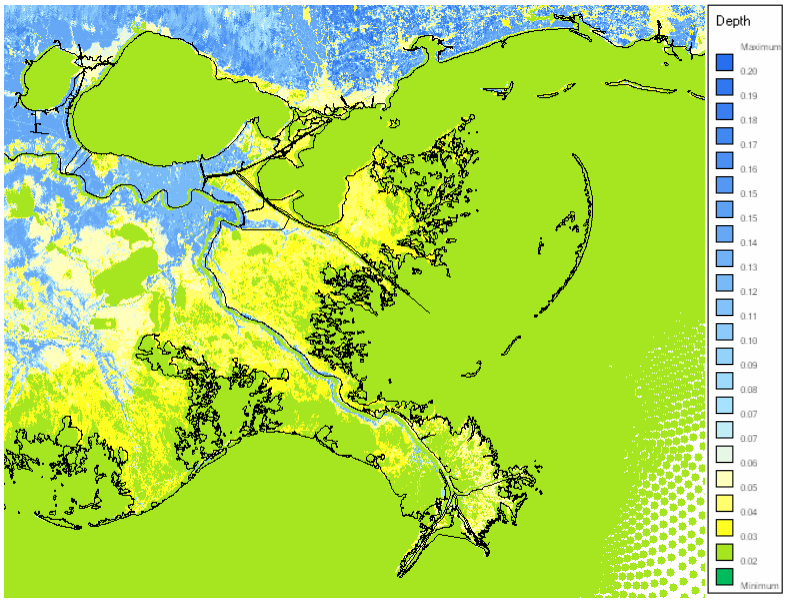

Figure 5.3 ADCIRC SL15 roughness values (Manning coefficient)

5.1.4 Boundary conditions

The forcing for the tidal calibration consists of tidal constituents on the open boundary offshore of the Chandeleur Islands. The amplitudes and phases of several tidal constituents are derived from a larger model, the Topex Poseidon database, at three points along the model boundary, see Figure 5.4. In between these points the values for amplitude and phase are linearly interpolated. At Southwest Pass the amplitudes derived from the Topex Poseidon database are larger than the measurements by NOAA (see Table 5.1 and Section 4.1.3). At the northern end of the boundary, exactly the opposite is the case. The tidal boundary is defined as astronomical constituents (amplitude and phase per constituent).

Table 5.1 Tidal constituents at boundary, derived from Topex Poseidon Database

Tidal constituent	Speed [°/hr]	South		Middle		North	
		Amplitude [m]	Phase [°]	Amplitude [m]	Phase [°]	Amplitude [m]	Phase [°]
K1	15.04	0.142	18	0.136	21	0.135	21
O1	13.94	0.141	12	0.132	14	0.131	14
P1	14.96	0.047	16	0.048	31	0.048	32
Q1	13.40	0.033	355	0.034	7	0.034	8
M2	28.98	0.018	120	0.041	144	0.041	145
S2	30.00	0.011	97	0.022	94	0.022	95
MF	1.10	0.009	347	0.008	351	0.008	351
N2	28.44	0.007	138	0.021	186	0.021	187
K2	30.08	0.004	59	0.007	30	0.007	31
MM	0.54	0.003	351	0.003	358	0.003	358

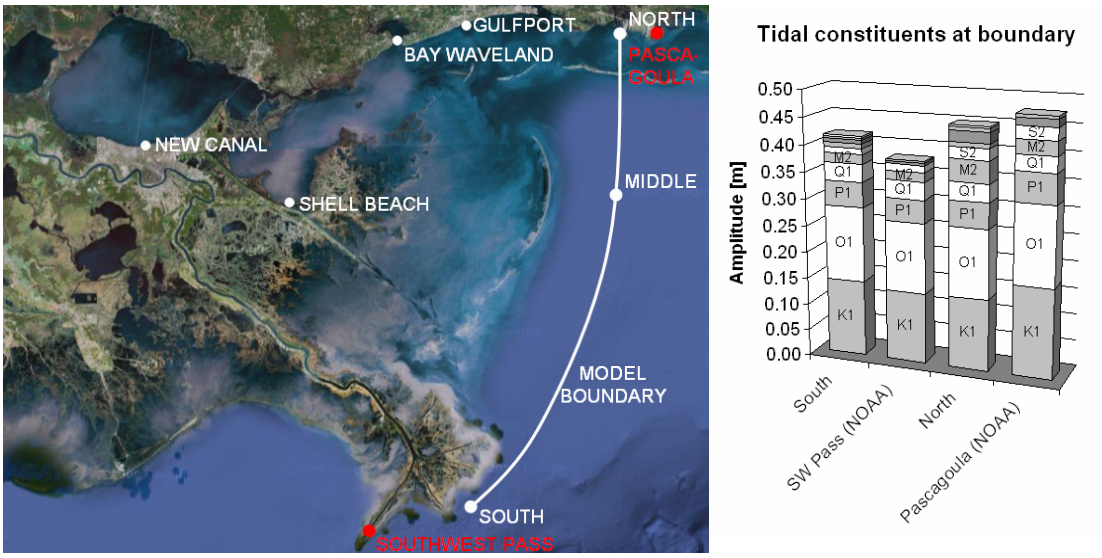

Figure 5.4 Location boundary conditions (Google Earth, 2009) and tidal constituents per location

5.1.5 Settings

The tidal calibration is performed with a 2D model, so velocities are depth averaged.

In order to make a descent decomposition of the water level excitation into tidal constituents, the run time of the model should be at least 1 month. With a record length of 30 days, most constituents can be extracted from the signal. Taking the spin-up time into account, the total model period is 39 days (01/04/2010 – 02/12/2010).

Once the model is calibrated, a longer simulation of the calibrated model will be performed to check all constituents in detail. If the record is longer, it is easier to distinguish the constituents and the results of the analysis will be more reliable. The minimum record length to distinguish two constituents can be calculated using equation (5.6) (Goring, 1984). With the smallest frequency difference begin 0.08° per hour between K1 and P1, as well as between K2 and S2, the record length to properly analyze all constituents should be at least 4500 hours (187.5 days).

$$T \geq \frac{360^o}{\Delta f} \tag{5.6}$$

where
T = length of record [hr]
Δf = difference in frequency between the two constituents [°/hr]

Based on the grid resolution the Courant-(Friedrichs-Levy) number, see (5.7), gives an indication of the maximum time step.

$$CFL = \frac{\Delta t \cdot \sqrt{g \cdot d}}{\{\Delta x, \Delta y\}} \leq 10 \tag{5.7}$$

Table 5.2 shows the maximum time step for several areas in the model. Model runs with a time step of 30 seconds did not produce more accurate results in the area of interest than runs with a time step of 5 minutes. To reduce modeling time, a time step of 5 minutes was used. Time steps larger than 5 minutes did result in more inaccurate results in Lake Borgne and the Biloxi Marsh.

Table 5.2 Time step according to Courant number for several areas in the model

Location	Minimal value of {Δx, Δy} [m]	Local depth [m]	Δt [min]
Model boundary near Gulf of Mexico	2000	50	15.05
Lake Borgne & Lake Pontchartrain	150	3	4.61
Rigolets	75	8	1.41
Chef Menteur	20	13	0.30
IHNC	25	7.5	0.49
MRGO	100	7.5	1.94

The water level in the model should be raised by 0.3 meter. This is the average difference between MSL and the reference level NAVD88, see Section 4.2.1. Raising the mean water level was accomplished by adding a term a_0 to the constituents. In order to decrease the spin-up time, the initial water level is also increased.

The threshold depth is set to 0.1 meter, the default value. If the water depth in a cell becomes larger than this value, the cell is considered wet. There is a rule of thumb for the threshold depth δ, see equation (5.8) (Deltares, 2009a). Using a tidal amplitude of 0.33 meter and 288 time steps per tidal period, the minimum threshold depth is then 0.008 meter. The values of other numerical parameters are set to default, see Table 5.3.

$$\delta \geq \frac{2 \cdot \pi \cdot |a|}{N} \tag{5.8}$$

where
$|a|$ = tidal amplitude [m]
N = the number of time steps per tidal period

Table 5.3 Values of numerical parameters in default run

Parameter	Value	Unit
Minimum record length	39	days
Time step	5	min
Threshold depth	0.1	m
Gravity	9.81	m/s^2
Water density	1020	kg/m^3
Temperature	21	degrees
Horizontal eddy viscosity	1	m^2/s
Horizontal eddy diffusivity	10	m^2/s
Marginal depth	-999	m
Smoothing time	60	min
Wall roughness slip condition	Free	
Drying and flooding check at	Grid cell centers and faces	
Depth specified at	Grid cell corners	
Depth at grid cell centers	Max	
Depth at grid cell faces	Mean	
Advection scheme for momentum	Cyclic	
Advection scheme for transport	Cyclic	
Horizontal Forester filter	On	
Vertical Forester filter	Off	
Correction for sigma-coordinates	Off	

5.2 Performance default run

Water levels are compared to NOAA measurements with respect to phase and amplitude. The tidal flux in the Rigolets, the Chef Menteur and the IHNC are compared with each other for the 60-30-10 ratio and compared with measured prisms. Measurements were performed by AECOM and for the development of the FVCOM model (see Section 4.3). The model in this study will be calibrated on the fluxes measured by AECOM, as these were measured most recently, in 2008 and 2009.

For checking the performance of the model compared to the NOAA measurements, graphs like Figure 5.5 are made. Points on the black line represent modeled amplitudes (left) or phases (right) of tidal constituents that equal the measured constituents. The green lines indicate results within 10% (left) or 20° (right) of the measured values. When the model results are within these intervals, the model is said to be calibrated sufficiently for tidal propagation.

Using all the default values in Delft3D-FLOW and the input data and boundary conditions as described before, the tidal amplitudes decrease too fast when propagating further into the model area. At Gulfport Harbor, see Figure 5.5, the amplitude and phase of the most important constituents is modeled well. A little further in the model domain at Bay Waveland, amplitudes have decreased too much. However, the phases of the largest constituents still have a deviation of less than 20° compared to the measurements, see Figure 5.6. Propagating towards Shell Beach and New Canal (West End), the amplitudes decrease further and the signal starts to lag behind, see Figure 5.7 and Figure 5.8.

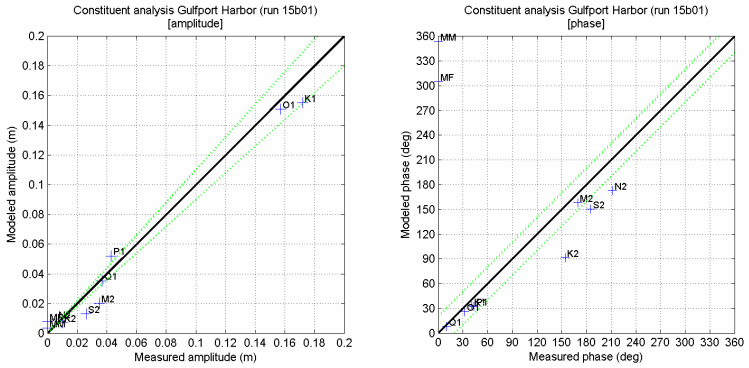

Figure 5.5 Constituent analysis Gulfport Harbor (default run)

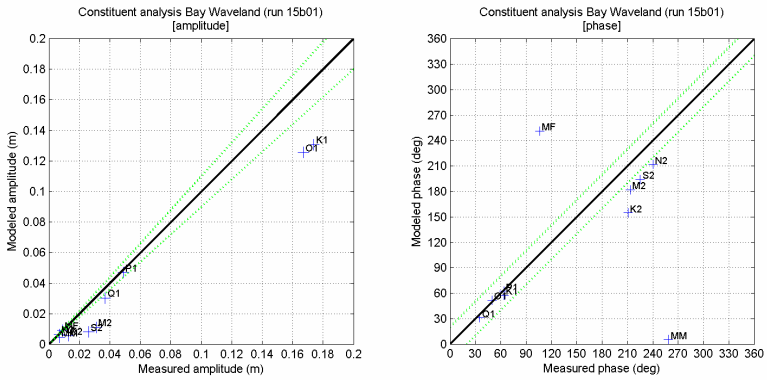

Figure 5.6 Constituent analysis Bay Waveland (default run)

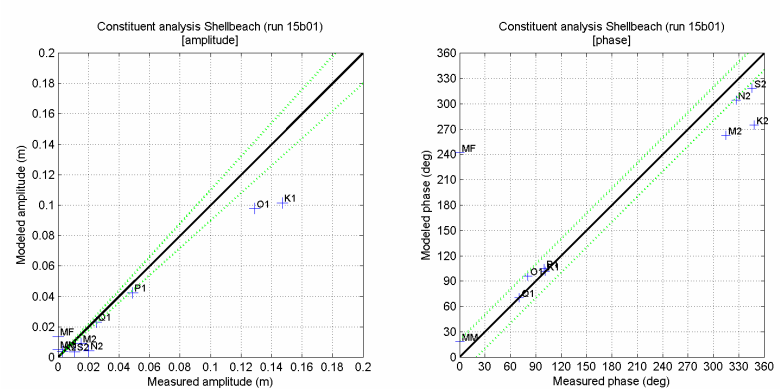

Figure 5.7 Constituent analysis Shell Beach (default run)

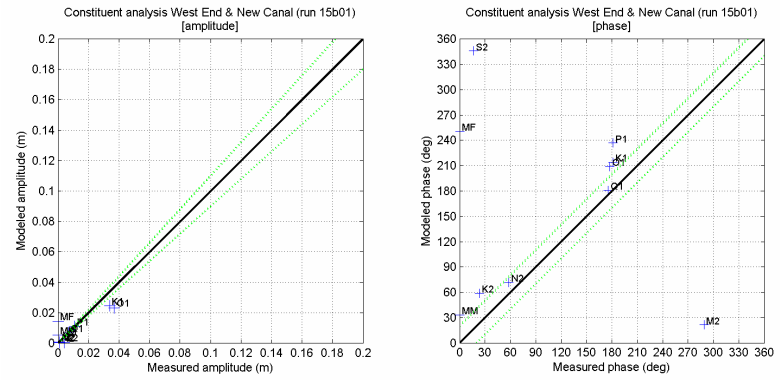

Figure 5.8 Constituent analysis New Canal (West End) (default run)

The AECOM measurements will be compared to the maximum flood flux in the model. The location of the measurements is indicated in Figure 5.9. At the same location in the model transects are added to collect discharge data.

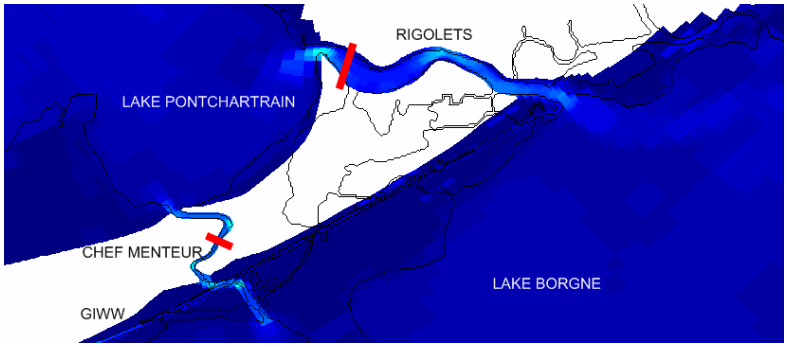

Figure 5.9 Location AECOM measurement transects indicated by red lines

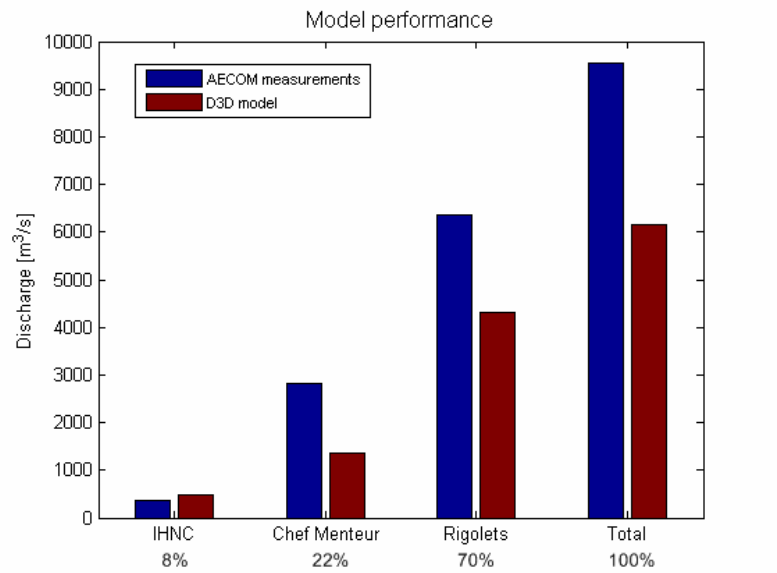

Figure 5.10 Comparison of tidal fluxes in passes (default run). Percentages give contribution of each channel to total flux into Lake Pontchartrain.

Table 5.4 Measured and modeled fluxes (default run)

Fluxes [m^3/s]	AECOM measurements	Delft3D modeling	Modeled ratio
Rigolets	6,371	4,299	70%
Chef Menteur	2,832	1,351	22%
IHNC	354	493	8%
TOTAL	**9,557**	**6,144**	**100%**

From Figure 5.10 and
Table 5.4 it follows that there is too little flow through each of the channels. This is one of the reasons why the tidal amplitude in Lake Pontchartrain is too low (Figure 5.8). Below each channel the percentage of the total flow through that channel is given. The flow through the Rigolets is high compared to the other channels.

The next section will deal with the changes that are made in the model set-up in order to gain better results with respect to water level elevations and fluxes.

5.3 Alterations in model

In order to augment the tidal amplitudes and fluxes, the roughness is reduced. From the preliminary data-analysis it already appeared that friction is dominant over local inertia in Lake Borgne. Therefore, reducing roughness to decrease the friction is the most efficient method to increase the amplitudes and decrease the phase lags in the model. This is confirmed by the results of the harmonic method that indicated that decreasing the roughness will lead to better results for tidal amplitudes in Lake Borgne and Lake Pontchartrain.

In all areas where significant flow velocities occur, the Manning values are adjusted. The roughness in marsh areas remains as in the ADCIRC SL15 model. This is done by decreasing the Manning values below 0.025 by a factor two. The roughness in the Rigolets and the Chef Menteur varies between 0.0167 and 0.0133. The roughness in the IHNC is set to 0.0167. In the MRGO, the Manning value is reduced to 0.0133.

These are more realistic values when considering the anticipated values for the roughness in the tidal passes as calculated in the preliminary data-analysis. That analysis indicated that the roughness in the channels should be very low, towards the limits of unrealistic values. The RMA2 model used even lower Manning values of 0.015.

To give an indication of the order of magnitude of the Manning roughness applied in the calibrated model, the equivalent Nikuradse roughness (*k*) height is calculated with equations (5.9) and (5.10). This has been calculated for the tidal passes and the MRGO, see Table 5.5. The roughness in the channels is given in Table 5.5. In the harmonic method for tidal propagation in the Pontchartrain Basin, c_f values around 0.0010 were used, which indicates the roughness of the channels in the data analysis is lower than in the Delft3D model.

$$k = 12 \cdot R \cdot 10^{\frac{-1}{5.75 \cdot \sqrt{c_f}}} \tag{5.9}$$

$$c_f = \frac{g \cdot n^2}{R^{\frac{1}{3}}} = \frac{g}{C^2} \tag{5.10}$$

where
R = hydraulic radius of channel [m]
c_f = friction coefficient [-], see (5.10)
n = Manning roughness coefficient [s/m$^{1/3}$]

Table 5.5 Manning and Nikuradse roughness in the tidal passes and the MRGO

Channel	Hydraulic radius R [m]	Manning roughness n [m$^{1/3}$/s]	Friction factor c_f [-]	Nikuradse roughness k [m]
Rigolets	8	0.0167	0.0014	0.0022
Chef Menteur	13	0.0167	0.0012	0.0015
IHNC	7.5	0.0167	0.0014	0.0020
MRGO	8	0.0133	0.0009	0.0002

In addition, the cross-section of several tidal passes is increased. This leads to larger fluxes in the passes, as well as larger amplitudes in Lake Pontchartrain. Starting point for the changes is the 60-30-10 flux ratio between the Rigolets, Chef Menteur and IHNC, and the depths and cross-sections as determined with the harmonic method. The increase of the cross-sectional area is accomplished by increasing the depth of the cells in the channel. The height and location of the land cells along the channel banks have not been altered, see Figure 5.11.

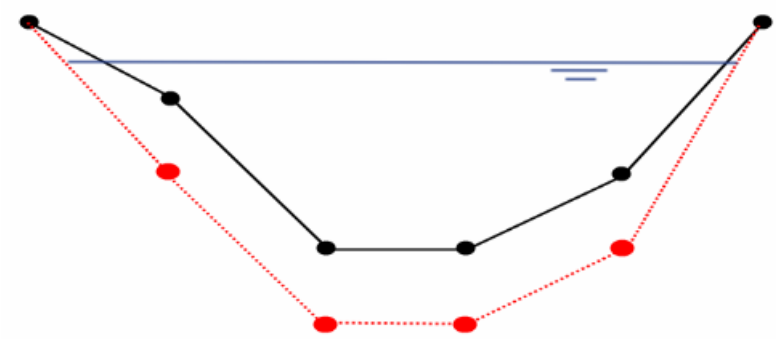

Figure 5.11 Example of adjustment of cross-sectional area of tidal passes and the MRGO: the bank height remains unchanged

Since the flux through the Rigolets is very high compared to the other tidal passes, the cross-section of this channel has not been altered. The minimal depth of the Chef Menteur pass is increased to 13 meter, so the deeper parts in the channel remain intact. Near the bends of the Chef Menteur, the width decreases in the original bathymetry. The minimum width in the bends has been increased to 230 meter. The widest part of the Chef Menteur is 370 meter. Due to the interpolation in the IHNC, the cross-sectional area of the channel has decreased compared to the original dataset. Therefore, the minimum depth of the IHNC is increased to 8 meter, and the width is increased to 250 meter. The new cross-sectional area of all tidal passes is comparable to those used for the best-fit run in the harmonic analysis.

The MRGO has also undergone some manual alterations. Since there are several bends in the MRGO, the orientation of the grid does not always follow the MRGO. This has had consequences for the interpolation of the bathymetry and the roughness. Therefore, these values were manually adjusted. The channel has an average width of 250, with an average depth of 7.5 meter.

From Figure 5.12 it can be seen that part of the Biloxi Marsh did not get flooded during high water. In the right plot, it shows that several grid cells have a bed level above 0.57 meter. With a tidal elevation of maximal 0.67 meter at the boundary and a threshold depth of 0.1 meter, this is the critical bed level for flooding of the cell. Due to the large cell size in the Biloxi Marsh (the minimal cell width is 150 meter), the small channels that carry the flow in reality are not represented in the model bathymetry. Besides this, some cells may have an unrealistic height. As established in the background of the SL15 bathymetry, the marsh areas for which the height was not known got assigned a value of 0.8 m. As this area is interpolated on the relatively coarse grid, the channels are not represented, and the bed level is unrealistically high too. To make sure all cells in the Biloxi Marsh flood during spring tide, the bed level is lowered to a maximum value of 0.30 meter. This is the minimal value for all cells in the Biloxi Marsh to be flooded.

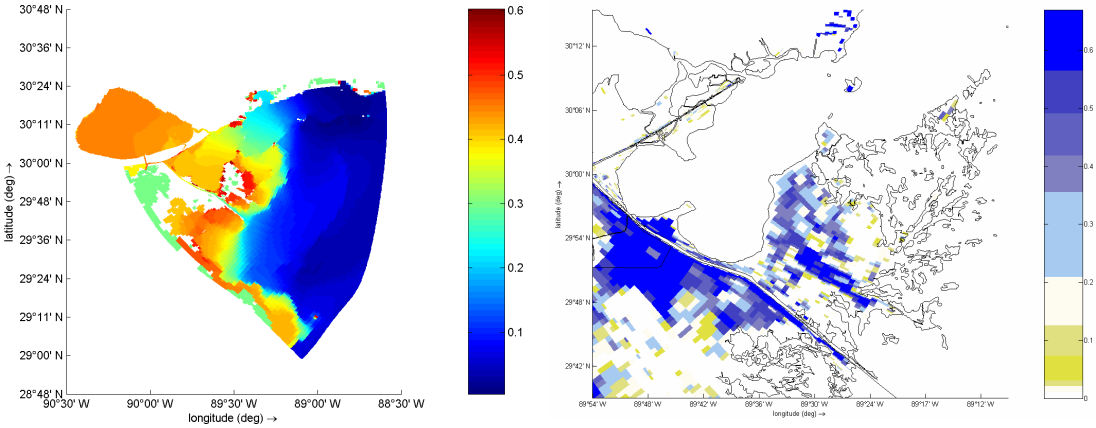

Figure 5.12 Left: instantaneous water level (m) in default run; right: bathymetry

Other parameters and model input has remained the same as the first run, mostly default. Changing the viscosity does not lead to better model results.

5.4 Performance calibrated run

The model performance with adjusted bathymetry and roughness falls within the set interval for calibration for the most important constituents O1 and K1, see Figure 5.13, Figure 5.14, Figure 5.15 and Figure 5.16 for tidal amplitudes and phases. Table 5.6 sums up the modeled amplitudes and phases.

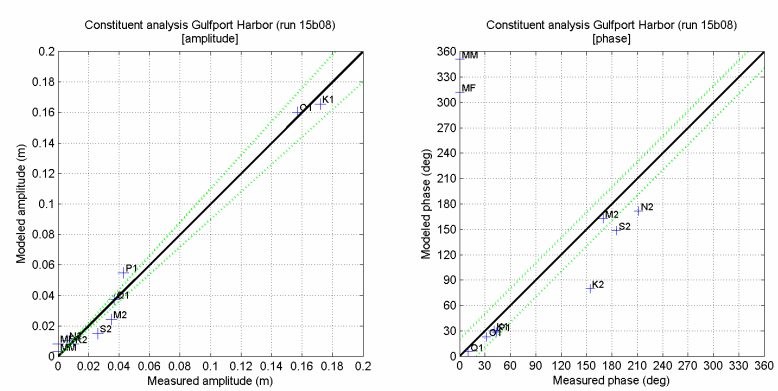

Figure 5.13 Constituent analysis Gulfport Harbor (calibrated)

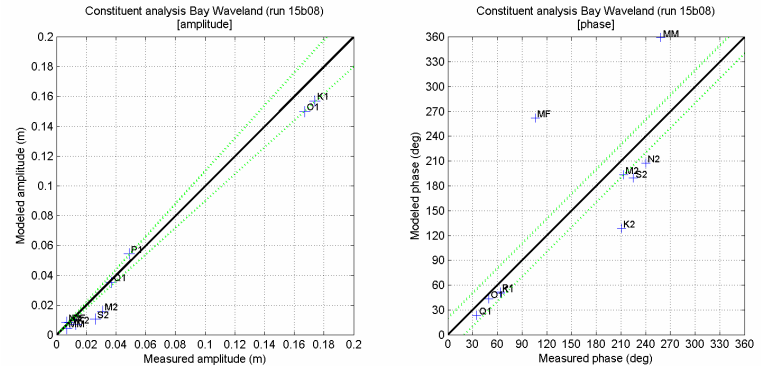

Figure 5.14 Constituent analysis Bay Waveland (calibrated)

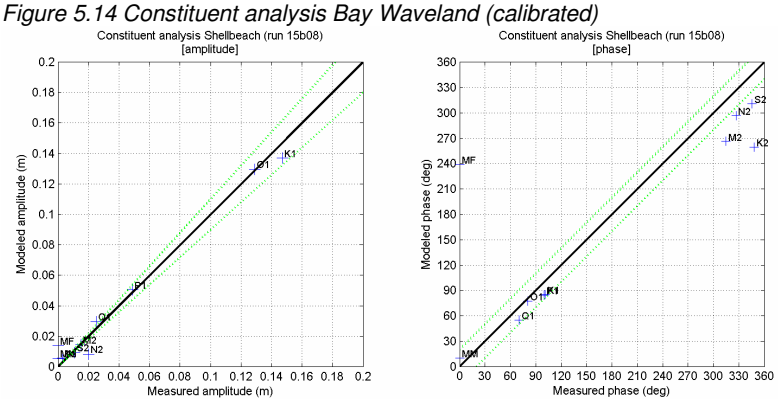

Figure 5.15 Constituent analysis Shell Beach (calibrated)

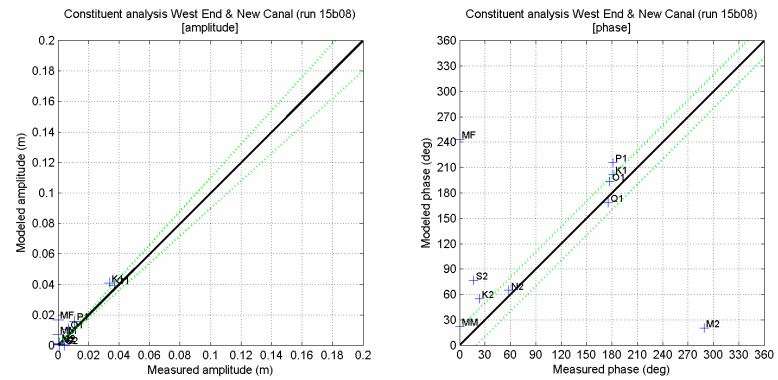

Figure 5.16 Constituent analysis New Canal (West End) (calibrated)

Table 5.6 Modeled tidal constituents (calibrated)

Consti-tuents	Shell Beach measured		Shell Beach modeled		New Canal measured		New Canal modeled	
	Amplitude [m]	Phase [°]	Amplitude [m]	Phase [°]	Amplitude [m]	Phase [°]	Amplitude [m]	Phase [°]
MM	0.000	0.0	0.005	10.0	0.000	0.0	0.007	22.1
MF	0.000	0.0	0.013	238.8	0.000	0.0	0.016	243.4
Q1	0.025	70.3	0.029	54.8	0.007	175.5	0.010	168.5
O1	0.129	80.6	0.129	77.2	0.037	177.5	0.038	193.7
P1	0.049	99.7	0.050	84.2	0.011	181.2	0.015	215.9
K1	0.147	101.3	0.136	85.0	0.034	181.5	0.040	201.7
N2	0.020	326.8	0.008	296.8	0.001	58.2	0.000	64.7
M2	0.015	314.9	0.014	266.3	0.001	288.8	0.001	32.6
S2	0.011	345.7	0.009	311.1	0.004	16.4	0.000	69.1
K2	0.003	348.2	0.005	259.7	0.001	23.5	0.000	52.2

The model performance is judged by the tidal amplitudes rather than phases. As explained in the model assumptions, amplitudes are important for water exchange between the lakes and the Gulf of Mexico, while phases are not important for the yearly averaged dynamic equilibrium that will be modeled later. Figure 5.17 shows the total water level elevations for the default and calibrated run, compared to the measurements. It can be seen that the calibrated model performs better. Only at New Canal in Lake Pontchartrain the amplitude has increased too much compared to the measurements. As will be demonstrated later this section, the total flux to Lake Pontchartrain shows a very good match to the measured values. Therefore, the increased tidal amplitude at New Canal is accepted.

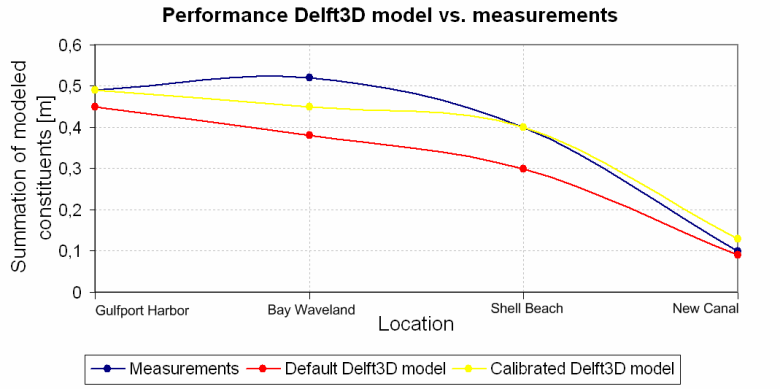

Figure 5.17 Tidal propagation measurements versus Delft3D modeling results

The phases in the calibrated model still lag behind on the measurements. This can be explained by currents or circulations that are not modeled. An example is the absence of wind and wind-driven currents. The restricted representation of wind in the ADH model was considered a restriction for that model study as well. Also, the boundary condition consists of tidal constituents only. There could be large-scale currents near the continental shelf that increase the tidal propagation from the Gulf of Mexico towards Lake Borgne. Taking the nontidal water level elevations into account as forcing at the open boundary was already recommended by Rego et al. (2010) in the H3D study.

Besides wind and currents around the continental shelf, the river discharges might also influence the tidal propagation. This has not been taken into account for modeling tides, it will be added in the next step when modeling salinities.

Figure 5.18 shows the performance of the calibrated model for fluxes in the tidal passes. The flux-ratio between the channels is indicated at the bottom of the figure. Table 5.7 gives the fluxes in the default run and the calibrated run compared to the AECOM measurements.

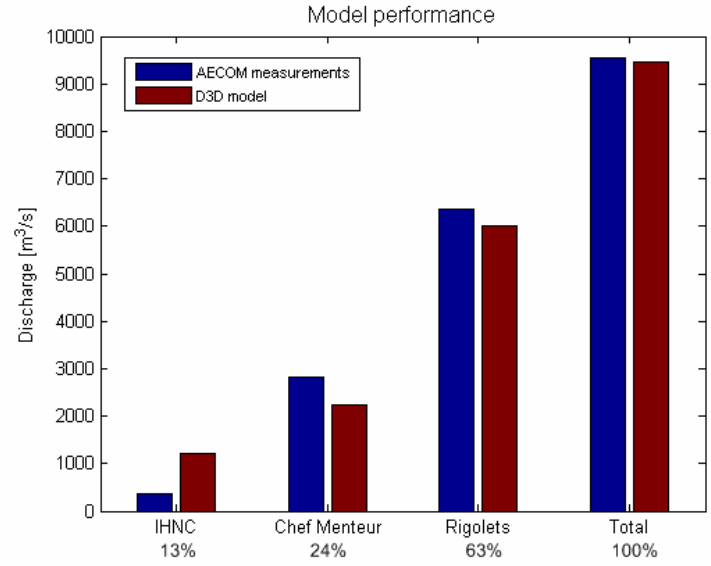

Figure 5.18 Comparison of tidal fluxes in passes (calibrated)

Table 5.7 Tidal fluxes in calibrated model versus AECOM measurements

	Default run [m^3/s]	**Calibrated run [m^3/s]**	**Ratio of calibrated run**	**Calibrated vs. AECOM measurements**
Rigolets	4,299	6,000	63%	+18%
Chef Menteur	1,351	2,250	24%	-21%
IHNC	493	1,200	13%	+239%
TOTAL	**6,144**	**9,450**	**100%**	**-1%**

The ratio between the channels has improved. The flux through the IHNC is much larger than measured, but is close to 10%. The total modeled flux to Lake Pontchartrain is to 1% equal to the measured flux. This means the initial cross-sectional areas of the MRGO and the tidal passes was too small. The combination of cross-section and friction that was used based on the preliminary data-analysis is more representative. The limited cross-sectional area can be explained by the fact that for the MRGO and the tidal passes the post-Katrina configuration was used in the SL15 bathymetry. For the MRGO it was already established that Hurricane Katrina caused shoaling. Shoaling might have occurred in the tidal passes as well. If the surveys were made before the system had restored the old cross-section, the channel configuration does not contain the erosion yet. Therefore, cross-sections might be too small in the bathymetry comparing to the current situation in which the tidal elevation are measured.

5.5 Conclusions

A structured grid was set-up for the Delft3D-FLOW module. The main focus lies on the channels that facilitate the tidal propagation. Each tidal pass is six cells wide. In Lake Borgne and the MRGO the grid resolution is smallest with grid cells 150 meter wide. Towards the boundary the cell size increases to 1500 x 2020 meter. The grid contains 53,000 nodes.

The bathymetry is taken from the ADCIRC SL15 model. The roughness also originates from this model and is expressed in Manning values. The boundary at the Gulf of Mexico contains three points with information of the ten most important tidal constituents from the Topex Poseidon Database. In between the points the information is linearly interpolated.

The model is run for 39 days with a time step of 5 minutes. Most model parameters were left on default values. The amplitudes decrease too fast when propagating through the model. Also the phase lag increases too much compared to measured values. The flux through the tidal passes between Lake Borgne and Lake Pontchartrain is too small.

The roughness is decreased and the cross-sectional areas of the tidal passes and the MRGO are increased. The tidal amplitudes show good comparison with the measured values. Only the phase difference is larger than using the initial bathymetry and roughness. The tidal fluxes show very good comparison to the measurements. Since tidal volumes are more important than phases when studying salinity, the model is considered calibrated on tidal propagation.

With the applied boundary conditions and bathymetry the model is calibrated properly for tidal propagation when using the model for the purpose of modeling a dynamic equilibrium of yearly averaged salinity. Recommendations for further modeling are done in the next section. Before salinity is added to the model, the gathered data that influence the salinity is summed up and analyzed in the next chapter. After that, the model will be used to reproduce the dynamic equilibrium with respect to salinity.

5.6 Recommendations for future model studies

The model is calibrated for tidal elevations, but there are still some improvements that can be made in future modeling. In order to decrease the phase difference between model and measurements, it is necessary to take more processes into account than just tides. Wind and wind-driven currents are currently not modeled, while they might have an impact on tidal propagation. The boundary conditions consist of tidal constituents only. Adding river discharges and large-scale currents along the boundary would allow hydrodynamic model calibration. The necessary increase of cross-sectional area could be explained by possible shoaling of the channels by Hurricane Katrina that was not yet eroded when the bathymetry was surveyed. Therefore it is recommended to perform new surveys of the MRGO, the Rigolets, the Chef Menteur Pass and the IHNC for future model studies.

6 Data analysis for salinity

The Delft3D model is calibrated for tidal water elevations and fluxes. Before modeling the dynamic salinity equilibrium, the data with respect to salinity are treated first. This chapter will deal with all the data and studies that were performed to get better insight in the salinity patterns in the Pontchartrain Basin. The set-up is comparable to Chapter 4. First all gathered data are summed up. The data cover the daily river discharges in the Pontchartrain Basin, the wind intensities and directions, and salinity measurements at several locations in the Pontchartrain Basin. The data of 2008 and 2009 are compared to see if there are any relations. A quick calculation is made to get more insight in the stratification in the Pontchartrain Basin, using the estuarine Richardson number. This chapter will conclude with previous model studies of salinity around the Mississippi Birdfoot and in the Pontchartrain Basin.

6.1 Gathered data

To model the yearly averaged dynamic equilibrium of salinity, yearly averaged discharges will be used. Also the daily average discharge for 2008 and 2009 are given, since these data will be used for the data analysis. Also the wind data are given for 2008 and 2009 to be used in the pre-analysis. This section will conclude with salinity data for 2008 and 2009 at several stations in the model area.

6.1.1 River discharges

In the model several rivers are taken into account. These are the Mississippi River, the Pearl River and several rivers discharging in Lake Pontchartrain and Lake Maurepas. These rivers are the Tchefuncte River, Tangipahoa River, Tickfaw River, and the Amite and Comite River. The rivers that discharge into Lake Borgne and Lake Pontchartrain are shown in Figure 6.1.

Figure 6.1 Rivers discharging in and near Lake Pontchartrain (Google Earth, 2009)

For the calculation of the yearly averaged discharges of rivers in the project area, data of the U.S. Geological Survey (USGS) are used. The stations with the most extensive data sets are often located far upstream of the river mouth. The volume drained downstream of the river gage cannot be ignored in most cases. Roblin (2008) investigated the relationship between the location of the river gages and the discharges per unit area for several tributaries of the Pontchartrain Basin. She found that the discharge per unit area is relatively independent of location along a tributary, see relation (6.1).

$$Q_{down} = \alpha \cdot Q_{up} \tag{6.1}$$

Where
Q_{down} = downstream discharge per unit drainage area [$m^3/s/km^2$]
α = factor calculated by Roblin [-], see Table 6.1
Q_{up} = upstream discharge per unit drainage area [$m^3/s/km^2$]

Table 6.1 Relationship between upstream and downstream discharges (Roblin, 2008)

River	Downstream gage	Upstream gage	α (Roblin)	R^2 Error
Amite	Denham Springs	Darlington	1.0166	0.8978
Tangipahoa	Robert	Osyka	1.0260	0.7893
Bogue Chitto	Bush	Tylertown	1.0468	0.9212
Pearl	Bogalusa	Jackson	1.1119	0.8577
Tickfaw	Holden	Liverpool	0.9165	0.9450
Comite	Comite	Olive Branch	1.0723	0.9383

Also, the discharge per unit area does not vary per tributary according to Roblin, see (6.2). This relationship holds for all tributaries of the Pontchartrain Basin due to the consistency of topography and climate throughout the watershed. However, this formula results in one value for each day. More valuable information is how the discharge varies per day or month.

$$\overline{Q_{river}} = 0.018637 \cdot A_d^{-0.018577} \tag{6.2}$$

where
$\overline{Q_{river}}$ = average long-term daily flow
A_d = total drainage area

Combining both relations found by Roblin makes it possible to calculate the daily averaged discharges for all tributaries using the daily averaged discharge at a certain gage, see relation (6.3). The gage with daily discharge data located furthest downstream will be used.

$$Q_{river,total} = \frac{A_{d,total} \cdot \alpha}{A_{d,gage}} \cdot Q_{river,gage} \tag{6.3}$$

where
$Q_{river,total}$ = total river discharge [m^3/s]
$A_{d,total}$ = total drainage area of the river [m^2]
$A_{d,gage}$ = drainage area of the river until the location of the gage [m^2]
$Q_{river,gage}$ = daily average discharge measured at gage location [m^3/s]

For all rivers in the model domain the yearly averaged discharge has been calculated, see Table 7.2. More information about discharge locations or confluence of tributaries will be treated next.

Table 6.2 Multiplication factors for each tributary in the model area

River	$A_{d,total}$ [km^2]	Location gage	USGS site number	$A_{d,gage}$ [km^2]	α (Roblin)	Multiplication factor [-]	Yearly averaged discharge [m^3/s]
Pearl	20,658	Bogalusa	02489500	17,024	1.1119	1.35	381
Bogue Chitto	3,142	Bush	02492000	3,142	1.0468	1.00	57
Amite	4,597	Denham Springs	07378500	3,315	1.0166	1.41	83
Comite	900	Comite	07378000	736	1.0723	1.31	18
Tangipahoa	2,107	Robert	07375500	1,673	1.0260	1.29	42
Tchefuncte	498	Folsom	07375000	247	1.0000	2.02	9
Tickfaw	1,896	Holden	07376000	640	0.9165	2.72	29

From the figures in this paragraph, it can be concluded that the months July until November are dry months, while March through June form the wet season.

6.1.1.1 *Mississippi River*

The Mississippi River is the largest river in the model area. The Lower Mississippi River, downstream from Cairo, has no locks or dams. Only levees are present, to protect the surrounding areas from flooding, and structures to control the discharge. The Old River Control Structure distributes the water at the divergence of the Mississippi River and the Atchafalaya River at a 70-30 rate.

The Mississippi River flows into the Gulf of Mexico at Southwest Pass, South Pass and Pass a Loutre at an estimated ratio of 30%,10% and 10% respectively (ERDC, 2009). The area where the river branches off into these three passes is called Head of Passes, see Figure 6.2. The remaining 50% of the Mississippi River discharge seeps out through several crevasses upstream of Head of Passes, mostly at the east side of the river. Through each of the crevasses of Baptiste Colette and Grand Pass flows about 10% of the Mississippi River discharge, through Cubits Gap and West Bay each about 5% (ERDC, 2009). The remaining 20% of crevasse flow reaches the Gulf of Mexico west of the river.

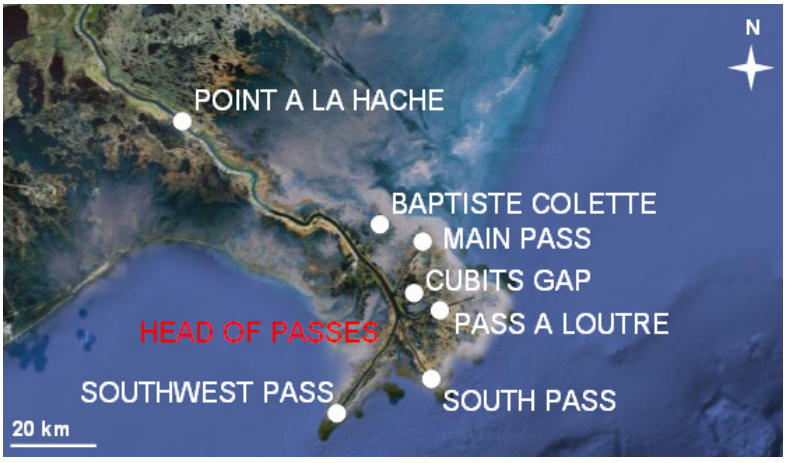

Figure 6.2 Project area

For a representative discharge of the Mississippi River the gage at Baton Rouge, upstream of New Orleans, is used (USGS, station ID 07374000). The data used consists of the mean of daily mean discharges from May 17, 2007 until September 30, 2009. The yearly averaged discharge of the Mississippi River is 15,340 m^3/s. The daily discharge data of 2008 and 2009 are plotted in Figure 6.3. This is the total Mississippi discharge. The yearly averaged flow through each pass is given is Table 6.3.

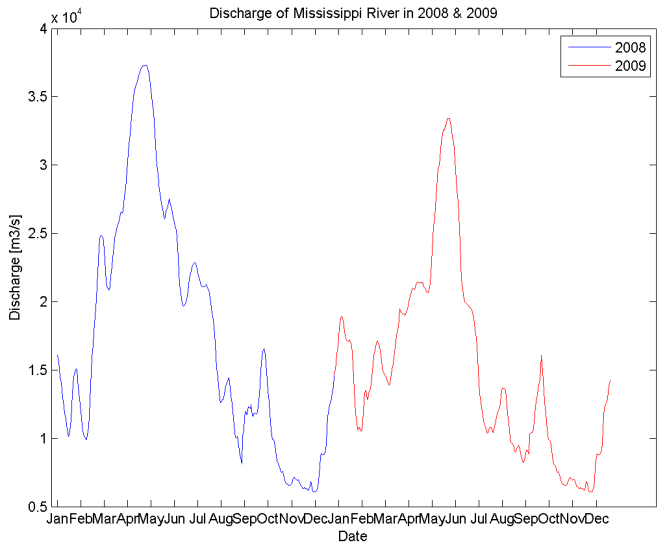

Figure 6.3 Daily discharge of Mississippi River in 2008 and 2009.

Table 6.3 Yearly averaged discharge of Mississippi River for several location at Birdfoot

Location	Yearly averaged flow [m^3/s]	Percentage of total Mississippi flow
Southwest Pass	4,602	30%
South Pass	1,534	10%
Pass a Loutre	1,534	10%
Baptiste Colette	1,534	10%
Grand Pass	1,534	10%
Cubits Gap	767	5%
West Bay	767	5%
Other crevasses	3,068	20%
TOTAL	**15,340**	**100%**

In times of high discharges, the Bonnet Carré Spillway is used to control the water level of the Mississippi River. The Bonnet Carré Spillway is a manmade controllable crevasse with 350 floodgates. It is located approximately 20 km west of New Orleans and drains its water in Lake Pontchartrain. Table 7.4 shows the opening times of the structure.

Table 6.4 Opening of Bonnet Carré Spillway (Sikora and Kjerfve, 1985; Wikipedia, 2010)

Year	Number of days opened	Number of flood gates opened
1937	48	285
1945	57	350
1950	38	350
1973	75	350
1975	13	225
1979	45	350
1983	35	350
1997	31	298
2008	31	160

The last time the floodgates were opened in 2008,see Table 6.5. The average flow was 3,199 m^3/s, the maximum flow 4,531 m^3/s (MVN USACE, 2010).

Table 6.5Number of bays opened at the Bonnet Carré Spillway in 2008

Date	Total number of bays opened
April 11	38
April 12 till 15	84
April 16	90
April 17	110
April 18	135
April 19 till 29	160

6.1.1.2 Pearl River

The Pearl River, see Figure 4.1, is the main contributor of fresh water in Lake Borgne. The Pearl River collects its largest western tributary, the Bogue Chitto River, near the city of Bush (Stewart et al., 2005). The most southern gage with discharge data for the river is upstream of this point, at Bogalusa (USGS, station ID 02489500). The available data run from October 1, 1938 until September 30, 2009. The data at this gage are used to calculate the total Pearl River discharge at the mouth, using the multiplication factor as calculated by Roblin. The yearly averaged discharge for the Pearl River is 381 m^3/s. The discharge of the Bogue Chitto River is added to this. Since the Bogue Chitto flows into the Pearl River close to Bush, it is assumed that the discharge data of the gage at Bush (USGS, station ID 02492000) are equal to the total discharge of the Bogue Chitto River. The multiplication factor is therefore 1.00. The data at Bush run from October 1, 1937 until September 9, 2009. The yearly averaged discharge of the Bogue Chitto River is 57 m^3/s. This means the total yearly average discharge of the Pearl River is 438 m^3/s.

The daily averaged discharge of the Pearl River in 2008 and 2009 is plotted in Figure 6.4. The Pearl River splits into the West and East Pearl River after collecting the Bogue Chitto River, about 80 km above the mouth. The West Pearl River bends towards the Rigolets while the East Pearl River discharges in Lake Borgne. There is no discharge ratio known between the East and West Pearl River.

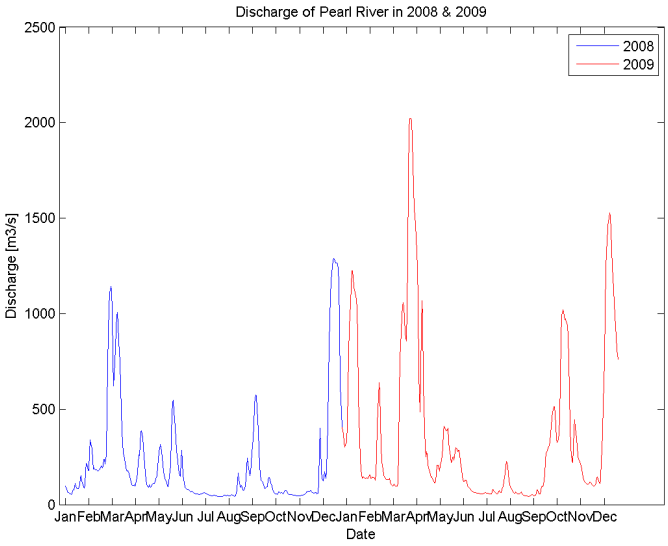

Figure 6.4 Discharge of Pearl River in 2008 and 2009

6.1.1.3 *Rivers discharging into Lake Pontchartrain*

Several rivers discharge into Lake Pontchartrain. The main rivers are the Tangipahoa and the Tchefuncte rivers. The water from rivers discharging into Lake Maurepas reaches Lake Pontchartrain via Pass Manchac. These are the Amite-Comite and the Tickfaw rivers. Another source of fresh water is the drainage system of the City of New Orleans. The drainage system makes up for 4% of the total freshwater input into Lake Pontchartrain (Sikora and Kjerfve, 1985). Since this is such a small portion of the total fresh water, it will not be elaborated further.

Combining the USGS data and Roblin's factor with the total drainage area of the Tangipahoa River (NWMC, 2010), the mean of daily averaged discharge is determined to be 42 m^3/s. The daily discharge data for 2008 and 2009 are plotted in FIGURE. The discharge of the Amite River is plotted in the same figure to show the large resemblance between the two rivers. This confirms the theory of Roblin that the discharge per unit area does not vary per tributary.

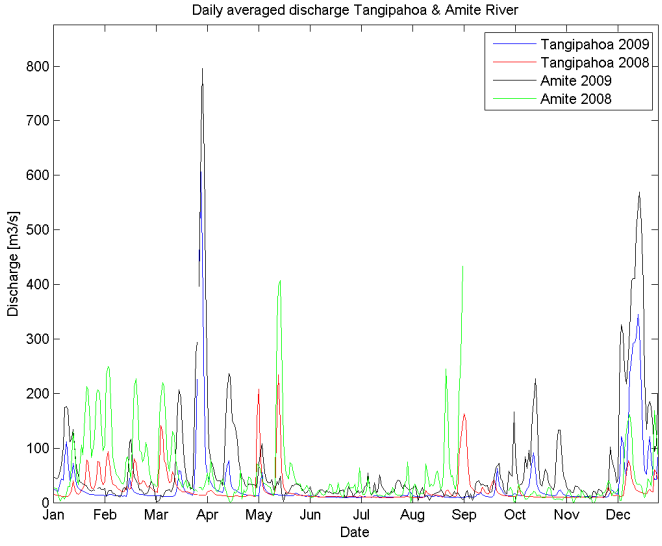

Figure 6.5 Daily averaged discharge of the Amite and Tangipahoa Rivers in 2008 and 2009.

The Tchefuncte River collects the Bogue Falaya River at Covington. Together, the two rivers drain an area of 498 km^2 (US EPA, 2010). Since there is no factor relating up- and downstream discharge calculate by Roblin, α is assumed to be 1.00. This results in a yearly averaged discharge of 9 m^3/s.

Data about the drainage area of the Tickfaw River originates from the American Society of Agricultural and Biological Engineers (ASABE, 2010). The yearly averaged discharge of the Tickfaw River is 29 m^3/s.

Water of the Amite River is partially diverted via the Amite Diversion Canal to the Blind River. The discharge of the Blind River will be included in the Amite River. This means that a gage upstream of the Blind River can be used, at Denham Springs (USGS, station ID 07378500, data range: 1983/09/01-2009/09/30). The yearly averaged discharge of the Amite River is 83 m^3/s. For 2008 and 2009 the daily discharge is plotted in Figure 6.6.

Near Baton Rouge, the Comite River flows into the Amite River. It is however not considered in the discharge of the Amite River at Denham Springs. The total drainage area of both rivers is 5581 km^2 (Goldsteen,1993). The most downstream gage for the Comite River with discharge statistics is near the city of Comite (USGS, station ID 07378000, data range 1944/10/01-2009/09/30). The yearly averaged discharge of the Comite River is 18 m^3/s.

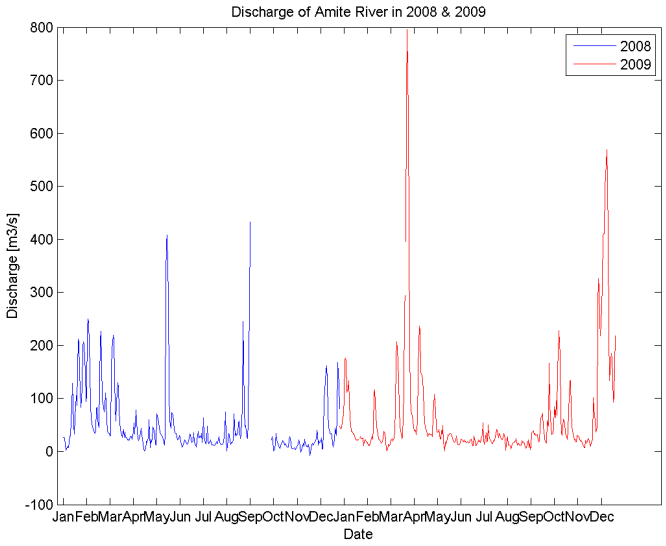

Figure 6.6 Amite River discharge in 2008 and 2009

6.1.2 Wind

Next to tidal flux and river discharges, wind is an important factor in salinities and stratification in the project area. The wind causes a surface current in the same direction. This causes set-up at one side of the lake. In order to compensate for this set-up, water flows in the opposite direction over the bottom of the lake. In the case of a stratified lake, the surface current consists of fresh water, while the bottom current consists of more saline water. This means that the set-up side of the lake becomes fresher, while the side where the wind is blowing from becomes more saline.

Along the Mississippi and Louisiana coastline easterly (northeasterly through southeasterly) winds prevail during autumn, winter and spring. During summer, the wind changes direction to south and southwest. During the winter cold fronts frequently pass by. High- and low-pressure systems pass by from west to east, causing strong winds every 3 to 10 days. After the passage of the cold front, strong north and northeast winds are experienced for several days (Walker et al., 2005). In Appendix B monthly wind roses are plotted for Shell Beach and New Canal for 2009 and part of 2008.

This means that during the summer, with S-SW winds, Lake Pontchartrain will have a lower salinity. Fresher surface water from Lake Borgne is pushed into Lake Pontchartrain towards the North. Over the bottom the more saline water flows towards the South and the tidal passes. During autumn, winter and spring the western side of Lake Pontchartrain and Lake Borgne have lower salinities than the eastern side.

6.1.3 Hurricanes

The modeling of hurricanes is not an easy practice, since a combination of factors determine the storm surges and flow patterns. Factors like wind speed and direction, air pressure and the track of the hurricane all play an important role. In this study it will not be attempted to model hurricanes. However for the analysis of the salinity data, the impact of hurricanes is taken into account. That way a quantitative prediction can be made about the necessity of hurricane modeling for predicting salinities in the Pontchartrain Basin, eventually with the Violet Diversion in place. It is expected that the hurricane surge will cause an increase in salinity due to the supply of saline Gulf water. What the effect on salinities is, and how long the effects will be noticeable, will be assessed in the preliminary data-analysis.

The comparison of data takes place for 2008 and 2009. Therefore only these years will be described in terms of hurricanes.

The year 2008 had an active hurricane season, see Figure 6.7 (left). The two most important hurricanes influencing the salinity in the project area are Gustav and Ike. On August 31, Hurricane Gustav made landfall in Louisiana. Only two weeks later, on September 13, Hurricane Ike made landfall on Galveston Island. The storm surge caused by Ike reached the Louisiana shoreline.

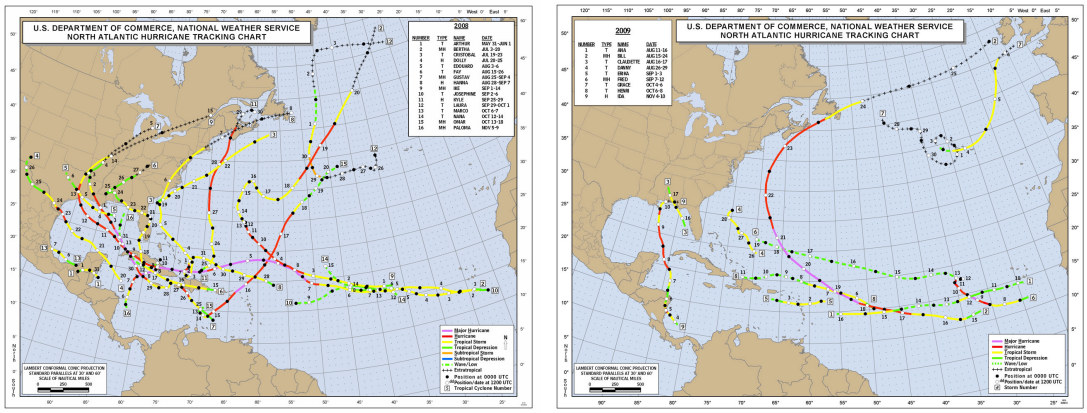

Figure 6.7 Hurricane tracking chart for the North Atlantic, 2008 (left) (NWS NHC, 2010a) and 2009 (right) (NWS NHC, 2010b)

The year 2009 was a calmer year than 2008 in terms of hurricanes and tropical storms in the Gulf of Mexico, see Figure 6.7 (right). In 2009 tropical storm Claudette made landfall in Florida mid August but did probably not have any influence on salinity in the project area. Hurricane Ida weakened into a tropical storm after reaching the Mississippi Birdfoot.

6.1.4 Salinity

The average salinity in Lake Borgne is 7 ppt (parts per thousand). In Lake Pontchartrain, the mean salinity is 1.2 ppt in the west to 5.4 ppt in the east (Sikora and Kjerfve, 1985). The annual variations in salinity can be as high as 8 ppt. The water column is usually well mixed vertically. Weak stratification can occur near the tidal passes.

There are two institutes that have useful long-term records of salinity measurements in the project area. The U.S. Geological Survey (USGS) and the Louisiana Department of Natural Resources (LADNR) have combined efforts to gather and store measurement data in the Coastwide Reference Monitoring System (CRMS, 2010). The following data are extracted from SONRIS (SONRIS, 2010). Figure 6.8 shows the locations of CRMS stations with yellow dots. The red dots are the stations of which data are used in this project. The four digits next to each dot is the respective station number. Table 6.6 contains data about the locations of the CRMS stations and the start and end date of the salinity time series. This table also contains the average salinity over the entire time series.

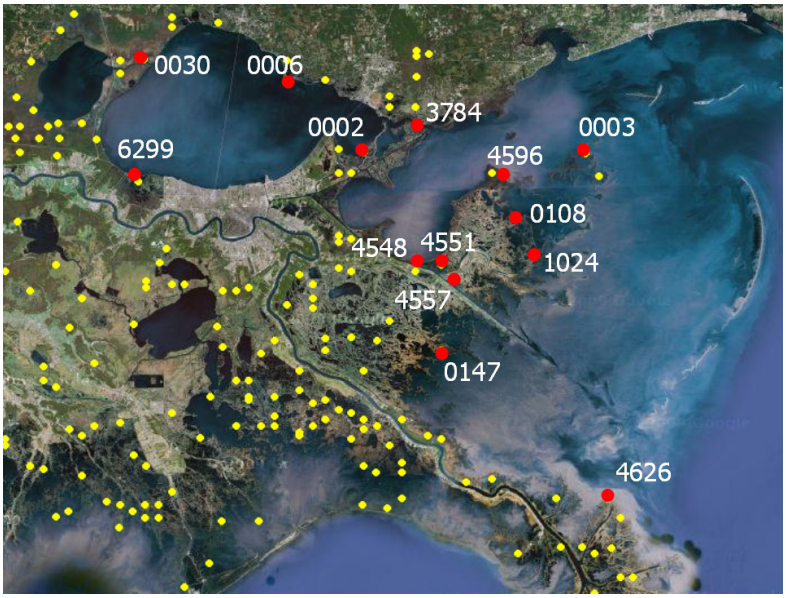

Figure 6.8 Location CRMS stations (CRMS, 2010)

Table 6.6 Start and end date of salinity time series per CRMS station

Station nr	Location	Start date	End date	Yearly average [ppt]
CRMS0002	Chef Menteur Pass	29/09/2007	31/12/2009	6.9
CRMS0003	Biloxi Marsh (eastern tip)	01/11/2007	12/10/2009	19.6
CRMS0006	Lake Pontchartrain (east)	28/09/2007	06/01/2010	4.8
CRMS0030	Pass Manchac	09/05/2007	23/12/2009	3.4
CRMS0108	Biloxi Marsh (inside)	07/12/2007	12/10/2009	13.1
CRMS0147	Breton Sound	08/06/2006	12/05/2009	9.5
CRMS0159	Mississippi River (South Pass)	27/06/2007	18/12/2009	1.3
CRMS1024	Biloxi Marsh (south)	26/03/2008	28/10/2009	16.3
CRMS3784	Along Rigolets	18/01/2008	17/11/2009	6.8
CRMS4548	Shell Beach	23/01/2008	11/12/2009	9.8
CRMS4551	MRGO (north of La Loutre)	23/01/2008	17/12/2009	10.7
CRMS4557	MRGO (south of La Loutre)	23/01/2008	17/12/2009	12.9
CRMS4596	Biloxi Marsh (Lake Borgne)	01/11/2007	12/10/2009	11.3
CRMS4626	Mississippi Birdfoot (east)	26/06/2007	24/11/2009	3.1
CRMS6299	Bonnet Carré Spillway	29/01/2008	14/12/2009	4.3

The average salinity does not give any information about seasonal changes in salinity or the impact of certain wind or discharge events on the salinity. Therefore the daily averaged salinity is plotted for 2008 and 2009. In order to present the data in an organized way, stations are grouped per area. First the salinities in the Biloxi Marsh are given for 2008 and 2009 in Figure 6.9. The salinities for the stations in Lake Borgne are given in Figure 6.10. The 2008 and 2009 daily salinities in Lake Pontchartrain are plotted in Figure 6.11.

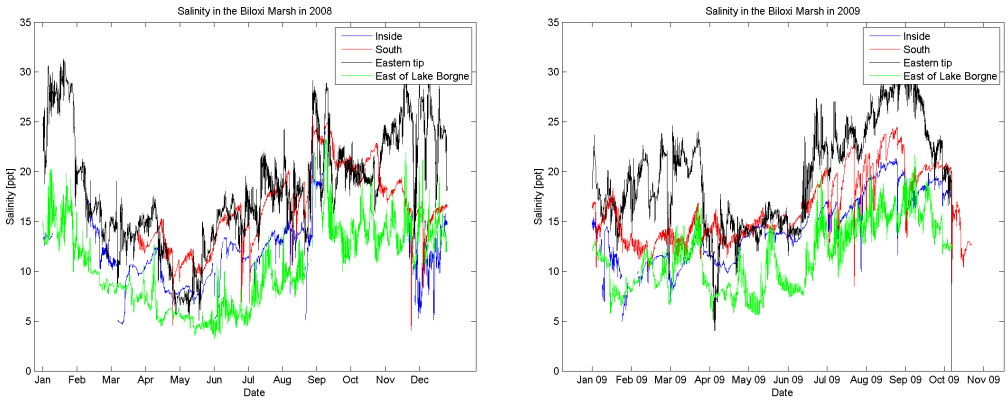

Figure 6.9 Salinity in the Biloxi Marsh in 2008 (left) and 2009 (right)

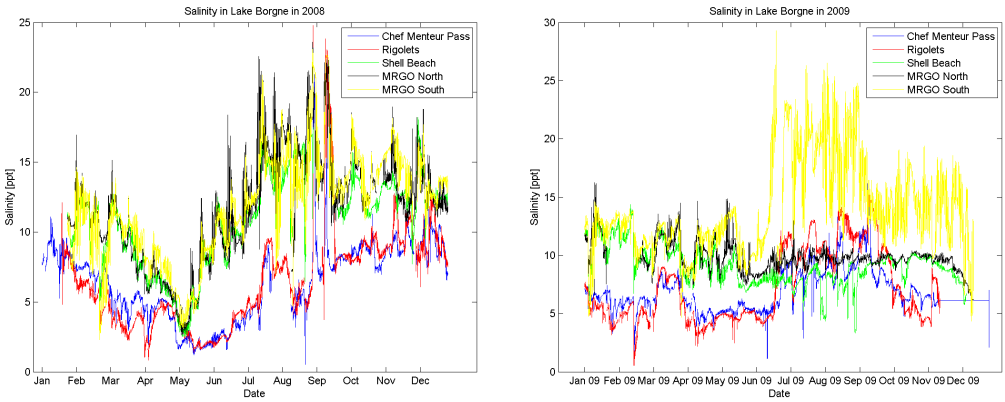

Figure 6.10 Salinity in Lake Borgne in 2008 (left) and 2009 (right)

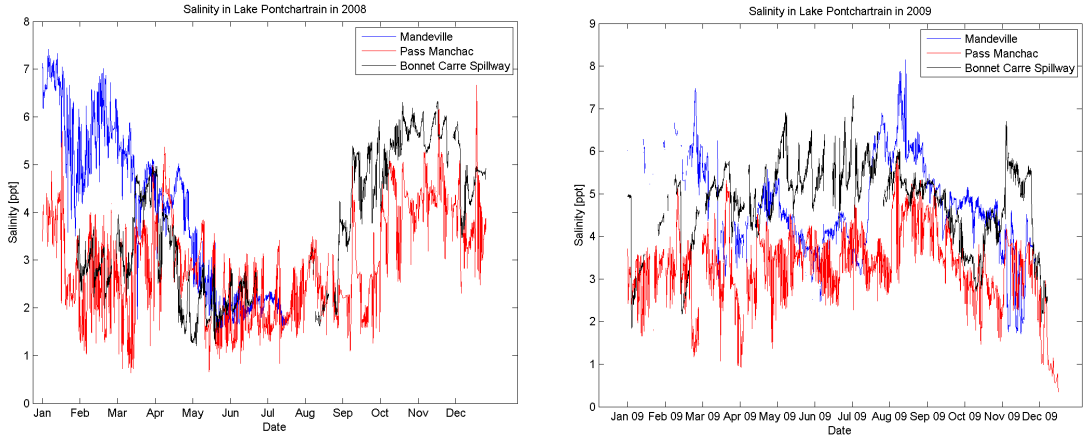

Figure 6.11 Salinity in Lake Pontchartrain in 2008 (left) and 2009 (right)

6.2 Pre-analysis of model data

This section will deal with the gathered data just as was done with the data concerning tidal propagation. The analysis will give an insight in seasonal trends and the impact of extreme events. With estimated flow velocities the estuarine Richardson number will be calculated. This number can give more insight in the stratification in the project area.

6.2.1 Relation between gathered data

This section contains an analysis of salinity data in the project area. The salinity data are compared to discharge data of the most important rivers in the project area which will also be modeled. Wind data are used to get an insight in mixing directions. Wind can increase mixing when pushing fresh water into a more saline environment or the other way around. Occurrence of hurricanes is also considered in the data analyses.

First the stations in Lake Pontchartrain will be analyzed. Per section an area closer to the Gulf of Mexico will be treated. After Lake Pontchartrain the focus will shift towards Lake Borgne and the tidal channels that connect both lakes. The discharge of the Pearl River will be taken into account on this point. The MRGO will also be studied here. The last area is the Biloxi Marsh. The Mississippi River will only be treated here, since the influence is expected to be largest here.

6.2.1.1 Lake Pontchartrain

From Figure 6.12 it can be seen that the seasonal variation in Lake Pontchartrain is hard to distinguish, as salinities are already very low (between 2 and 7 ppt). Around March there seems to be a seasonal low, while at the end of the year the salinity drops again. Using discharge data of the Amite and Tangipahoa River, the salinity data at Mandeville will be analyzed. Then the effects of the opening of the Bonnet Carré Spillway will be analyzed.

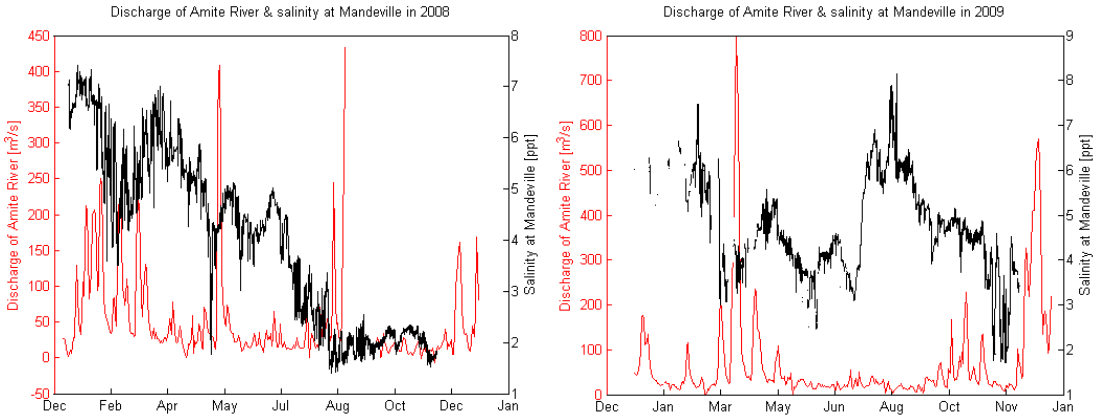

Figure 6.12 Discharge of Amite River versus salinity at Mandeville in 2008 (left) and 2009 (right)

The discharge of the Amite River is taken to be representative for all rivers discharging in Lake Pontchartrain. In the section were the discharge data are collected, it was already established that the Tangipahoa River shows a similar seasonal discharge trend. At the end of January 2008 the discharge of the Amite River increases. The three small peaks can be seen in the decrease of salinity at Mandeville. The salinity series at the Bonnet Carré Spillway starts later but the salinity at this station also seems to react to the discharge peaks in February. Due to the directional spreading of the wind in January, the fresh river water spreads faster to the salinity stations east and south of the river mouths. In April the discharge is minimal in both rivers, explaining the increase in salinity at Mandeville. The discharge peak in May leads to a sudden drop of salinity at Mandeville, but the values recover quickly to a more sensible value for the time of year. Since the direction of the wind changes from SSE to SSW between April and May, the influence of the river discharges on the salinity at Mandeville increases. The salinity was already lower at the Bonnet Carré Station due to the opening of the spillway. Since the data set of the Mandeville station does not contain data from half July on, it cannot be said what the impact of the increased discharge in September is. In 2009, the first distinct decrease in salinity takes place in February, after the discharge peak of the Amite River. In March and April the river discharge peaks. This can also be seen in the salinity at Mandeville. However, as soon as the discharge returns to values below 200 m^3/s, the salinity increases again. This can be explained by the SSE direction of the wind, probably pushing more saline water from the tidal passes towards Mandeville.

A change in wind direction to SSW in May could explain the salinity changes until July. The north/northeastern winds in October and December in combination with the increased discharges explain the lower salinities at these months, as the river water is pushed into Lake Pontchartrain. The effects of the increased discharge in December cannot be checked at Mandeville due to lack of data, but the salinity at the Bonnet Carré and Pass Manchac stations decreases.

The Bonnet Carré Spillway was opened from April 11 until April 29 2008. Halfway April a drop in salinity can be distinguished from over 3 ppt to an average of 2 ppt. After closure of the spillway, the salinity starts to increase again in begin May. It takes a few months, until September, to reach the average salinity of 5 ppt. This is also the average salinity in 2009.

At Mandeville a decrease of salinity is best distinguishable in May 2008. The influence of the opening of the Bonnet Carré Spillway at Mandeville is minimal due to the southeastern wind direction in April. Looking at the Mandeville and Bonnet Carré data of 2009, the seasonal drop in salinity is approximately from May until July. This seasonal change in salinity can also be seen at other stations along the Louisiana coastline, which will be attended to later.

Overall, it can be seen from these data that the lake does not react instantly to a change in fresh water supply. In Chapter 4 it was already established that the estimated flushing time of the lake is 60 days. The disposal of fresh water also depends on the wind direction. For example, the salinity at Pass Manchac is lower than at Mandeville from February until April, coinciding with a SSE wind direction. When the wind turns to a SSW direction from May until July, salinity at Mandeville and Pass Manchac show equal values.

6.2.1.2 Lake Borgne

First the seasonal changes in the tidal passes of the Rigolets and the Chef Menteur Pass will be discussed. The stations in the MRGO and at Shell Beach will be treated as representative for Lake Borgne. After discussing seasonal changes and the impact of the Pearl River, two other distinct features in the salinity data will be explained by hurricanes and closure of the MRGO.

The Rigolets and the Chef Menteur Pass have a comparable salinity. They are likely to be influenced most by the Pearl River discharge. There are no significant fluctuations in Shell Beach or Lake Pontchartrain that precede or follow the fluctuations at the tidal passes, so it is safe to assume that they react simultaneously and neither is to be considered as a forcing of the other. The tidal passes show the same trends as at Shell Beach and in the MRGO, only approximately 5 ppt lower. This is due to the location of the stations. The stations in the tidal passes are located closer to the relatively fresh water (approximately 5 ppt) of Lake Pontchartrain and further away from the saline water (approximately 35 ppt) of the Gulf of Mexico. Due to the equal variation in salinity at Shell Beach, the MRGO and the tidal passes, the seasonal fluctuations at these stations will be treated simultaneously.

The seasonal low in salinity in the tidal passes seems to occur from April until June of July. This is a little earlier than Lake Pontchartrain, which appeared to be May until July (based on 2009 Mandeville data). In the MRGO and at Shell Beach, the low salinities occur from March until June 2008, so a little earlier than in the tidal passes. The fact that the salinity decreases first at Shell Beach, followed by the tidal passes and last in Lake Pontchartrain, could suggest that the Mississippi River discharge is governing in the seasonal changes. The time lag is then explained by residence time of the fresher water into the system of Lake Pontchartrain. This will be discussed later.

The discharge peak of the Pearl River in 2008 is at the beginning of March, which can be recognized in the salinity at Shell Beach, see Figure 6.13. The salinity at the tidal passes seems to decrease earlier. This is explained by the SSE winds in March. The peak at the end of May cannot be seen in the tidal passes, probably since the salinity has already reached a minimum of 2 ppt which is equal to the salinity in Lake Pontchartrain.

In July the salinity increases at the tidal passes but in August the increased Pearl River discharge decreases the salinity again. The discharge peak in September is probably overcome by other factors, like the hurricane season. The 2008 hurricanes and their effects will be treated after the influence of the Pearl River.

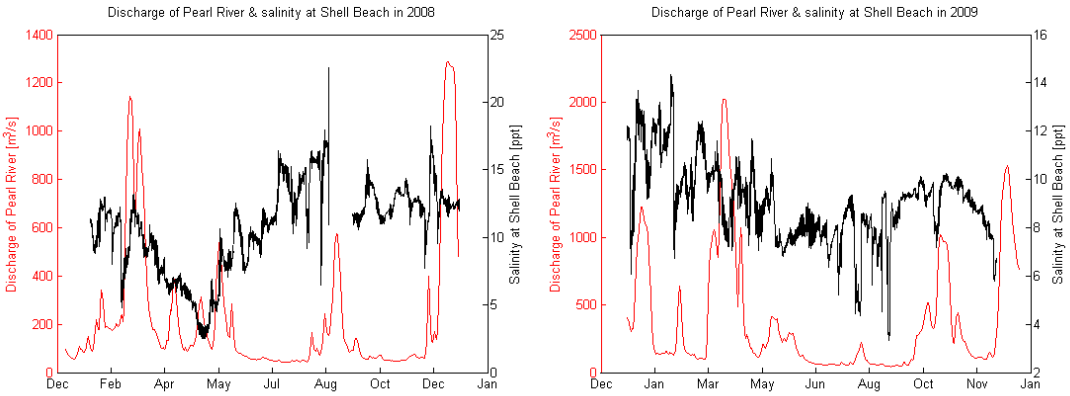

Figure 6.13 Discharge of Pearl River versus salinity at Shell Beach in 2008 (left) and 2009 (right)

The discharge peaks in December 2008 and January and February 2009 probably explain the decreased salinity in the tidal passes in 2009.This does not hold for Shell Beach however. This can be explained by the ESE winds in December 2008. At the end of the year 2009, from October until December, the discharge of the Pearl River increases again. This can be seen in the salinity of the tidal passes. However, a decrease in salinity at Shell Beach is not distinct, which was to be expected with the northeastern wind dominating in November and December 2009.

Another remarkable feature is the increased salinity in March and April in the Rigolets and the Chef Menteur Pass. This increase in salinity can also be distinguished at Shell Beach and the MRGO, however not as clear. The Pearl River has the highest discharge of that year in the same period, and wind from southeastern direction dominates in this period. The increased salinity in the eastern part of Lake Borgne can be explained by the more saline bottom current that counteracts the wind set-up and the west of Lake Borgne.

Leaving the Pearl River discharge and returning to the salinity data of the tidal passes and Shell Beach and the MRGO, there are still two features to be explained. First the two salinity peaks in August and September 2009 in the tidal passes will be addressed. Later it will be explained why the salinity at the MRGO, south of La Loutre, has a significant higher salinity from June 2009 on than the northern side of the MRGO and Shell Beach.

The landfall of Hurricane Gustav in Louisiana explains the first salinity peak at the tidal passes. Only two weeks later, on September 13 hurricane Ike made landfall in Texas. The second peak in salinity in the tidal passes can be contributed to the storm surge caused by Ike. From these salinity data it can be seen that the impact of hurricanes can be significant, increasing the salinity from 7 to approximately 25 ppt. However, it also appears that the influence is only for a very short term, in the order of days after passing of the hurricane. In 2009 tropical storm Claudette did not have any influence on the salinities in mid August. The influence of tropical storm Ida on salinities is hard to estimate, since data from November and December 2009 lack. Looking at the salinity at Shell Beach, it decreases due to the increased discharge of the Pearl River. It can therefore be said that the influence of Ida did not exceed the influence of the Pearl River.

In June the salinity in the southern part of the MRGO increases as it does in 2008. However, the salinity in the northern part and Shell Beach both remain constant to the level in May. This is explained by the construction of the rock closure structure in the MRGO. The salinity station called MRGO South lays southward of this closure, while the MRGO North and Shell Beach are situated north of the closure. There is no supply of more saline water to these latter stations from the MRGO. Therefore the salinity in Lake Borgne decreases, which can be recognized by comparing the salinity at Shell Beach and the tidal passes. The fact that the salinity in the tidal passes is higher than at Shell Beach can be explained by the supply of saline water by tidal motion between the Biloxi Marsh and the Louisiana/Mississippi coastline.

6.2.1.3 Biloxi Marsh

The 2008 salinity in the Biloxi Marsh shows that the salinity is highest at the eastern tip most of the time. The salinity is lowest east of Lake Borgne. This can be explained by the difference in salinity of the water south of the Biloxi Marsh (Chandeleur Sound) and in Lake Borgne. First the stations closest to Lake Borgne (Inside, East of Lake Borgne) will be analyzed to check for comparisons or differences with the previous conclusions. After, the stations closer to Chandeleur Sound (South, Eastern tip) will be analyzed.

Both station follow seasonal trend with a decreased salinity in the months February until September 2008. The fluctuations in the salinity signal are too small to directly link to river discharges. Due to the high residence times in the marshes, the peaks in the salinity will be damped as the fresh water penetrates further into the marshes. However, at the end of August or start of September two salinity peaks are distinguishable. These are caused by hurricanes Gustav and Ike, as discussed before. Looking at the 2009 data, the salinity East of Lake Borgne shows more fluctuations. Inside the Biloxi Marsh the salinity follows the same trend. The seasonal salinity dip occurs from half March until half June. During this period the salinity increases twice, half April and half May. This can be explained by a high discharge from the Mississippi as well as the Pearl River, which decrease the salinity to a very low value. It reaches the lowest value in the area, equal to the salinity in the tidal passes. As soon as the discharge decreases, more saline water mixes and the local salinity gradients become smaller.

At the Eastern tip of the Biloxi Marsh, the salinity seems exceptionally high in January 2008. This can be explained by the lack of northern wind. It can be seen that in 2008 there is no strong dominance of northern winds that push fresher water from Lake Pontchartrain into Lake Borgne. In January 2008 more southern winds occur, which pushes more saline surface water of the Gulf into the project area. From February until June the salinity is lowest. This means the seasonal low in salinity occurs a little earlier (about a month) than the seasonal changes in Lake Borgne. Looking at the discharge of the Mississippi River in 2008, see Figure 6.14, a decrease in salinity in April occurs only shortly after the discharge peak in April. This confirms the idea formulated earlier (for Lake Borgne and the tidal passes) that the Mississippi River is of large influence for the salinity in the project area. It is the same decrease in salinity that was established at Shell Beach and the tidal passes due to the increase in Pearl River discharge. Whether the decrease in salinity is caused by the Pearl River or Mississippi River discharge is hard to say from these data.

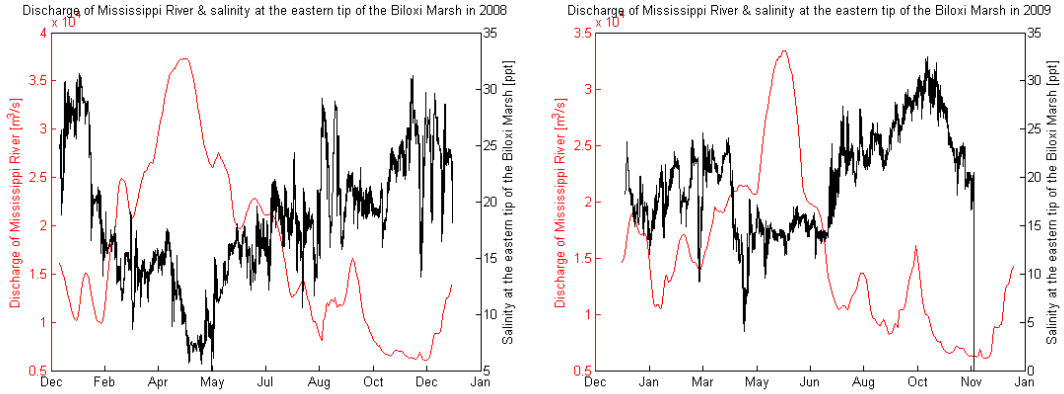

Figure 6.14 Discharge of Mississippi River versus salinity in the eastern tip of the Biloxi Marshes in 2008 (left) and 2009 (right)

In August and September the salinity peaks due to hurricanes Gustav and Ike are present. In 2009, the salinity gradient over the Biloxi Marsh is smaller for the station Inside and South. However, the salinity gradient over the station at Eastern Tip and South of the Biloxi Marsh has increased. During the start of the year, the salinity is low compared to a year before (20 versus 30 ppt). This can be explained by the high Mississippi River discharge in December 2008 and January 2009. In March a similar salinity drop occurs. The salinity drop at the beginning of April is a lot harder to explain. It cannot be confirmed at the other stations. With the wind- and discharge data now available, this sudden drop and recovery of salinity cannot be explained. At all stations the salinity increases towards October, to decrease again towards the end of 2009. This can be explained by increased discharge of the Pearl River. The small increase in Mississippi River discharge probably has a minimal influence due to the northern winds that dominate. This wind however increases the supply of fresh water from Lake Pontchartrain.

The minimum salinity during summer is almost equal at all stations in the Biloxi Marsh. It is caused by the large Mississippi River discharge, which is pushed towards the Biloxi Marsh by the southwestern winds.

6.2.1.4 *Correlation*

In order to quantify the relation between increased discharge and salinity, the correlation (*R*) is calculated, see equation (6.4). The discharge is correlated to the salinity. When shifting the data several days, a better correlation can be reached. This is an indication of the time it takes for the discharge to reach a certain location.

$$R_{x,y} = \frac{\mathrm{cov}(X,Y)}{\sigma_x \cdot \sigma_y} \tag{6.4}$$

$$\mathrm{cov}(X,Y) = \frac{1}{n} \cdot \sum_{i=1}^{n} (x_i - \mu_x) \cdot (y_i - \mu_y) \tag{6.5}$$

where
cov*(X,Y)* = covariance of the datasets, see (6.5)
σ = standard deviation of dataset
n = number of elements in one dataset
μ = mean of dataset

Table 6.7 contains the results for several stations. The initial correlation indicates the correlation when plotting discharge of the Mississippi or Pearl River versus salinity at a station. The next column gives the number of days the discharge series should be shifted in time (delayed) for the best correlation. The best correlation is given in the last column. All values are negative since a high discharge causes a low salinity.

Table 6.7Correlations between the Mississippi and Pearl River discharge and the salinities at several stations

Station	Location	Mississippi River			Pearl River		
		Initial correlation	Days shift	New correlation	Initial correlation	Days shift	New correlation
Mississippi Birdfoot							
0159	MR South Pass	-0.5501	2	-0.5583	-0.0591	24	-0.2804
Lake Borgne							
4548	Shell Beach	-0.7902	0		-0.0291	65	-0.5586
4551	MRGO north	-0.7648	0		-0.0620	53	-0.5159
4557	MRGO south	-0.7576	0		-0.1134	66	-0.5305
Biloxi Marsh							
0003	BM eastern tip	-0.7662	13	-0.8085	-0.0278	23	-0.2966
0108	BM inside	-0.5312	11	-0.5814	-0.0527	16/17	-0.3033
1024	BM inside south	-0.6943	3	-0.6948	-0.4727	19	-0.5251
4596	BM, east of LB	-0.7920	13	-0.8237	0.0247	3	-0.0457
Tidal Passes							
0002	Chef Menteur	-0.7630	29	-0.8516	0.0856	35	-0.2981
3784	Rigolets	-0.6900	16	-0.7218	0.0199	41	-0.3587
Lake Pontchartrain							
0030	Pass Manchac	-0.3027	74	-0.7142	0.0210	15/34	-0.1623
6299	Bonnet Carré	-0.6267	25	-0.7157	0.0174	83	-0.5492

The best correlation between the Mississippi River discharge and the salinity in the Biloxi Marsh is obtained by an approximate 13 days delay in discharge. For Lake Borgne a comparable day shift would be expected, but the best correlation is occurs for zero days delay. The same can be seen in the MRGO. The correlations at these stations are better than those in the Biloxi Marsh. Note that the best correlation for the station at South Pass is reached at a 2-day shift. The number of days to shift the discharge series to obtain the best correlation increases from the Biloxi Marsh through the tidal passes into Lake Pontchartrain. Overall in the area of interest an average correlation of over -0.75 is reached, which increases towards -0.85 when shifting the discharge series.

For the Pearl River it is expected that the shift have to occur for a smaller number of days for Lake Borgne and the Biloxi Marsh since the river mouth is closer. In contrary, this analysis shows that the number of days to shift the discharge series is larger, also the best correlation is significantly lower than for the Mississippi River. The discharge of the Pearl River seems to reach the Biloxi Marsh faster then Lake Borgne.

6.2.1.5 Conclusions

At all the areas, Lake Pontchartrain, Lake Borgne and the Biloxi Marsh, the rivers have a significant influence on the salinities. Discharge peaks lead to lower salinities, sometimes with a delay of a few days. The magnitude of the influence of the rivers depends on the wind direction.

The wind can push the fresh water towards a salinity station which results in a smaller response time and lower salinities. Also the other way around; when the wind is directed from the station towards the river mouth, the salinity decreases less.

The seasonal decrease in salinity seems to be from February to June in the Biloxi March. In Lake Borgne this seems to be from March till June. The delay of a month could be explained by the time it takes for the fresh water of the Mississippi River to reach Lake Borgne after it has reached the Biloxi Marsh. The seasonal low in salinity in Lake Pontchartrain seems to be from May till July. This supports the theory that the Mississippi River has a large influence on salinities in the Pontchartrain Basin.

The effects of the opening of the Bonnet Carré Spillway in 2008 can be seen in the salinities in Lake Pontchartrain. Hurricanes that cause a storm surge in the Pontchartrain Basin cause a sudden increase in salinity to a value of approximately 25 ppt, but this increase is of a short duration. The storm surge imports saline water into Lake Borgne, but the water levels falls after such a short time period that no mixing has occurred.

The stations in the MRGO and at Shell Beach respond to the closure of the MRGO. The stations north of the closure show lower salinities compared to the same period the year before and compared to the station south of the closure. Due to the closure, there is no more tidal propagation through the MRGO.

A correlation analysis between Mississippi and Pearl River discharge and salinity shows that at all location the correlation with the Mississippi River is best. The Mississippi River discharge seems to reach Lake Borgne within a day, while it takes 13 days to affect the salinities in the Biloxi Marsh. Since the Pearl River mouth is closer to Lake Borgne and the Biloxi Marsh, better correlations and shifting over shorter periods are expected. However both expectations seem to be false.

6.2.2 Stratification

The estuarine Richardson number ($R_{i,E}$) gives an impression of the type of stratification in an estuary. It is the ratio of the energy it takes to mix the discharge with the tidal currents to the potential energy of the tidal motion, see (6.6) (Kranenburg, 1998).

$$R_{i_E} = \frac{\Delta\rho \cdot g \cdot d \cdot Q_r}{\rho \cdot A \cdot u_T^3} \tag{6.6}$$

where
$\Delta\rho$ = water density difference between lake and river [kg/m^3]
g = gravitational acceleration [m/s^2]
d = water depth in estuary [m]
Q_r = river discharge [m^3/s]
ρ = water density in estuary [kg/m^3]
A = cross-section of river mouth [m^2]
u_T = rms-value of the flow velocity in the river mouth due to the tidal motion [m/s]

A low value for the estuarine Richardson number is associated with a well-mixed estuary, while a large value indicates horizontal stratification. Exact numbers are not known, since it differs per situation. A good estimate for the interval for the transition from well-mixed to stratified is given in (6.7).

$$0.08 < R_{i_E} < 0.8 \tag{6.7}$$

For the estuarine Richardson number of Lake Borgne, only the Pearl River flow is taken into account since it is the nearest river mouth. The area is the width of the lake multiplied by the depth. Lake Pontchartrain can be better schematized as a lake rather than an estuary. But in order to get some insight in the possibility of horizontal stratification in the Delft3D model, the same formula is used. For Lake Pontchartrain all river discharges are taken into account. Since there has been no model effort yet, the flow velocities need to be estimated. The estimated values can be found in Table 6.8 for Lake Borgne as well as Lake Pontchartrain. These are based on realistic tidal flow velocities. The channels connecting both lakes have been analyzed as well. Just as Lake Pontchartrain these are not estuaries, but it is interesting to get some insight in the stratification parameter. The cross-sectional area of the channels is used, with the tidal flux as discharge. The density difference between the lakes indicates the energy necessary for mixing. The velocities estimates are equal to those of the lakes.

Table 6.8 Parameter values for the calculation of the estuarine Richardson number

Parameter	Unit	Lake Borgne	Rigolets	Chef Menteur	IHNC	Lake Pontchartrain
$\Delta\rho$	[kg/m^3]	13	13	13	13	7
d	[m]	3.0	13.0	13.0	8.0	3.7
Q_r	[m^3/s]	438 (Pearl River)	6,000	2,250	1,200	181
ρ	[kg/m^3]	20	7	7	7	7
A ($b*d$)	[m^2]	90,000	10,200	2,260	1,070	117,000
u_T	[m/s]	0.5 – 1.0	0.5-1.0	0.5 – 1.0	0.5 – 1.0	0.5 – 1.0
$R_{i,E}$	**[-]**	**0.74 – 0.09**	**85.7 – 10.7**	**145.7 – 18.2**	**163.5 – 20.4**	**0.36 – 0.05**

In both lakes the estuarine Richardson numbers are in the transition zone between well mixed and stratified. As the velocities decrease, the stratification increases. In the channels the column is horizontally stratified. As the formula holds for estuaries and not for a situation like the tidal channels, it is not certain that stratification will occur. However this analysis indicates that horizontal stratification might occur in the channels in the Delft3D model.

6.3 Previous model studies

Two studies focused on the effects of discharge and wind on the Mississippi River plume. The first study of Walker et al. (2005) uses satellite images, while the second study of Rego et al. (2010) uses the numerical model H3D to study the plume. The last study discussed here is the FVCOM model study of the Pontchartrain Basin. The performance of the FVCOM model on tidal propagation was discussed previously; here the performance on salinity will be treated.

6.3.1 Structure of the Mississippi River plume

The study by Walker et al. is not as much a modeling study as a data analysis. It will be discussed here since it will help gain more insight in the circulation around the Mississippi Birdfoot and can explain the results of the analysis of salinity data of the previous chapter.

Walker used satellite images of sea surface temperature around the Mississippi Birdfoot to study the flow patterns. However, surface temperatures are near isothermal in the summer months. That makes it hard to distinguish significant flow patterns. Therefore, Walker used the reflecting properties of sediment and chlorophyll concentrations to study the Mississippi plume during those months. Walker tried to explain the plume by discharge data, wind stresses and slope eddies.

The total Mississippi River discharge directly influences the size of the plume. During the months March, April and May, when the discharge is highest, the surface plume is largest. During the months August, September and October the Mississippi discharge is at its lowest. The plume is therefore smallest.

The plume extends farther west than east. This is due to the large discharge of Southwest Pass. The dominating easterly winds only enhance this pattern. Prevailing winds from southeast direction push the water towards the west. However, the water that flows out at the eastern side does not pass the Birdfoot but gets pushed into the southern areas of Breton and Chandeleur Sound. This in contrary to what happens during northeasterly winds.

As said before, northeasterly winds are associated with the passage of a cold front. It pushes the fresh water south around the Birdfoot to the west, in the direction of the Atchafalaya Bay. After approximately 4 days the winds return to their typical eastern direction.

During the summer winds from the south and southwest prevail. The plume gets pushed northward. Some discharge from Southwest Pass reaches the eastern side of the Birdfoot. Fresh water from Main Pass and other channels at the east side penetrates far into Breton and Chandeleur Sound. This flow pattern persists typically for 4 to 6 weeks.

There is another factor, besides discharge volumes and seasonal prevailing winds, to determine the orientation of the Mississippi River plume. South of the Mississippi River delta, large eddies occur due to large-scale wind circulations, also known as (anti)cyclones. If the river flow is directed in eastward direction, it reaches the continental shelf relatively fast. When such a slope eddy is present, the fresh water flows far into the Gulf due to the strong current, see Figure 6.15. Northward intrusion of the Loop Current towards the delta can have the same effect. First, the water is pushed eastwards, after it is transported southwards.

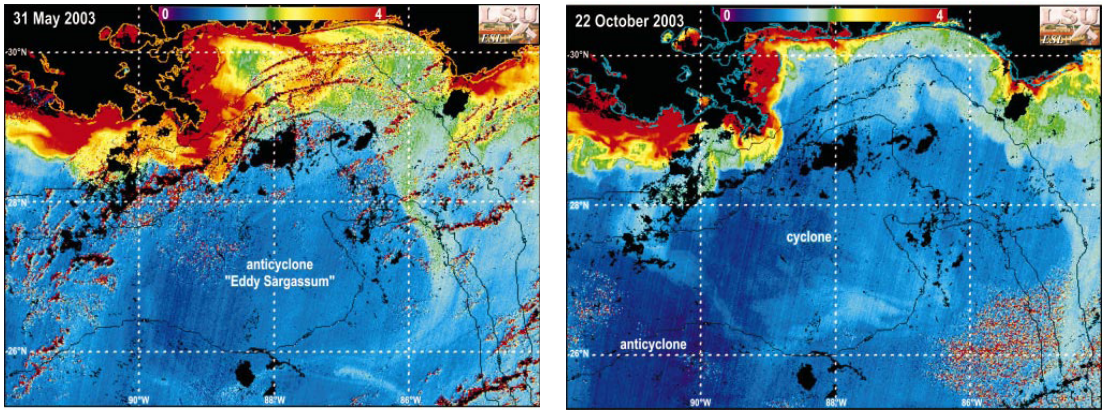

Figure 6.15 The anticyclone (left) transports the chlorophyll a eastward, while the cyclone (right) causes a westward direction (Walker et al., 2005)

The frequency of occurrence of slope eddies and intrusion of the Loop Current is important to estimate the southward transport of fresh water and residence times on the continental shelf. However, for this study these events might not be of large influence since salinities monthly averaged.

6.3.2 Modeling of Mississippi River diversion regimes

The study by Rego et al. (2010) was already treated in Section 4.3.5. After calibration on tidal propagation, the model was calibrated for sediment transport based on satellite observations of the river plume. By adjusting the vertical diffusivity-to-viscosity ratio, the model was calibrated qualitatively for vertical mixing. The satellite images, integrated over the top 2 meter, were used for the model validation.

After the model was calibrated, the passage of cold fronts was modeled. In the winter the prevailing winds are north-northeast. The Mississippi River plume is blown southwest ward into the Gulf. During the passage of the cold front, which takes about 4 days, the winds rotate clockwise. Thereby the plum gets pushed northwards and reattaches to the coast approximately near the mouth of the Atchafalaya River. After the cold front has passed, the winds turn north-northeast again and the plume retreats.

The last goal of the study was to simulate several diversion locations to study their impact. In the five scenarios developed, the total Mississippi River discharge was diverted eastward, westward or both with different ratios. Also a scenario was run with the total Mississippi River discharge at the Atchafalaya Bay. The latter scenario was the only one were the conservation of sediment was worse than the current situation. The best scenario in terms of sediment conservation was to divert 70% of the Mississippi discharge to the west and 30% to the east. Both sides of the delta will be protected. However, when a project focuses only on either side of the delta, this might not be the preferred scenario. Figure 6.16 shows the deposited sediment thickness under the 70-30 diversion regime. The location of the diversion is indicated with the white dot, located approximately halfway between Venice and Port Sulphur.

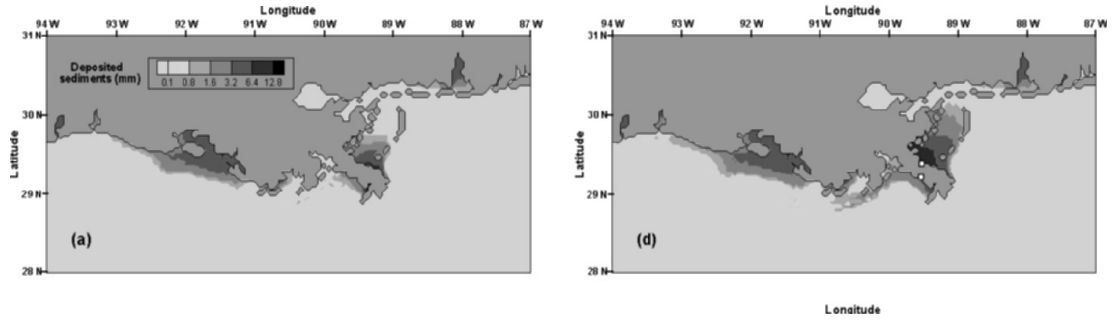

Figure 6.16 Deposited sediment thickness converted to yearly rates under existing conditions (left) and a 70-30 (west – east) diversion ratio (right) (Rego et al., 2010)

Two limitations of the modeling process are described to be a lack of data and exclusion of certain sediment processes. A lack of suspended sediment data and shelf current observations prevents a more qualitative calibration. Sediment processes that are not taken into account are sediment re-suspension and the cohesive nature of the Mississippi River sediment. It is said however that the absence of the slope eddies and the Loop Current is no limitation to the model application, since the area of interest focuses on the continental shelf.

6.3.3 Modeling of Violet Diversion scenarios with FVCOM

The FVCOM model (Georgiou et al., 2007) was already discussed in Section 4.3.2. For reaching a dynamic equilibrium initial salinities were used, see Figure 6.17. These values were based on measurements from 1997 until 2002. Using tidal forcing and river discharges averaged for the month March, a yearly averaged situation was generated. This leads to a dynamic equilibrium near river mouths. The model has not been calibrated for salinities, only for tidal elevations and fluxes.

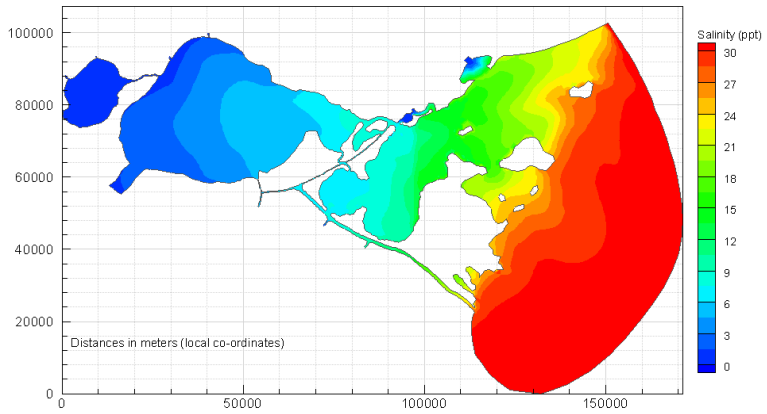

Figure 6.17 Initial salinity for the FVCOM model, based on yearly averaged salinities (Georgiou et al., 2007)

Four diversion scenarios were modeled: the baseline condition and constant flows of 142, 283 and 425 m^3/s (5,000, 10,000 and 15,0000 cfs respectively). The baseline condition was actually split up in two cases: the MRGO in pre-summer 2009 condition (open) and 90% constricted after completion of the closure structure.

First the response time of the system was determined, see Table 6.9. This is based on the first period of the diversion. Once the salinity has decreased in Lake Borgne, the gradients become smaller and response times will decrease.

Table 6.9 Response time of Lake Borgne for several diversion scenarios

Diversion flow [cfs]	Diversion flow [m^3/s]	Time it would take to fill Lake Borgne [months]
5,000	142	16
10,000	283	2
15,000	425	1.3

Using a constant flow of 10,000 or 15,00 cfs, the Chatry target salinities could be met within two months. The response time of the Biloxi Marsh is smaller than determined; after one month salinity is decreased is the entire Marsh. The discharge of the Pearl River helps to keep the saline Gulf water out and therefore enhances the effect of the diversion, see Figure 6.18.

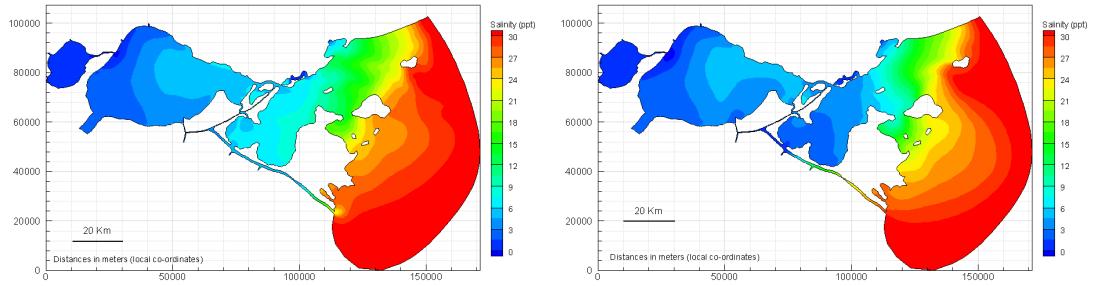

Figure 6.18 Salinities in Pontchartrain Basin calculated with FVCOM in baseline condition (left) and with 10,000 cfs diversion scenario at Violet (right) (Georgiou et al., 2007)

The second series of simulations were performed for an annual period of diversion. Firstly, the baseline condition with closure of the MRGO, but no diversion discharge results in a salinity decrease of 20% in one year in Lake Borgne, the Biloxi Marsh and the eastern part of Lake Pontchartrain, see Figure 6.19. The second scenario contains a peak diversion flow of 5,000 cfs (142 m^3/s) during March and April and a minimum flow of 2,000 cfs (57 m^3/s) during the other months. The closure of the MRGO is implemented for this as well as the other annual diversion scenario. The average salinities decrease only slightly compared to the constricted MRGO without diversion. This is explained by the low diversion flow in all months but March and April. The third scenario contains a peak diversion flow of 15,000 cfs (425 m^3/s) during March and April and 650 cfs (18 m^3/s) during the other months. This leads to a significant reduction of salinities in Lake Borgne and eastern Lake Pontchartrain, see Figure 6.20.

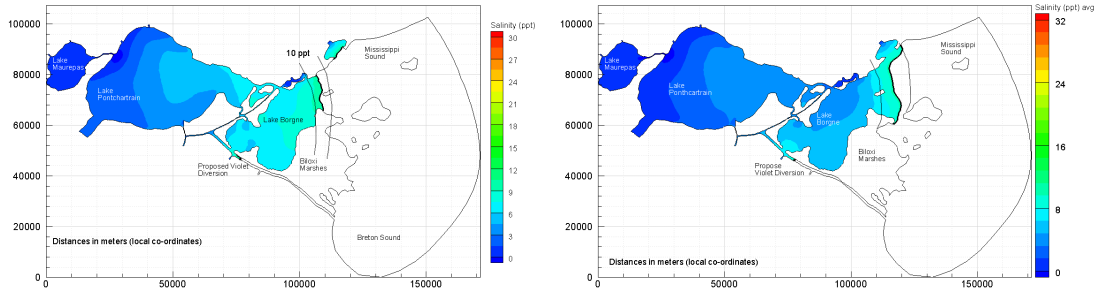

Figure 6.19 Surface salinities in Lake Borgne and Lake Pontchartrain after a simulation of a year with open MRGO (left) and with completed MRGO closure structure (right) (Georgiou et al., 2007)

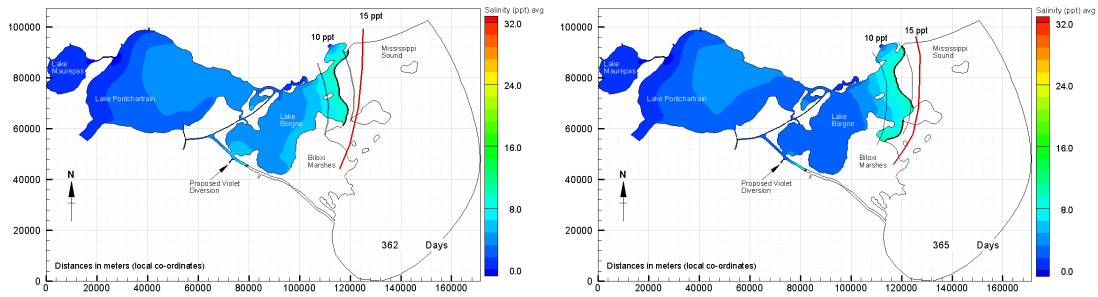

Figure 6.20 Surface salinities in Lakes Borgne and Lake Pontchartrain after a simulation of a year for the annual 5,000 cfs scenario (left) and annual 15,000 cfs scenario (right) (Georgiou et al., 2007)

Salinity plots in the report are surface salinities in order to give a good indication of the advancement of fresh water into the model area and the salinities in shallow waters. The model indicated that the water column is well mixed in Lake Borgne, the Biloxi Marsh and eastern Lake Pontchartrain.

Two main restrictions of this study are given. Firstly the study did not look into the feasibility of the diversion flows, which depends on the available head of the Mississippi River. Secondly, the Central Wetlands Area (CWA) was not represented in the model. The diverted flow was introduced into the model domain at the Bayou Dupre gate.

6.3.4 Conclusions

The size and orientation of the Mississippi River plume is largely determined by the river discharge and wind directions. The large discharge at Southwest Pass orientates the plume westward, which is enhanced by the (south)eastern winds. During the passage of a cold front the Mississippi discharge gets pushed into the southern areas of Breton and Chandeleur Sound. Large scale eddies occur near the continental shelf due to wind circulations. The eddies take the fresh water into the Gulf. The Loop Current has the same effect.

The FVCOM model was not calibrated for salinities, only for tidal water levels and fluxes. The model was used to model several scenarios for the Violet Diversion. The closure of the MRGO alone results in 20% lower salinities in Lake Borgne, the Biloxi Marsh and eastern Lake Pontchartrain. With a constant flow of 10,000 or 15,000 cfs (283 respectively 425 m^3/s) the Chatry salinity targets are met within two months. The Pearl River has a positive effect on salinities by keeping the saline Gulf water out of Lake Borgne. A diversion with 15,000 cfs (425 m^3/s) during March and April and 650 cfs (18 m^3/s) during the other months leads to a significant reduction of salinities in Lake Borgne and eastern Lake Pontchartrain.

6.4 Recommendations for Delft3D modeling

The large influence of the wind on salinities in the Pontchartrain Basin was proven both by the preliminary data-analysis as by previous model studies. The wind causes a circulation in stratified area. The fresh water at the top of the water column is pushed by the wind in the same direction, while the more saline at the bottom flows in opposite direction. The wind was not taken into account for the tidal propagation and it was already concluded that this was one of the limitation of the calibration process. Therefore a salinity simulation will be performed with wind. This might give a qualitative indication of the error caused by neglecting wind effects.

Under the effects of wind, the correlation between salinity and river discharges was determined. The influence of the Mississippi River was larger than that of the Pearl River at all locations. The Mississippi River discharge seems to reach Lake Borgne within a day, while it takes 13 days to affect the salinities in the Biloxi Marsh. With a flushing time of 60 days for Lake Pontchartrain, the Delft3D model should be close to dynamic equilibrium within two or three months. All these time scales are determined with variable discharges, while this study will only focus on yearly averaged discharges.

The Loop Current, (anti)cyclonic eddies and other nontidal water level elevations are not negligible when modeling tides in around the Mississippi Birdfoot. It was already concluded that the Delft3D model performance on tidal propagation was not as desired, probably by not taking these currents into account. Salinities in the Delft3D model might be underestimated due to the absence of these currents in the boundary conditions.

At the same time, water of the Mississippi River that is not drained at the east side of the river (within the model domain) will not reach the model area. In reality it might flow into Chandeleur Sound under the influence of (wind-driven) currents. This could result in overestimation of salinities. The influence of the boundary on salinities in the area of interest (Lake Borgne and the Biloxi Marsh) should be investigated.

From the modeling of Violet Diversion scenarios with the FVCOM model, it appeared that the closure of the MRGO decreased salinities in Lake Borgne and the Biloxi Marsh. This is supported by the results of the preliminary data-analysis, that showed that the salinities in the northern part of the MRGO remained at the low summer salinities after the closure was completed. The salinities south of the closure did rise due to decreased Mississippi River discharge. As the MRGO closure is completed and irreversible, this should be modeled first. The relative impact of the Violet Diversion can then be compared to the present situation with the closure in place. Otherwise, comparing the Violet Diversion with the MRGO closure to pre-closure results, the relative impact of the Diversion would be overestimated.

7 Model validation for salinity

This section will deal with the model performance on salinity modeling. Starting point is the Delft3D-FLOW model that has been calibrated for tidal propagation earlier in this study. First the input data with respect to river discharges and salinities are elaborated, using the gathered data of the previous section. Then the results of the 2D and 3D model will be analyzed, keeping in mind the results of the data-analysis. The next step is a tracer analysis to get more insight in the contributions of every source on several locations. These results will be compared to the results of the previous model studies to see if the hydrodynamics are well represented in the Delft3D model. The closure of the MRGO and a scenario for the Violet Diversion are simulated. Relative changes due to the diversion are explained and interpreted to give a preliminary advice about the impact of the diversion.

7.1 Hydrodynamics and salinity

The calibrated hydrodynamic model is expanded with salinity. The set-up and performance of the salinity model is explained in this section. The model is set up in such a way that a dynamic equilibrium will be reached. This means that salinity reaches an equilibrium based on yearly averaged discharges, but tide-driven currents shift the equilibrium back and forth over a tidal cycle. When the dynamic equilibrium is reached, the results can be compared to yearly averaged salinities in the project area as presented in Section 6.1.4. With the dynamic equilibrium, seasonal changes in salinity will not be modeled.

7.1.1 Model set up

For the simulation of salinity, the same hydrodynamic model is used as for the tidal calibration. In the FLOW-module of Delft3D the user can tick off processes and constituents. When modeling salinity, the concentration will be taken into account as well as the influence of salinity on density (Deltares, 2009a). Salinity can affect the density which can cause gradients in density in horizontal or vertical direction. Due to these gradients, density driven currents can occur. These currents can be taken into account in the FLOW-module. In depth-averaged modeling the vertical density gradients are not taken into account. This could lead to bad model results when in reality stratification occurs, like in the tidal passes. Using multiple layers in the vertical could then lead to better results.

The boundary condition for tidal constituents is the same as in the calibrated model. A uniform salinity of 25 ppt is assigned to the tidal flow entering the model area, which is a representative value of the salinity in the Gulf of Mexico near the Louisiana coast.

There are seven rivers discharging into the model area. For all rivers the yearly averaged discharge is used in order to model the dynamic equilibrium. Table 8.1 shows the yearly averaged discharge per source in the model. The salinity of all river discharges is 0 ppt.

Table 7.1 River discharges (yearly averaged) into model domain

River	Location	Yearly averaged discharge [m^3/s]
Mississippi River	Cubits Gap / Grand Pass	2301
	Baptiste Colette	1534
	Pass a Loutre	1534
Pearl River	East	190
	West	190
Tchefuncte River		9
Tangipahoa River		42
Amite, Comite & Tickfaw Rivers	Pass Manchac	130

The discharge of the Mississippi River is divided over several passes and crevasses. The crevasses of Cubits Gap, Grand Pass and Baptiste Colette discharge into the model area. At Head of Passes, discharge from Pass a Loutre is taken up in the model. The discharge per location was already established in Section 6.1.1. In total 35% of the Mississippi discharge enters the model, in agreement with the measurements of ERDC (2009). The remaining 65% flows out at the western side of the Mississippi River, outside the model area, and will therefore not be taken into account.

The bathymetry of the Pearl River is poorly represented in the model due to grid resolution and orientation. Therefore, the East and West Pearl river will be included in the model separately at each respective mouth in stead of one representative discharge further upstream. A ratio of 50-50 will be assumed between the East and West Pearl River.

The Tickfaw, Comite and the Amite River are added up and enter the project area at Pass Manchac, since Lake Maurepas is not represented in the model.

A non-uniform initial salinity is imposed to reduce the spin-up time, see Figure 7.1. The values are based on yearly averaged salinities, as reported in Section 6.1.4.

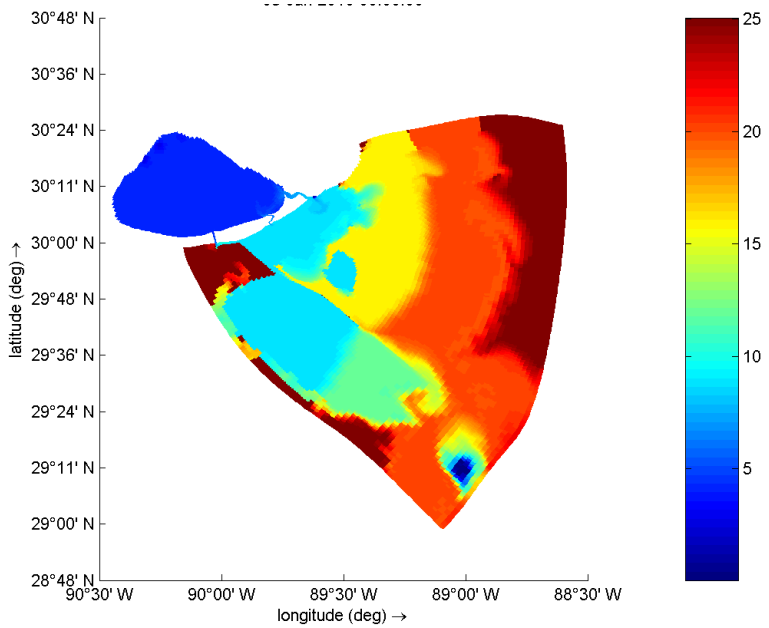

Figure 7.1 Initial salinity (parts per thousand) in model based on measurements

7.1.2 Performance FLOW-module

The first salinity simulation was performed with the discharges and the initial salinity added to the model calibrated on tides. In the entire model area salinities were too low compared to measurements. Therefore the grid was refined by a factor two. This did not have any effect on model results except for the increased detail in the Biloxi Marsh and at Bayou Bienvenue. Next, the eddy diffusivity was changed from 10 m^2/s to 1 m^2/s. This also did not lead to better results with respect to salinity. The same holds for a smaller time step. Since all these changes did not result in better model performance, it will not be treated in more detail.

The model calibration on tidal propagation was performed using a depth-averaged model. In order to simulate in three dimensions, 10 σ-layers were used. The difference between these two models is treated first. Next, the high gradient that occurs near the Mississippi River discharge is handled by introducing a salinity gradient over the boundary. In the previous section it was established that wind has a large influence on the orientation of the Mississippi River plume. Therefore a run was performed with ESE wind. All changes and their effects are summed up in Table 7.2.

Table 7.2 Alterations in Delft3D salinity model and their effects

Alteration in model	Results	More information
Grid refinement by factor 2	Negligible	-
Eddy diffusivity from 10 to 1 m^2/s	Negligible	-
Decrease time step by factor 2	Negligible	-
2D to 3D (10 σ-layers)	More salt water intrusion	Section 7.1.2.1
Salinity gradient over boundary	Density driven currents	Section 7.1.2.2
Wind (ESE)	Faster tidal penetration into Lake Borgne	Section 7.1.2.3

7.1.2.1 2D versus 3D modeling

The model was first run depth-averaged, with the same setting as were used in the calibration process. The only difference is that the Biloxi Marsh has not been lowered in these simulations. The Mississippi discharge was introduced into the model at a single location, at Pass a Loutre. The same run was performed with 10 σ-layers in the vertical. All layers covered 10% of the total water depth. The boundary condition for tides remained the same as in the 2D simulation. Over the entire depth a salinity of 25 ppt was assigned. For the 3D turbulence the k-Epsilon model was chosen (default setting). The results after two months of simulation are given in Figure 7.2.

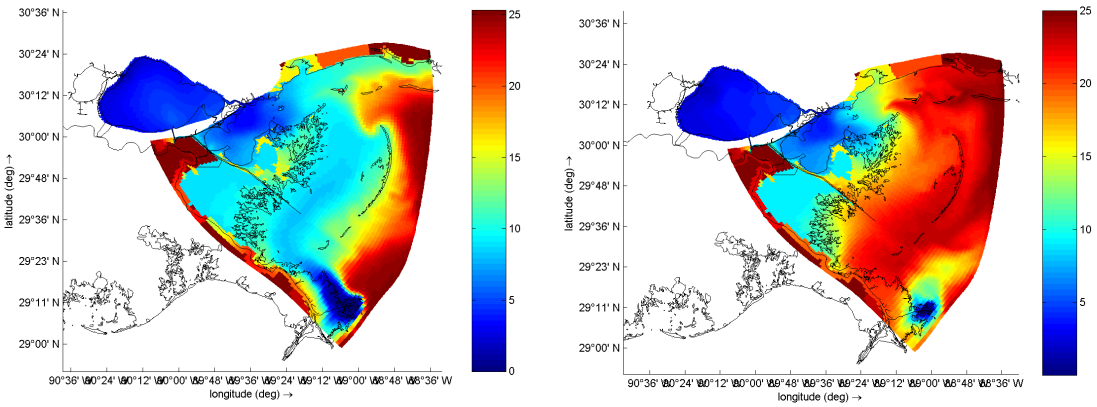

Figure 7.2 Salinities after 2 months simulation in depth averaged model (left) and in top layer of 3D modeling with 10 σ-layers (right)

In the depth-averaged model, the Mississippi River discharge is pushed into Chandeleur Sound by the saline water from the boundary. The entire model is too fresh as the water from the Gulf does not penetrate into the model area beyond the Chandeleur Islands. In the 3D-model the upper layer is much more saline than in the 2D-model. Using multiple layers vertical salinity gradients are modeled and horizontal gravitational circulation occurs. Due to the river discharges the fresh surface water flows towards the Gulf of Mexico, while the more saline Gulf water flows at depth into the model area. In the Pontchartrain Basin gravitational circulation cannot be neglected, therefore all model runs should be performed in 3D.

The discharge of the Mississippi River is located close to the boundary where water with a much higher salinity enters the model. High gradients occur. To reduce these gradient, the salinity is differentiated over the boundary. This is treated in the next section.

7.1.2.2 *Spatially varying salinity over boundary*

In order to reduce the salinity gradients near the Mississippi River discharge, the salinity imposed at the boundary is decreased from north to south. The boundary is divided into three sections, see Figure 7.3. The location of the section as well as the imposed salinity is based on the salinities near the boundary in the 3D salinity simulations. Around the Mississippi Birdfoot the salinity was around 10 ppt at the surface and increasing to 25 ppt with increasing depth, while north of the Chandeleur Islands the salinity was 25 ppt over the entire depth. Therefore section three has a salinity of 25 ppt over the entire width and depth. Section 1 has a surface salinity of 10 ppt over the entire width. The salinity at the bottom is 25 ppt. Over depth the salinity is linearly interpolated. The second section is linearly interpolated between both section in horizontal and vertical direction. Table 7.3 gives the values at either ends of all sections.

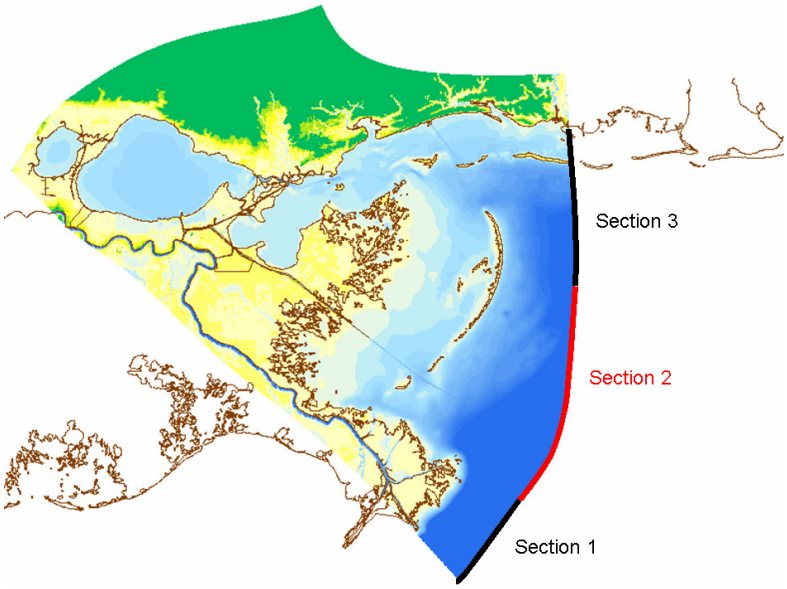

Figure 7.3 Section for differentiation of salinity over model boundary

Table 7.3 Salinity specified for the boundary sections

Salinity (ppt)	**Layer 1**		**Layer 10**	
	South	North	South	North
Section 1	10	10	25	25
Section 2	10	25	25	25
Section 3	25	25	25	25

The results of the model with spatially varying boundary salinity is compared to the initial 3D model with a salinity of 25 ppt over the entire boundary, see Figure 7.4. Both simulations were performed for 6 months.

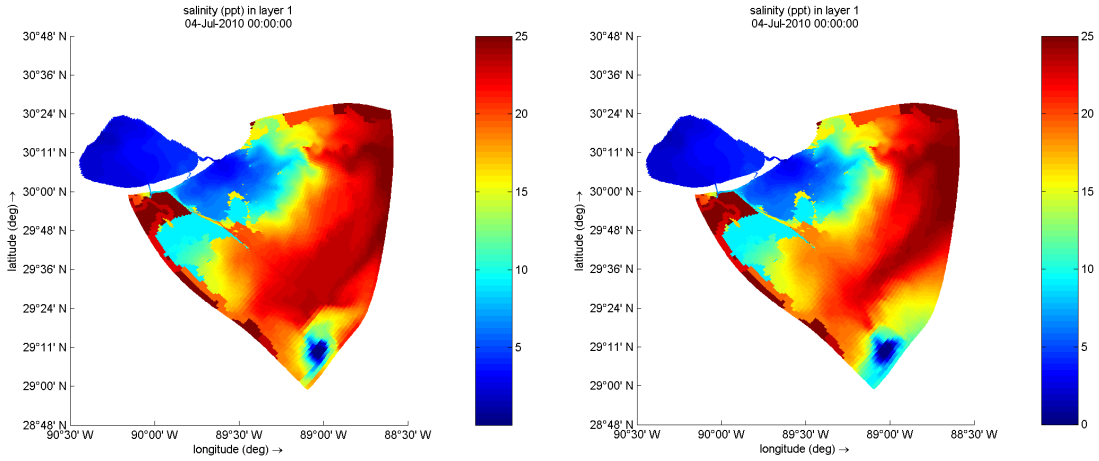

Figure 7.4 Salinity after 6 months simulation with uniform (25 ppt) boundary (left) and spatially varying boundary (right)

The southern part of the open boundary shows smaller salinity gradients. The salinity variation over the boundary is compensated by a density difference. The density is larger at the northern end which causes a density driven flow in southward direction. This flow concentrates around the Chandeleur Islands. It has no influence however on the salinity in Lake Borgne. The model remains equally fresh in Lake Borgne when using a spatially varying boundary.

7.1.2.3 Wind

Two studies that focused on the Mississippi River plume were treated before. Both studies concluded that wind has a large effect on the orientation of the plume. This was supported by the preliminary analysis of salinity data. The effects of wind on this model were studied by a single run by adding a wind of 5.4 m/s under a 112.5° angle (ESE). This is the prevailing wind in February until April.

The model was only run for a period of six months. A dynamic equilibrium was not reached at that point. Therefore no conclusion can be drawn with respect to the influence of wind on salinity in Lake Pontchartrain. It was clear however that the wind accelerated the penetration of the tide and the Mississippi River discharge into Chandeleur Sound for all layers. For the influence of the wind on the dynamic equilibrium in the Pontchartrain Basin a longer simulation should be performed.

7.1.2.4 Baseline condition

With the experience of these salinity simulations, the baseline condition was modeled. Ten σ-layers were used with each a thickness of 10% of the water depth. The horizontal eddy diffusivity was set to 10 m^2/s. The river discharges as previously described were used. This means the Mississippi River discharge was divided over 3 locations as given in Table 8.1. The MRGO is not restricted. The salinity at the boundary was set uniform to exclude density driven currents around the Chandeleur Islands. Wind was not taken into account. The model was run for 2 years with a time step of 5 minutes.

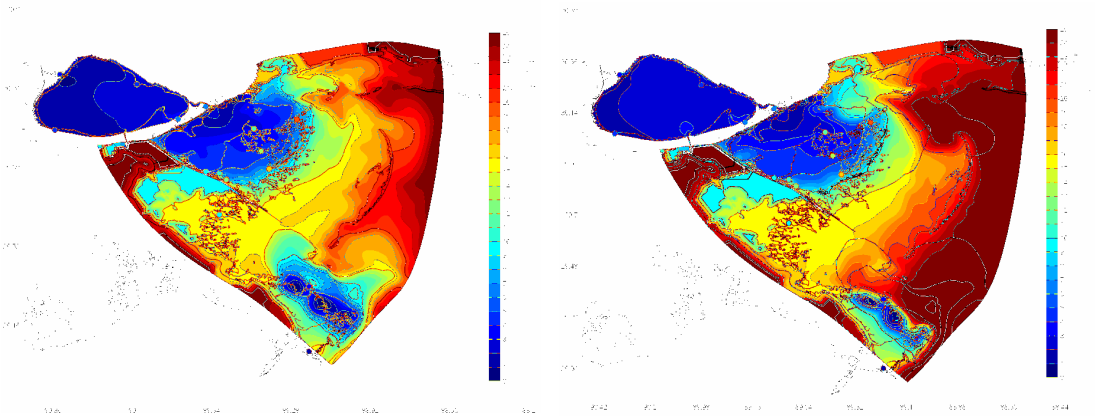

Figure 7.5 Salinity in upper layer (left) and bottom layer (right) after 2 years simulation with baseline conditions. White contour lines are 5 ppt contour lines of upper layer, colored dots are measured yearly averages.

Figure 7.5 shows the salinities in the upper (left) and bottom layer (right). It can be seen that in Lake Pontchartrain and the tidal passes the salinities are a good match to the measured values. Along the MRGO and at Shell Beach the model is slightly too fresh. The stations in the Biloxi Marsh and Lake Borgne are approximately 10 ppt more saline in reality than in the model. At these locations, the water column is well mixed. This in contrary to the estuarine Richardson number calculated in Section 6.2.2, that indicated stratification in Lake Pontchartrain and Lake Borgne. Offshore of the Biloxi Marsh, the system is more stratified.

7.1.2.5 Conclusions

The Delft3D FLOW-module computes too low salinities in the area of interest. The overall salinity in Lake Borgne is approximately 10 ppt too low. The salinities in Lake Pontchartrain show good resemblance to measured values.

The large deviation in salinities in Lake Borgne can be explained by the definition of the boundary condition. A uniform salinity was applied, while this is not representative. A larger model to derive salinities at locations along the boundary was not available. As described before, a change in boundary salinities can have large impacts on currents. A second error is introduced by only applying tidal constituents as boundary forcing. Large-scale circulations in the Gulf of Mexico, either wind or density driven, that reach until the Chandeleur Islands are not taken into account. A larger model to derive current velocities at boundary locations was not available.

7.2 Tracer analysis

The Delft3D FLOW model results in too low salinities in Lake Borgne. The deviation from yearly averaged measurement values is approximately 10 ppt at several locations in Lake Borgne and the Biloxi Marsh. In order to explain in more detail why the model results shows such low salinities in Lake Borgne, a tracer analysis can be performed. All sources in the model carry a tracer. This way the contribution of each source can be checked at several locations in the model. The tracer analysis is elaborated next.

The Delft3D WAQ-module is used for water quality modeling. The module does not calculate the hydrodynamics; these should be imported from Delft3D FLOW. With this information the advection-diffusion-reaction equation is solved on the same grid as was used for the hydrodynamics. A wide range of substances can be modeled. In this study only tracers will be used.

The first step in setting up the tracer analysis is the coupling of the hydrodynamic data of the FLOW model. The hydrodynamics of a one spring-neap cycle (14 days) are imported. The water levels at the end of the file should be equal to the water levels at the start of the hydrodynamic file. After each spring-neap cycle the hydrodynamics are read from the start. In this step, the grid and bathymetry of the FLOW-model are also imported. The same number of layers in the FLOW-model will be used in the WAQ-model.

The second step is to define the processes that are taken into account. The continuity is set to one for the initial conditions, the tidal forcing at the boundary and all river sources. Five conservative tracers are defined. The first tracer is given to all water particles in the initial condition. The second tracer is coupled to the tidal forcing at the boundary. The third tracer is coupled to the discharge of the Mississippi River. The Pearl River discharge is coupled to the fourth tracer. All rivers discharging into Lake Pontchartrain are coupled to the fifth tracer.

The results of the water quality module are saved at each grid cell for a 2D horizontal plot per layer each 30 minutes. In addition, observation points can be defined, the information was saved separately for all layers at each location. The third option is to visualize the results per pre-defined section. The information per section was saved depth averaged. For the observation points as well as for the section, information is saved daily.

During the coupling of the hydrodynamics to the water quality module, inactive cells are removed. No layers or cells were aggregated.

The dispersion in both directions was left to the default value of 1 m^2/s. The vertical diffusion was obtained from the coupled hydrodynamics with a scale factor of 1. In the WAQ-module this diffusion value is added to a constant value, which was left at the default value of 1 x 10^{-7} m^2/s. As this value is small compared to the computed diffusion, it is negligible. The adding is a mandatory part of the WAQ-module. The water density was set to 1020 kg/m^3. No wind was taken into account as this was also the case for the FLOW-model.

The model was run for two years with a time step of 10 minutes. Integration method 16 is used. This is an implicit upwind scheme in the horizontal direction. In the vertical a centrally discretized scheme is used. The concentrations are calculated with an iterative solver.

7.2.1 Results

The results of the tracer analysis are discussed here. Figure 7.6 shows the nine sections in which the model area is divided. Each cell is assigned to a section, but no cell is assigned double. During the water quality simulation the origin of each water particle is recorded. Each water particle that enters the model domain has a value belonging to the source: the boundary (tidal forcing) or one of the river. During the entire simulation the water particle keeps the same value. The water column can thus be divided per source. Figure 7.7 shows the average composition of the water column for each section.

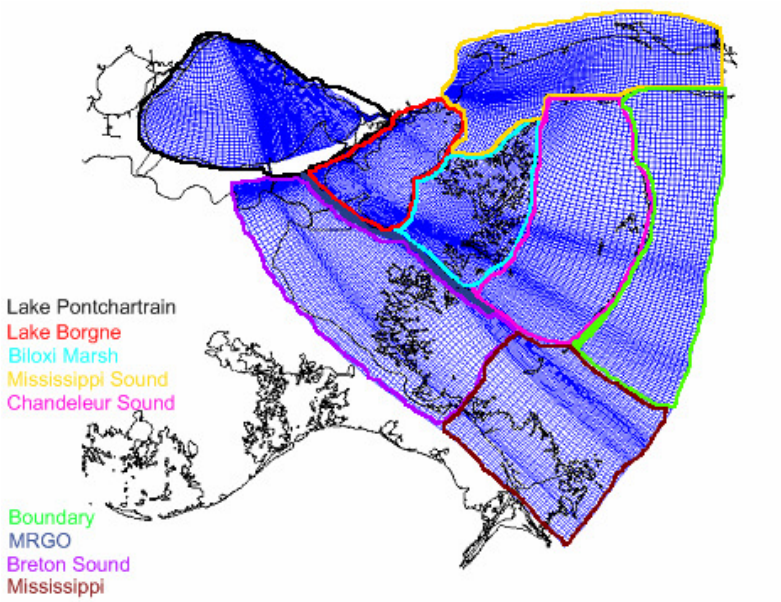

Figure 7.6 Sections in tracer analysis

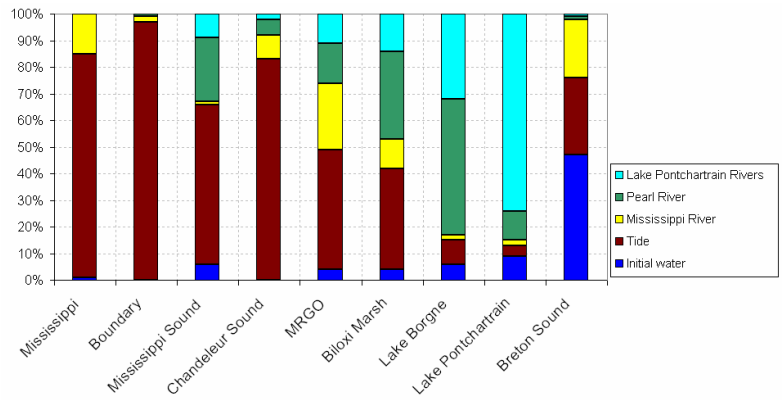

Figure 7.7 Contribution of each source per observation section after 3 years of simulation

The tidal signal decreases when moving away from the boundary. In the Biloxi Marsh 40% of the water is from tidal propagation, which is already significantly less than in Chandeleur Sound (over 80%). The riverine sources are more represented in the Biloxi Marsh. While in the MRGO and Mississippi Sound the tidal propagation makes up for 50% respectively 60% of the water, in Lake Borgne just 10% of the water originates from the boundary. This explains the low salinities in the FLOW-model. This could be explained by the fresh water plume of the Pearl River that keeps out the saline Gulf water without mixing, a phenomenon that was also observed in the FVCOM study (Section 6.3.3).

The Mississippi River discharge has only a limited area of influence. Via Chandeleur Sound and the MRGO the fresh water reaches the Biloxi Marsh. The influence of the Mississippi River in Lake Borgne and Lake Pontchartrain is minimal. This in contrary to the high correlation coefficient that was calculated using discharge and salinity measurements (Section 5.2.1). It could be explained by the definition of the boundary in combination with the relative model domain.

In previous model studies on salinity, it was proven that the Mississippi River plume can be oriented in such a way that discharges on the western side of the Birdfoot are transported into Chandeleur Sound. This effect is not taken into account in this model study. This could be accomplished by either changing the boundary condition with respect to salinities and flow velocities near the Birdfoot, or by increasing the model domain in southern and western direction.

The discharge of the Pearl River has a large influence on salinities in Lake Borgne; it makes up for 40% of the water. Water in the Biloxi Marsh comes for approximately 30% from the Pearl River. Only a small portion of the Pearl River discharge flows to Lake Pontchartrain. The rest of the Pearl River discharge flows Gulfward either through the MRGO or through Mississippi Sound and Chandeleur Sound.

The influence of the rivers discharging into Lake Pontchartrain decreases towards the open boundary, opposite to the amount of initial water still in the system. Thirty percent of the water in Lake Borgne comes from the Lake Pontchartrain Rivers. From there it is divided between the MRGO and Mississippi Sound.

At all sections initial water is still present at different percentages. This leads to the conclusion that the model is not in equilibrium after 3 years. A different run was performed to get a better insight of the time it takes to reach equilibrium. From Figure 7.8 it follows that after four years of simulation, equilibrium is still not reached as there still is some initial water in the system.

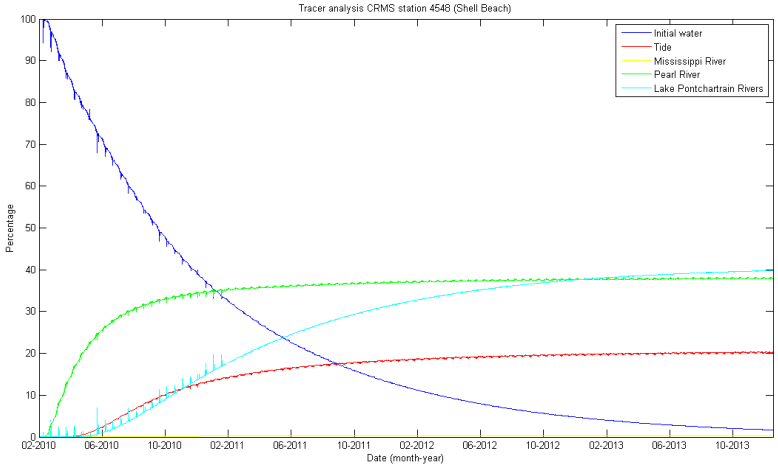

Figure 7.8 Tracers at Shell Beach (CRMS4548) over time

7.2.2 Recommendations for further modeling

The tracer analysis proves that the hydrodynamic has not reached dynamic equilibrium after four years. Therefore it is important to simulate the scenarios for a period longer than dour years. If the simulation is interpreted before dynamic equilibrium is reached, the results will not be reliable.

The underestimation of the intrusion of tides and its transport and underestimation of the Mississippi River discharge is explained by the definition of the boundary condition, as only tidal constituents are used. From previous model studies it already became clear that nontidal water level elevations and currents in the Gulf of Mexico can contribute to tidal propagation.

Due to lack of time and data the hydrodynamic model is not expanded in size to cover a larger part of the Gulf of Mexico. Neither have new boundary conditions been defined due to a lack of knowledge about the currents near the continental shelf. It is recommended that for future modeling an effort is made to enlarge the model domain or to include currents in the boundary conditions.

With the current hydrodynamic model the Violet Diversion is modeled. As the salinities in Lake Borgne and the Biloxi Marsh are too fresh, the relative impact of the Violet Diversion on yearly averaged salinities cannot be investigated. Therefore it will only be assessed how large the area of influence of the diversion is. In addition, the impact of the closure of the MRGO is investigated. From previous model studies it appeared that the closure decreased salinities in Lake Borgne. It will be investigated if this phenomenon also occurs in the Delft3D model.

7.3 Scenarios

The tracer analysis has given more insight in the performance of the 3D FLOW-model. Due to the limited tidal transport, the model has too low salinities in Lake Borgne, Lake Pontchartrain and the Biloxi Marsh. Besides this, it is clear that the model time should exceed 2 years before dynamic equilibrium is reached. Despite these conclusions, the model is not calibrated for salinity. Simulating a scenario for the Violet Diversion will only give an insight in relative changes in salinity. Since the MRGO is closed since July 2009 but was not closed in the baseline condition model before, the closure will be modeled first.

7.3.1 Baseline condition with MRGO closure

In July 2009 the closure of the MRGO was completed. A rock dam of 450 meter wide (bottom width) was constructed about half a kilometer south of Bayou La Loutre. The rock dam is elevated to 2.5 meter above NAVD88.

This rock dam was inserted to the bathymetry in the baseline FLOW-model. The results for the salinity in the upper layer can be found in Figure 7.9 (left) with lines of equal salinity from the baseline condition without MRGO closure (right).

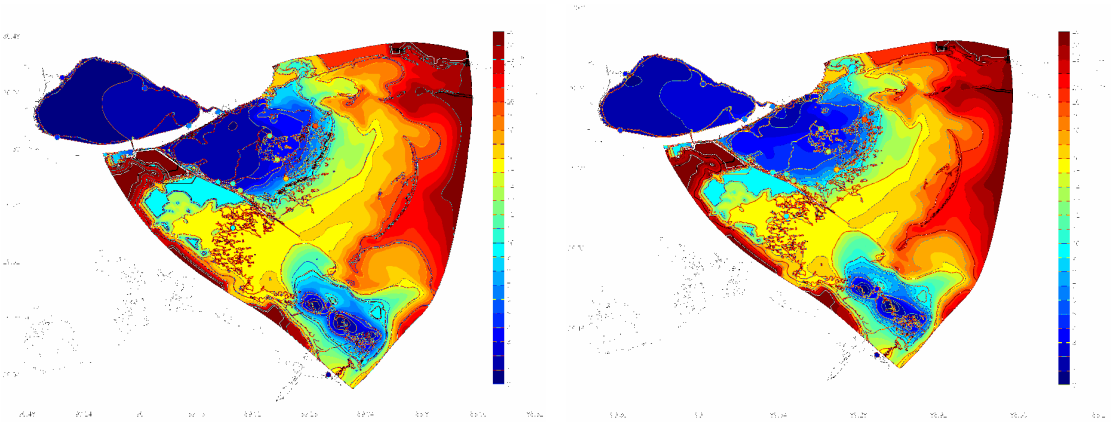

Figure 7.9 Salinity in upper layer after 2 years of simulation with MRGO closure (left) and without MRGO closure (right)

With the closure of the MRGO the salinities in Lake Borgne decrease. This can be explained by the absence of tidal penetration into Lake Borgne via the MRGO. The only tidal propagation into Lake Borgne takes places at Mississippi Sound. Also Lake Pontchartrain is slightly fresher with closure of the MRGO, since fresher water enters the lake via the tidal passes than in the baseline situation. The decreased salinity in Lake Borgne and Lake Pontchartrain were also modeled with FVCOM (Section 6.3.3). Gulfwards of the Biloxi Marsh there is no difference in salinity in the simulations with or without MRGO closure.

7.3.2 Violet Diversion

For the Violet Diversion several scenarios have been developed to get more insight in how the system would react. The U.S. Army Corps of Engineers has performed a preliminary model study to investigate the impact of the MRGO closure and several diversion scenarios (USACE, 2009b). It was concluded that with a 6400 cfs (181 m^3/s) diversion flow the Chatry optimum salinity targets would be met 40% of the time. This is with the MRGO closure structure in place.

In the FLOW-model the USACE diversion flow is rounded off to 190 m^3/s, which is equal to the yearly averaged discharge of both the West and the East Pearl River. Since the Central Wetlands Area is not well represented in the model bathymetry, the flow directly enters the MRGO at Bayou Dupre. This is where the Violet Canal and the MRGO currently meet. For large diversion flows a gate at Bayou Bienvenue would be constructed (USACE 2009d), however this is not taken into account for this study. The impact of the Violet Diversion on salinities can be seen in Figure 7.10.

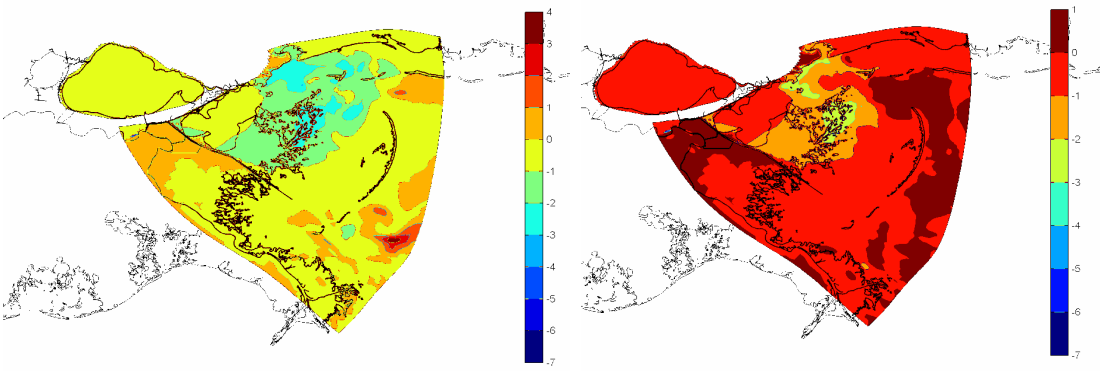

Figure 7.10 Difference plot of salinity between 3-year simulation with Violet Diversion and without diversion flow in the upper layer (left) and bottom layer (right), both with MRGO closure structure. Positive values indicate an increase in salinity.

The Violet Diversion has minimal effects on salinities in Lake Pontchartrain and Lake Borgne. This could indicate that the minimal salinity of Lake Borgne in the Delft3D model is around 7 ppt, the salinity after the closure of the MRGO. The salinity decreases in the Biloxi Marsh and Mississippi Sound. The far-reaching effect of the diversion can be explained by the underestimation of the transport by the tide and the Mississippi River. Since the modeled flow into Lake Borgne is not as strong as in reality, the area of influence of the diversion might in reality be smaller. At the model boundary an increase in salinity is observed. This could be explained by the increased flow of fresh surface water from Lake Borgne to the boundary. This increased flow pushes the tidal flow back to the boundary. The gravitational flow then causes an increased saline flow at larger depth. This is confirmed by the increase of salt wedge over the bottom, see Figure 7.10 right figure.

The 10 ppt and 15 ppt isohalines are indicated in Figure 7.11 with a red respectively blue line. The position of these isohalines are much further outside Lake Borgne than was the case with the FVCOM modeling (Georgiou et al., 2007). This was to be expected as the model was too fresh to calibrate for the baseline condition. Just outside of Lake Borgne the salinity gradients increase. This was also established in the Violet Diversion study with FVCOM.

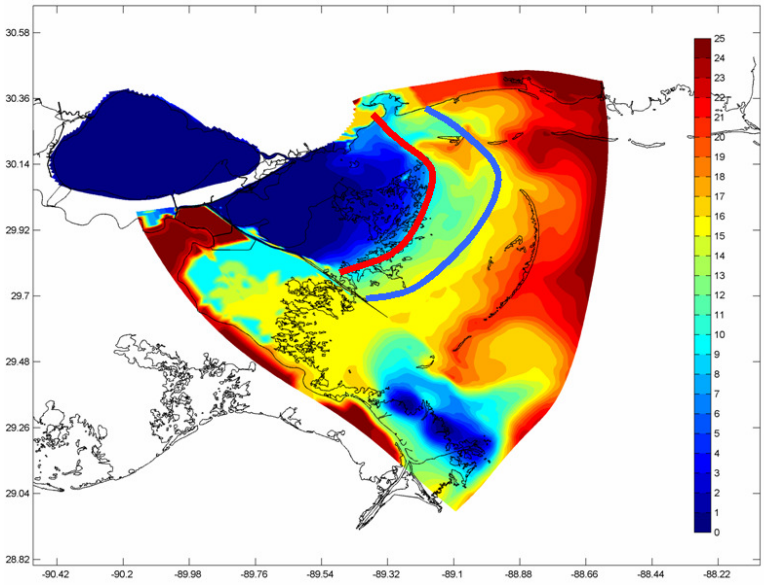

Figure 7.11 The 10 ppt and 15 ppt isohaline for the diversion scenario

7.4 Conclusions

The Delft3D FLOW-model that was calibrated for tidal propagation in the Pontchartrain Basin was extended for salinity modeling. The tidal flow entering the model has a salinity of 25 ppt. Initial salinities were based on the yearly averages of measured values.

Freshwater sources of the model are the Mississippi River discharging at three locations, the Pearl River at two locations and three rivers discharging into Lake Pontchartrain. Each river discharge has a salinity of 0 ppt. The goal was to calibrate the model for a dynamic equilibrium.

In the 2D model the salinities are depth averaged. Saline water from the boundary collides with the fresh water of the river discharges. This leads to a minimal tidal penetration into the model domain, which leads to a minimal transport of saline water into the project area. In a 3D model the saline water can enter the model over the bottom, while fresh water can leave the model domain at the surface. This is known as gravitational circulation. Salinities in the entire domain increase. In the Pontchartrain Basin the gravitational circulation and its effects are not negligible, therefore 3D modeling is inevitable. Despite the gravitational circulation, the model is still too fresh in the Biloxi Marsh and in Lake Borgne.

Near the Mississippi River discharge locations high salinity gradients occur. To solve this, a spatially varying salinity boundary is applied. The gradients near the Mississippi Birdfoot do indeed decrease, but a density driven current originates from north to south due to the difference in salinity along the boundary.

Wind is imposed in the model as it was proved from previous model studies that it has a large influence on the Mississippi River plume. The model had not yet reached dynamic equilibrium, but it could be concluded that the tide and the Mississippi River discharge penetrated further into the model. This does not mean the salinities change compared to the baseline condition, it could also mean that wind causes the dynamic equilibrium to be reached earlier.

With all these model studies, the model was still resulting in too low salinities in Lake Borgne and the Biloxi Marsh. Therefore a tracer analysis was performed. Each source was linked to a tracer to get more insight in the contribution of each source to several locations. After four years, equilibrium was not yet reached. Initial water was till in the system. Sections were defined to see what the water column of an area was build up from. The influence of the tide decreased when moving away from the open boundary. In the Biloxi Marsh, Lake Borgne and Lake Pontchartrain the tide filled less than half the lake. This explains the low salinities in the FLOW-model. A possible interpretation is that the plume of the Pearl River does not mix and keeps out the saline water from the Gulf. The Mississippi River has limited influence in the area of interest, which objects the high correlation earlier found in the data analysis. The Pearl River has a large influence on Lake Borgne and the Biloxi Marsh and flows towards the Gulf for a large extent. Therefore little discharge from the Pearl River reaches Lake Pontchartrain. The discharge of the rivers around Lake Pontchartrain reach Lake Borgne and flow towards the Gulf via the MRGO and Mississippi Sound.

With the FLOW-model the impact of the MRGO closure and a Violet Diversion scenario was studied. For the Violet Diversion a constant flow of 190 m^3/s was used, that flows directly into the MRGO at Bayou Dupre. The MRGO closure already resulted in lower salinities in Lake Pontchartrain, Lake Borgne and the Biloxi Marsh due to the absence of tidal propagation through the MRGO. The Violet Diversion made the area of interest even fresher. Since the model was not calibrated and a dynamic equilibrium was not reached, absolute salinities are not reliable.

8 Conclusion & Recommendations

The Delft3D FLOW-module was used for simulating the hydrodynamics of the Pontchartrain Basin. A grid was developed to follow the MRGO and the tidal passes between Lake Borgne and Lake Pontchartrain. In total the grid consists of a little less than 53,000 nodes. The bathymetry was extracted from the ADCIRC SL15 model. The depth-averaged model was calibrated for tidal amplitudes and phases of ten constituents, and for the tidal fluxes through the Rigolets, the Chef Menteur and the IHNC.

Salinity was implemented in the model by simulating initial salinity based on yearly averaged values of measurements. For the tide a salinity of 25 ppt is assumed, rivers are assumed to have 0 ppt salinity. For the Mississippi River the crevasses and Passes that are within the model domain are used. The discharge from the passes outside of the model domain, that might flow around the Mississippi Birdfoot, is not taken into account. The Pearl River and the rivers discharging in Lake Pontchartrain and Lake Maurepas are also implemented in the model. All discharges are yearly averages to obtain a dynamic equilibrium.

8.1 Conclusions

The Delft3D model for tidal propagation produced tidal constituents within 10% of the measurements. The modeled fluxes through the channels of the Rigolets, the Chef Menteur Pass and the IHNC were 1% accurate. In order to gain these results, friction in the flow areas was decreased by a factor two. The friction of the marshes remained unchanged. The cross-sectional area of the MRGO and the tidal passes between Lake Borgne and Lake Pontchartrain needed to be adjusted as well. This was already predicted by the application of the harmonic method for this area. The phases of the tidal constituents were underestimated. However, for the application of the model for salinities, phases are less important than the total water exchange between model areas. The model is considered calibrated for tides.

The depth-averaged salinity model did not perform well as stratification offshore of the Biloxi Marsh was not taken into account. In the 3D model, with ten σ-layers, gravitational circulation occurs: the saline water from the boundary was able to enter the model over the bottom, while the fresh discharge of the Mississippi River was able to leave the model. This increased the salinity in the model. However, salinities in Lake Borgne and Biloxi Marsh are still too low.

A tracer analysis showed that the tidal transport into the area of interest makes up for only a small portion of the water column. In addition, the influence of the Mississippi River is not as large as data analysis showed. The tracer analysis also showed that the time to reach an equilibrium situation was longer than four years. This could again indicate that the exchange mechanisms in the model are too small or maybe not even present at all.

From the data analysis it became clear that wind and large-scale currents, either tide- or wind-driven, have a large influence on flow patterns on the continental shelf around the Mississippi Birdfoot. Both wind effects and large-scale currents were not taken into account in this model study. This caused the tidal transport to Lake Borgne to be too small. In addition, the discharge of the Mississippi River that flows out at the western side will not enter the model domain, while previous model studies demonstrate that this does happen under the right wind conditions.

The MRGO closure that was completed in 2009 was not yet implemented in the bathymetry. Since the Violet Diversion will operate with the MRGO closure in place, a first run was performed with only the closure structure. It is evident that Lake Pontchartrain, Lake Borgne and the Biloxi Marsh become fresher. With a constant diversion flow of 190 m^3/s at Violet, the area of interest become even fresher. Since the model is not calibrated, no conclusions can be drawn towards meeting the Chatry limits.

8.2 Recommendations

The tidal calibration was performed with tidal forcing only. The amplitudes and phases of tidal constituents were used as boundary conditions. River discharges and large-scale (wind- or tide-driven) currents were not taken into account at first. Since the modeling of tidal phases did not produce desirable results, it is recommended to add river discharges and large-scale currents to the model to gain a complete hydrodynamic model. Calibration on tides might then result in more realistic friction parameters.

Taking the nontidal currents into account for the simulation can be achieved by setting up a model that represents a larger part of the Gulf of Mexico. In this larger model several processes should be implemented to generate large-scale currents along the continental shelf. Processes that should be taken into account are amongst others (but probably not only): wind, water temperature, salinity and air temperature. Wind and salinity should be added first as these processes will cause the largest difference in flow patterns compared to the current set-up of the calibrated model. Water and air temperature are of less importance. The goal of the larger model is to generate density- and wind driven currents like the (anti-)cyclones reported by Walker et al. (2005). Next to these currents, the Mississippi Birdfoot would be better represented in a larger model. In other studies it is proven that the Mississippi River discharge can be transported around the Birdfoot Delta. With a larger model this transport could also be simulated. This larger model could be used for the modeling of the Pontchartrain Basin or to extract the model boundaries for the present model.

For the calibration on tides the cross-sectional areas were enlarged. It was assumed that there might be a difference between surveyed and actual channel cross-sections due to shoaling by Hurricane Katrina. If the survey included the shoaling, but the sediments have eroded in the mean time, this could explain the difference. Therefore the SL15 bathymetry should be compared to more recent measurements to check the depth of the tidal channels.

For salinity simulations, the 2D model does not produce desirable results. The model performance increases when simulating in three dimensions due to the fact that gravitational circulation is taken into account. Therefore all transport simulations of the Pontchartrain Basin should be performed in 3D.

If a larger hydrodynamic and transport model is set up which also simulates the large-scale circulation in the Gulf of Mexico near the Mississippi Birdfoot, it might be able to calibrate the model. With a calibrated model more research can be performed into the discharge regimes of the Violet Diversion. The dynamic equilibrium that was attempted to achieve in this study, could then be replaced by a real-time simulation by using time series of wind, tides and discharges. Real-time simulations are important since the salinities in Lake Borgne and the Biloxi Marsh show distinct seasonal variations. In this baseline situation, different diversion regimes could be modeled. For example, during the months April and May a peak discharge could be diverted, while diverting a minimal flow during the other months. Only with this model, using constant or varying diversion discharges, the impact of the Violet Diversion on salinity gradients in Lake Borgne and the Biloxi Marsh could be quantified.

9 Literature

ADCIRC, 2010. *ADCIRC Development Group*. www.nd.edu/~adcirc/. Last consulted on February 22, 2010.

AECOM Environment, 2009. *90% Design Submittal GIWW Gate Hydraulic Numerical Design Inner Harbor Navigational Canal, Hurricane Protection Project.* Prepared for INCA/GERWICK JV, Metairie, Louisiana.

ASABE - Society of Agricultural and Biological Engineers, 2010. *ASABE Technical Library. Modeling of nonpoint sources in Tickfaw River Watershed.* http://asae.frymulti.com/abstract.asp?aid=20382&t=2. Last Consulted on April 20, 2010.

ASCE - American Society of Civil Engineers, Hurricane Katrina External Review Panel, 2007. *The New Orleans hurricane protection system: what went wrong and why*. American Society of Civil Engineers, Reston, Virginia.

Barras, J., S. Beville, D. Britsch, S. Hartley, S. Hawes, J. Johnston, P. Kemp, Q. Kinler, A. Martucci, J. Porthouse, D. Reed, K. Roy, S. Sapkota, and J. Suhayda, 2003. *Historical and projected coastal Louisiana land changes: 1978-2050.* USGS Open File Report 03-334, 39p (Revised January 2004).

Barras, J. A., 2006. *Land Area Change in Coastal Louisiana after the 2005 Hurricanes. A series of three maps.* U.S. Geological Survey Open-File Report 06-1274.

Battjes, J.A., 2002. *Stroming in waterlopen. Collegehandleiding CT3310.* Technische Universiteit Delft, Faculteit Civiele Techniek en Geowetenschappen, Opleiding Civiele Techniek, Sectie Vloeistofmechanica – April 2002.

Bunya, S., J.C. Dietrich, J.J. Westerink, B.A. Ebersole, J.M. Smith, J.H. Atkinson, R. Jensen, D.T. Resio, R.A. Luettich, C. Dawson, V.J. Cardone, A.T. Cox, M.D. Powell, H.J Westerink, and H.J. Roberts, 2010. *A High-Resolution Coupled Riverine Flow, Tide, Wind, Wind Wave, and Storm Surge Model for Southern Louisiana and Mississippi. Part I: Model Development and Validation.* American Meteorological Society, February 2010.

Blumenthal, S., 2010. *"No one can say they didn't see it coming"*. http://dir.salon.com/opinion/blumenthal/2005/08/31/disaster_preparation/index.html. Last consulted on May 11, 2010.

Brater, E.F., H.W. King, J.E. Lindell, and C.Y. Wei, 1996. Handbook of Hydraulics. McGraw-Hill, Boston, MA. 7th edition.

Chatry, M., R.J. Dugas, K.A. Easley, 1983. *Optimum salinity regime for oyster production on Louisiana's state seed grounds*. Marine Science, Vol 26, pp 81-94.

CHL ERDC – Coastal Hydraulics Laboratory, Engineer Research and Development Center, U.S. Army Corps of Engineers, 2009. *Seabrook Fish Larval Transport Study. Draft*. Vicksburg, Mississippi.

CRMS - Coastwide Reference Monitoring System, 2010. http://www.lacoast.gov/crms2/Home.aspx. Last Consulted on June 16, 2010.

Deltares, 2009a. *Delft3D-FLOW. Simulation of multi-dimensional hydrodynamic flows and transport phenomena, including sediments. User Manual version 3.14.* Deltares, Delft.

Deltares, 2009b. *Delft3D-RGFGRID. Generation and manipulation of curvilinear grids for Delft3D-FLOW and Delft3D-WAVE. User Manual version 4.00.* Deltares, Delft.

Deltares, 2010. *Website Deltares, Software.*www.deltares.nl. Software >> hydrosystems >> Delft3D, version 3.28.04. Last consulted on January 28, 2010.

Demas, C.R., P.A. Ensminger, D.J. Walters. Environmental Laboratory, U.S. Army Corps of Engineers. *Mississippi and Atchafalaya River Discharge and Suspended-Sediment Trends 1976-2007.*http://el.erdc.usace.army.mil/index.cfm. Last consulted on Friday September 25, 2009

DNR – Louisiana Department of Natural Resources, 1992. *Annual Monitoring Report, Violet Siphon Diversion, PO-1.* DNR Project No.:25030-91-30

Ebersole, B.A., J.J. Westerink, S. Bunya, J.C. Dietrich, M.A. Cialone, 2010. *Development of storm surge which led to flooding in St. Bernard Polder during Hurricane Katrina.* Ocean Engineering. Volume 37, Issue 1, Pages 91-103.

ERDC – U.S. Army Corps of Engineers, Engineer Research and Development Center, 2009. *West Bay Sediment Diversion Effects. ERDC Workplan Report. Draft.* Coastal and Hydraulics Laboratory, Vicksburg, MS.

Evers, D.E., J.G. Gosselink, C.E. Sasser, J.M. Hill, 1992. *Wetland loss dynamics in southwestern Barataria Basin, Louisiana (USA), 1945-1985*. Springer Netherlands, Volume 2, Number 3, September 1992. Abstract.

Georgiou, I., J.A. McCorquodale, A.G. Retana, D.M. FitzGerald, Z. Hughes, 2007. *Hydrodynamic and Salinity Modeling in the Pontchartrain Basin. Assessment of Freshwater Diversions at Violet with MRGO Modifications.* Pontchartrain Institute for Environmental Sciences, University of New Orleans, Boston University.

Goldsteen, J.B., 1993. *Danger all around: waste storage crisis on the Texas and Louisiana Gulf Coast.* University of Texas Press, p114.

Google Earth, 2009. http://earth.google.co.uk/. Google Earth 5.1.3533.1731

Goring, D.G., 1984. *Analysis of tidal river records by a harmonic regressive technique.* J. Hydrol., 78. 21-37

Gulfbase.org, 2010. *Resource Database for Gulf of Mexico Research, Lake Borgne.* http://www.gulfbase.org/bay/view.php?bid=lake1. Last consulted on February 24, 2010.

Gunter G., 1955. *Mortality of Oysters and abundance of certain associates as related to salinity*. Ecology. 36(4):601-619.

Hofmann, E.E., and S.J. Worley (1986). *An investigation of the Circulation of the Gulf of Mexico.* J. eophys. Res. 91 (C12), 14, 221-14,236

Jacobsen, R., 2007. *Assessing Baseline and Modified Astronomical Tide in the Pontchartrain Basin using ADCIRC.* URS Corporation and Louisiana State University, Department of Civil and Environmental Engineering, Baton Rouge, Louisiana.

C. Kranenburg, 1998. *Dichtheidsstromen, CT5302.* Faculteit Civiele techniek en Geowetenschappen, Technische Universiteit Delft.

LACPR - Louisiana Coastal Protection and Restoration Authority, 2007. *Integrated Ecosystem Restoration and Hurricane Protection: Louisiana's Comprehensive Master Plan for a Sustainable Coast.* Louisiana Coastal Protection and Restoration Authority, Baton Rouge, Louisiana.

LPBF - Lake Pontchartrain Basin Foundation, 2006. *Pontchartrain Coastal Lines of Defense Program.* Lake Pontchartrain Basin Foundation, Coastal Sustainability Program.

LPBF – Lake Pontchartrain Basin Foundation, 2006. *Comprehensive Habitat Management Plan for the Pontchartrain Basin. Final.* Lake Pontchartrain Basin Foundation.

LSU – Louisiana State University, 2006/2007. *GIS-Aided Water Quality Monitoring and Assessment System for Lake Pontchartrain*. Louisiana Water Resources Research Centre, LSU.

Martin K., D. Webb, G. Savant, and G. Lynch, 2009. *Lake Borgne Surge Barrier Study, Draft.* U.S. ERDC – U.S. Engineer Research and Development Center, Coastal and Hydraulics Laboratory, Vicksburg, MS.

McAnally, W.H., R.C. Berger, 1997. *Salinity Changes in Pontchartrain Basin Estuary Resulting from Bonnet Carré Freshwater Diversion. Numerical Model Investigation.* U.S. Army Corps of Engineers, Waterways Experiment Station, Technical Report CHL-97-2, February 1997.

MVN USACE - U.S. Army Corps of Engineers, New Orleans District, 2009. *Greater New Orleans Hurricane and Storm Damage Risk Reduction System (HSDRRS), 100 Year Design Map. Status June 2009.* http://www.mvn.usace.army.mil/hps2/pdf/100-Year%20Status%20Map_051209_Final.pdf. Last consulted on May 11, 2010.

MVN USACE - U.S. Army Corps of Engineers, New Orleans District, 2010. *Mississippi River Flood Control.* http://www.mvn.usace.army.mil/bcarre/2008%20operation.asp. Last consulted on April 15, 2010.

NOAA GEOID – National Oceanic and Atmospheric Administration GEOID, 2010. http://www.ngs.noaa.gov/GEOID/GEOID09/. Last Modified on March 17, 2010,

NOAA NDBC – National Oceanic and Atmospheric Administration's National Data Buoy Center, 2010. *Buoy SHBL1, Shell Beach, LA.* http://www.ndbc.noaa.gov/station_page.php?station=shbl1. *Buoy NWCL1, New Canal, LA.* http://www.ndbc.noaa.gov/station_page.php?station=nwcl1. Last Consulted on August 2, 2010

NOAA News – National Oceanic and Atmospheric Administration News, 2010. http://www.noaanews.noaa.gov/stories2005/images/katrina-flood-depth-estimation-09-03-2005.jpg. Last Consulted on May 11, 2010.

NOAA Tides and Currents - National Oceanic and Atmospheric Administration, Tides and Currents, 2010. *Stations Mayport (Bar Pilots Dock, 8720218), Virginia Key (8723214), Tampa (Old Port, 8726607), Apalachicola (8728690), Shell Beach (8761305), Grand Isle (8761724), Galveston (Pleasure Pier, 8771510), Corpus Christi (8775870), Madero (Tampico Harbor, Mexico, 9500966), New Canal (8761927), Southwest Pass (Pilots Station East, 8760922), Pascagoula (Dock E, Port of Pascagoula, 8741041), Gulfport (Harbor, 8745557). Bay Waveland (Yacht Club, 8747437), East Bank (East Bank 1, 8762372).* tidesandcurrents.noaa.gov. Last consulted on February 24, 2010.

NWMC - National Water Management Center, 2010. *Website Natural Resources Conservation Service. National Water Management Center. Louisiana Watershed Receives National Watershed Award.* http://wmc.ar.nrcs.usda.gov/news/lawatershed.html. Last consulted on April 20, 2010.

NWS NHC – National Weather Service, National Hurricane Center, 2010a. *2008 Atlantic hurricane season.* http://www.nhc.noaa.gov/2008atlan.shtml. Last consulted on July 12, 2010.

NWS NHC – National Weather Service, National Hurricane Center, 2010b. *2009 Atlantic hurricane season.* http://www.nhc.noaa.gov/2009atlan.shtml. Last consulted on July 12, 2010

Pawlowicz, R., B. Beardsley, and S. Lentz, 2002. *Classical Tidal Harmonic Analysis Including Error Estimates in Matlab using T-Tide.* Computers and Geosciences. Vol. 28, 929-937.

Rego, J.L., Meselhe, E., Stronach, J., and Habib, E., 2010. *Numerical Modeling of the Mississippi - Atchafalaya Rivers' Sediment Transport and Fate. Considerations for Diversion Scenarios.* Journal of Coastal Research, 26(2), 212-229. West Palm Beach (Florida), ISSN 0749-0208

Rivergages.com, 2010. *Water levels of Rivers and Lakes. U.S. Army Corps of Engineers.* rivergages.com. Last consulted on February 24, 2010.

Roblin, R.J., 2008. *Water Quality Modeling of Freshwater Diversions in the Pontchartrain Estuary.* University of New Orleans, Department of Civil and Environmental Engineering.

Sikora, W.B., B. Kjerfve, 1985. *Factors Influencing the Salinity Regime of Lake Pontchartrain, Louisiana, a Shallow Coastal Lagoon. Analysis of a Long-Term Data Set.* Estuaries. Vol. 8, No. 2A: 170-180.

SMAST/UMASSD - The School of Marine Science & Technology, University of Massachusetts – Dartmouth, 2004. *Marine Ecosystem Dynamics Modeling. The unstructured grid Finite Volume Coastal Ocean Model (FVCOM).* Last consulted on January 28, 2010. http://fvcom.smast.umassd.edu/FVCOM/index.html.

Stewart, J.G., C.S. Schieble, R.C. Cashner and V.A. Barko, 2005. *Long-term Trends in the Bogue Chitto River Fish Assemblage. A 27-year Perspective.* Humboldt Field Research Institute.

Templet, P.H., K.J. Meyer-Arendt, 1988. *Louisiana wetland loss: A regional water management approach to the problem.* Environmental Management, Vol 12, No. 2, pp. 181-192. Springer – Verlag, New York.

U.S. Army Corps of Engineers, New Orleans District, 2009a. *Coastal Restoration Plan and Structural Environmental Impacts Appendix. Appendix of the Louisiana Coastal Protection and Restoration Final Technical Report.* New Orleans.

USACE – U.S. Army Corps of Engineers, 2009b. *Mississippi River - Gulf Outlet (MRGO) Ecosystem Restoration Study Louisiana and Mississippi, Hydraulics and Hydrology, Preliminary Hydrodynamic and Hydraulic Modeling for a Proposed Freshwater Diversion in the Vicinity of Violet, Louisiana. Draft Modeling Report.* New Orleans District

U.S. Army Corps of Engineers, New Orleans District, 2010. *Mississippi River Gulf Outlet, Ecosystem Restoration Plan Feasibility Study.* www.mrgo.gov. Consulted on Wednesday January 20, 2010

USACE - U.S. Army Corps of Engineers, Team New Orleans – Frequently Asked Questions, 2010. http://www.mvn.usace.army.mil/ed/edss/faqs.asp#MLLW. Last Consulted on June 17, 2010

US EPA - U.S. Environmental Protection Agency, Louisiana, 2010. *Tchefuncte and Bogue Falaya Rivers. Fixing on-site sewage systems restores popular New Orleans area rivers.* http://www.epa.gov/nos/Success/state/la_tchef.htm. Last consulted on April 20, 2010.

USGS – U.S. Geological Survey (J. Barras), U.S. Department of the Interior, 2006. *Land Area Change in Coastal Louisiana After the 2005 Hurricanes: Marsh Communities.* Open-File Report 2006-1274. http://pubs.usgs.gov/of/2006/1274/. Last Consulted on June 22, 2010

USGS - U.S. Geological Survey, 2009. *Time-series of Daily Data 20-09-2008 till 19-09-2009 at station USGS 07374000 Mississippi River at Baton Rouge, LA.* http://waterdata.usgs.gov/la/nwis/dv/?site_no=07374000&agency_cd=USGS&referred_module=sw. Consulted on September 21, 2009

Walker, H.J., J.M. Coleman, H.H. Roberts, R.S. Tye, 1987. *Wetland loss in Louisiana*. Geogr. Ann. 69A (1): 189-200. Abstract.

Walker, N.D., W.J. Wiseman, L.J. Rouse, and A. Babin, 2005. *Effects of River Discharge, Wind Stress, and Slope Eddies on Circulation and the Satellite-Observed Structure of the Mississippi River Plume.* Journal of Coastal Research, 21(6), 1228-1244. West Palm Beach (Florida), ISSN 0749-0208

Westerink, J.J., R.A. Luettich, J.C. Muccino, 1993. *Modeling tides in the western North Atlantic using unstructured graded girds.* Tellus. 46A 178-199

Wikipedia, 2010. Wikipedia, the free encyclopedia. www.wikipedia.org. Articles: Gulf of Mexico, Bonnet Carré Spillway. Last consulted on February 23, 2010.

Wiseman, W.J., Jr, E.M Swenson, J. Power, 1990. *Salinity trends in Louisiana estuaries.* Estuaries. Vol 13 no 3, p265-271.

Yanagi, T., T. Takao, 1998. *Clockwise phase propagation of semi-diurnal tides in the Gulf of Thailand.* Journal of Oceanography. Vol 54, pp 143 to 150.

Zetler, B.D. and D.V. Hansen, 1970. *Tides in the Gulf of Mexico. A review and proposed program.* Bulletin of Marine Science.

A Schematization using the harmonic method

The propagation of the tide in the Pontchartrain Basin is schematized using the harmonic method. The assumptions for using this method are:

- No spin-up time is taken into account for this method. Therefore, results represent equilibrium situations.
- All channels are assumed prismatic (the cross-sectional area remains the same for the entire channel length).
- Deformation of the tide due to non-linear influences, e.g. variation of the cross-sectional area of the channel with water depth, are not taken into account.
- The channel geometry (A_s, B and R) is independent of depth, implying that the tidal water level elevation should be small compared to the total water depth.

First the tidal water level elevation, see equation (A.1), has to be rewritten using complex numbers, see (A.2) en (A.3).

$$\zeta(x,t) = \hat{\zeta}(x) \cdot \cos(\omega \cdot t - k \cdot x + \alpha) \tag{A.1}$$

$$\zeta(x,t) = \mathrm{Re}\left[\tilde{\zeta}(x) \cdot \exp(i \cdot \omega \cdot t)\right] \tag{A.2}$$

$$\tilde{\zeta}(x) = \hat{\zeta}(x) \cdot \exp(i \cdot (-k \cdot x + \alpha)) \tag{A.3}$$

$$\omega = \frac{2 \cdot \pi}{T} \tag{A.4}$$

$$k = \frac{2 \cdot \pi}{L} \tag{A.5}$$

where
ζ = amplitude of water level elevation [m]
$\hat{\zeta}$ = location dependent amplitude [m]
ω = tidal frequency [rad/s], see (A.4)
T = tidal period [s]
k = wave number [rad/m], see (A.5)
L = tidal wave length [m]

The one dimensional continuity equation (equation (A.6)) and the linearized equation of motion (equation (A.7)) can be expressed in only the water level elevation ζ, see equation (A.8).

$$B \cdot \frac{\partial \zeta}{\partial t} + \frac{\partial Q}{\partial x} = 0 \tag{A.6}$$

$$\frac{\partial Q}{\partial t} + g \cdot A_s \cdot \frac{\partial \zeta}{\partial x} + \kappa \cdot Q = 0 \tag{A.7}$$

$$\frac{\partial^2 \zeta}{\partial t^2} - c_0^2 \cdot \frac{\partial^2 \zeta}{\partial x^2} + \kappa \cdot \frac{\partial \zeta}{\partial t} = 0 \tag{A.8}$$

$$\kappa = \frac{8}{3 \cdot \pi} \cdot c_f \cdot \frac{Q}{A_s \cdot R} \tag{A.9}$$

$$c_0 = \sqrt{\frac{g \cdot A_s}{B}} \tag{A.10}$$

where
B = channel width [m]
Q = discharge [m^3/s]
g = gravitational acceleration [m/s^2]
A_s = stream-carrying cross-sectional area of channel [m^2]
κ = factor in linearized expression for friction [s^{-1}], see (A.9)
c_0 = propagation speed of wave without friction [m/s], see (A.10)
c_f = friction coefficient [-]
R = hydraulic radius of channel [m]

The ratio between friction and inertia can then be expressed by equation (A.11).

$$\sigma \equiv \frac{\kappa}{\omega} = \frac{8}{3 \cdot \pi} \cdot c_f \cdot \frac{\hat{Q}}{\omega \cdot A_s \cdot R} \tag{A.11}$$

As κ and σ are both dependent on the discharge amplitude ($\hat{Q}$), iterations are necessary to solve these equations. The use of the friction factor κ limits the length of the schematized channels. As the discharge varies over the channel, κ will also vary over channel length. Only if the channel length is limited, κ can be considered constant over the entire channel.

Continuing with equation (A.8), it is expected that the solution consists of two wave components, propagating in opposite direction. Dismissing the tidal time variation and substituting κ and k_0 (equation (A.12)), the differential equation (A.13) is attained.

$$k_0 = \frac{\omega}{c_0} \tag{A.12}$$

$$\frac{d^2 \tilde{\zeta}}{dx^2} + k_0^2 \cdot (1 - i \cdot \sigma) \cdot \tilde{\zeta} = 0 \tag{A.13}$$

Equation (A.13) results in a exponential solution. Therefore, equation 8.16 is substituted into equation (A.13), which leads to equation (A.15).

$$\tilde{\zeta}(x) = \exp(P \cdot x) \tag{A.14}$$

$$P^2 + k_0^2 \cdot (1 - i \cdot \sigma) = 0 \tag{A.15}$$

This equation leads to two complex square roots, which are denoted by p and –p, see equation (A.16).

$$p = i \cdot k_0 \cdot (1 - i \cdot \sigma)^{\frac{1}{2}} \tag{A.16}$$

This can be substituted in equation (A.6) and then in equation (A.7), leading to the general solutions in equations (A.17) and (A.18).

$$\tilde{\zeta}(x) = C_+ \cdot \exp(-p \cdot x) + C_- \cdot \exp(p \cdot x) = \tilde{\zeta}_+(x) + \tilde{\zeta}_-(x) \tag{A.17}$$

$$\hat{Q}(x) = \frac{i \cdot \omega \cdot B}{p} \cdot \left[C_+ \cdot \exp(-p \cdot x) - C_- \cdot \exp(p \cdot x) \right] = \frac{i \cdot \omega \cdot B}{p} \cdot \left(\tilde{\zeta}_+ - \tilde{\zeta}_- \right) \tag{A.18}$$

The complex constant C_+ and C_- have to be determined from the two boundary conditions for amplitudes and phases.

The aforementioned equations hold for a prismatic channel of limited length. The Pontchartrain Basin is schematized as a number of serial or parallel channels, see Figure A.1.

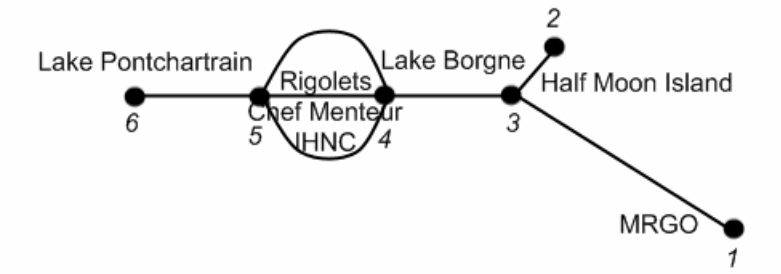

Figure A.1 Schematization of the Pontchartrain Basin for application of harmonic method

All elements (channels and lakes) are represented as line elements between two nodes. For example, Lake Borgne is the channel between node 3 and node 4, while the tidal passes are schematized as three different channels between nodes 4 and 5.

For each channel in the schematization two of the four quantities ($\tilde{\zeta}_0, \tilde{\zeta}_l, \tilde{Q}_0, \tilde{Q}_l$) are given as boundary conditions. The other two can be calculated when equations (A.17) and (A.18) are rewritten into (A.19).

$$\begin{aligned} \tilde{\zeta}_l &= L \cdot \tilde{\zeta}_0 + M \cdot \tilde{Q}_0 \\ \tilde{Q}_l &= N \cdot \tilde{\zeta}_0 + O \cdot \tilde{Q}_0 \end{aligned} \tag{A.19}$$

where *L, M, N* and *O* are complex constants per channel, see equation (A.20).

$$\begin{aligned} L = O &= \cosh(p \cdot l) \\ M &= -\frac{p}{i \cdot \omega \cdot B} \cdot \sinh(p \cdot l) \\ N &= -\frac{i \cdot \omega \cdot B}{p} \cdot \sinh(p \cdot l) \end{aligned} \tag{A.20}$$

Since the complex constants *L, M, N* and *O* are all dependent of the discharge amplitude (via p, equation (A.16)), the solution can only be obtained by iteration.

For the calculation of the ratio of friction to inertia, see equation (A.11), a representative discharge is formulized, see equation (A.21).

$$\tilde{Q}_{rep}^3 = \frac{\left(\tilde{Q}_1 + \tilde{Q}_2\right) \cdot \left(\tilde{Q}_1^2 + \tilde{Q}_2^2\right)}{4} \tag{A.21}$$

For more information about the harmonic method, reference is made to Battjes (2002).

B Wind roses

For two stations wind roses are plotted per month. Data from the National Data Buoy Center (NDBC) are available at Shell Beach and New Canal. Location of the stations can be found in Table 9.1. The monthly wind roses are plotted in Figure 9.1 until Figure 9.12. From August until December, data at Shell Beach are also available for 2008. The other data are from 2009. Be aware that the wind speed scale varies per wind rose, so per month and per station.

Table 9.1 NOAA NDBC gage information for Shell Beach and New Canal Stations (NOAA NDBC, 2010)

	Shell Beach	New Canal
Station ID	SHBL1	NWCL1
Station number	8761305	8761927
Longitude	-89.673	-90.113
Latitude	29.868	30.027
Anemometer height above site elevation	10 m	11.9 m

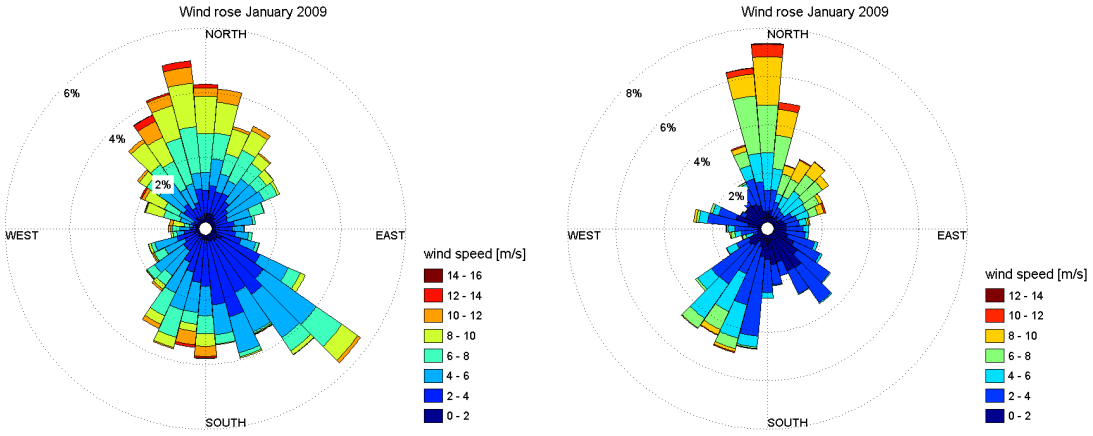

Figure 9.1 Wind rose January 2009 for Shell Beach (left) and New Canal (right)

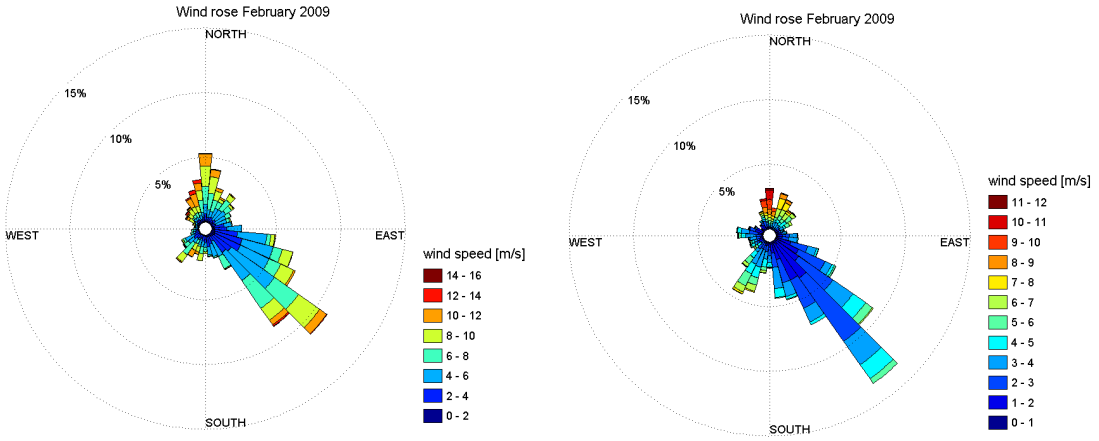

Figure 9.2 Wind rose February 2009 for Shell Beach (left) and New Canal (right)

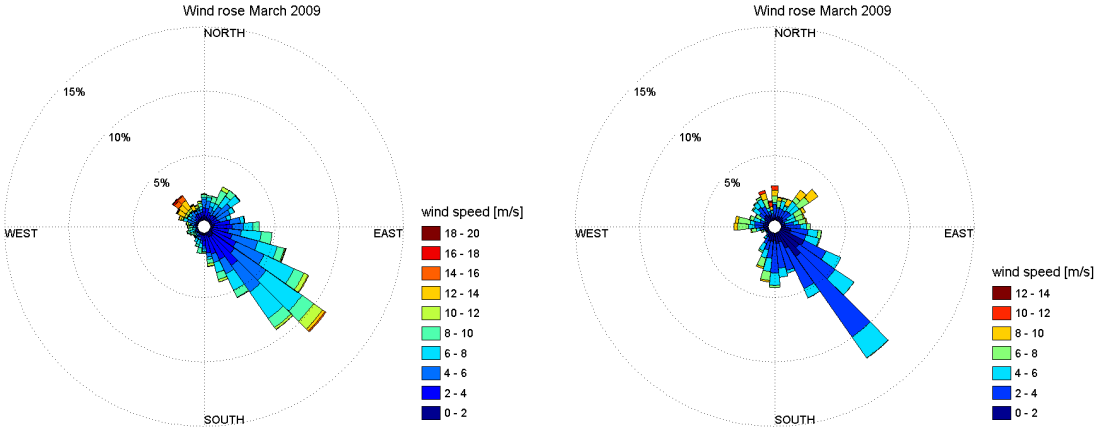

Figure 9.3 Wind rose March 2009 for Shell Beach (left) and New Canal (right)

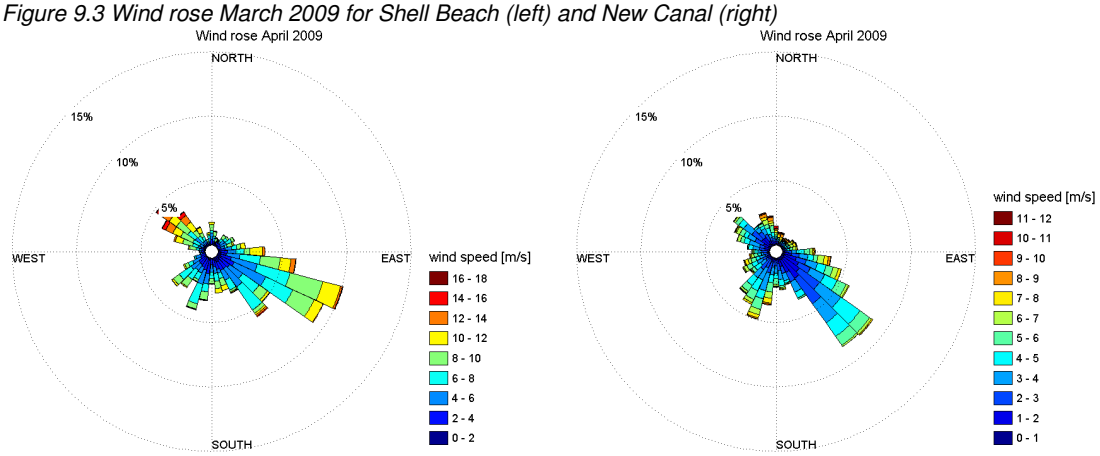

Figure 9.4 Wind rose April 2009 for Shell Beach (left) and New Canal (right)

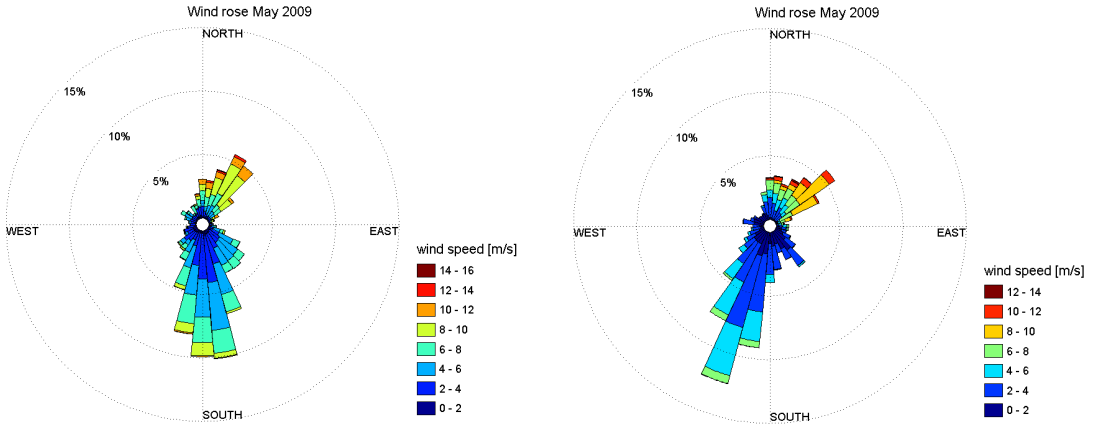

Figure 9.5 Wind rose May 2009 for Shell Beach (left) and New Canal (right)

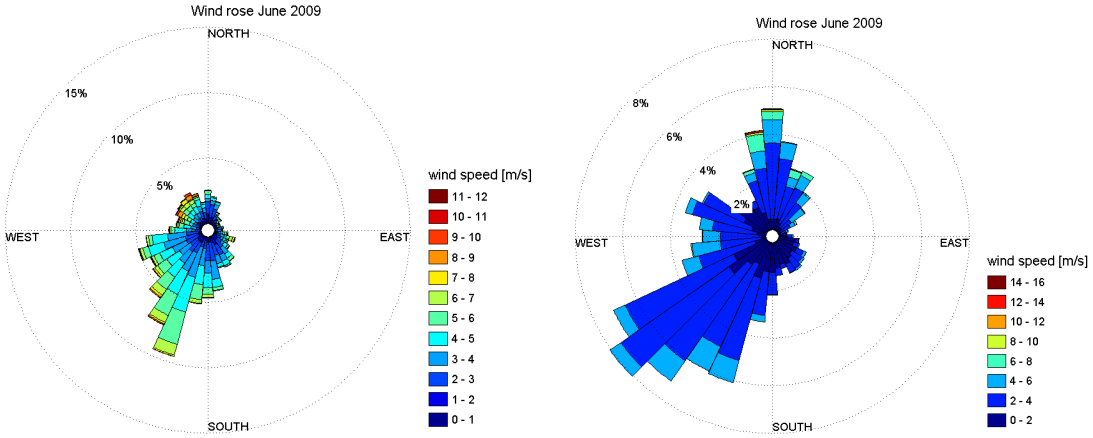

Figure 9.6 Wind rose June 2009 for Shell Beach (left) and New Canal (right)

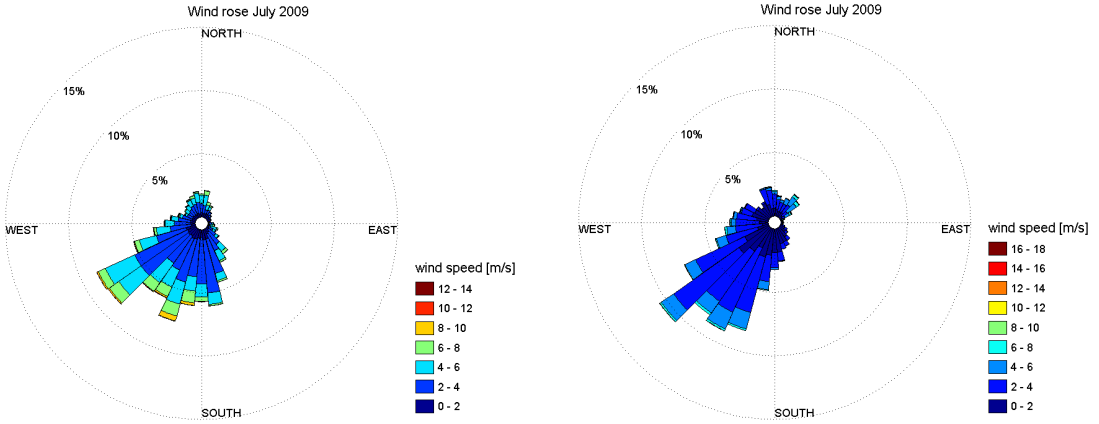

Figure 9.7 Wind rose July 2009 for Shell Beach (left) and New Canal (right)

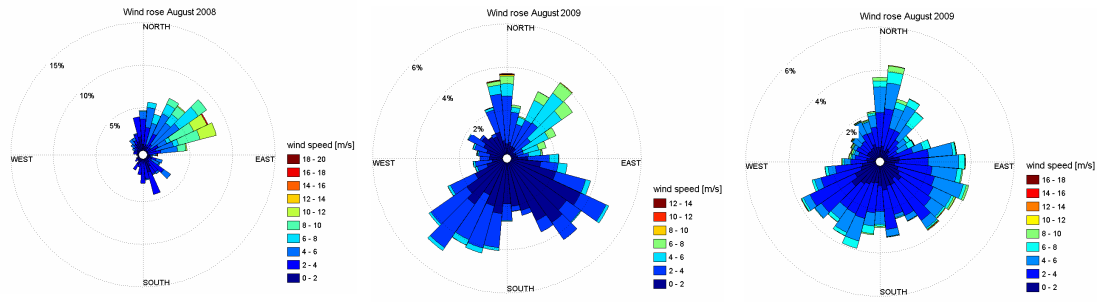

Figure 9.8 Wind rose August 2008 Shell Beach (left), 2009 Shell Beach (middle) and 2009 New Canal (right)

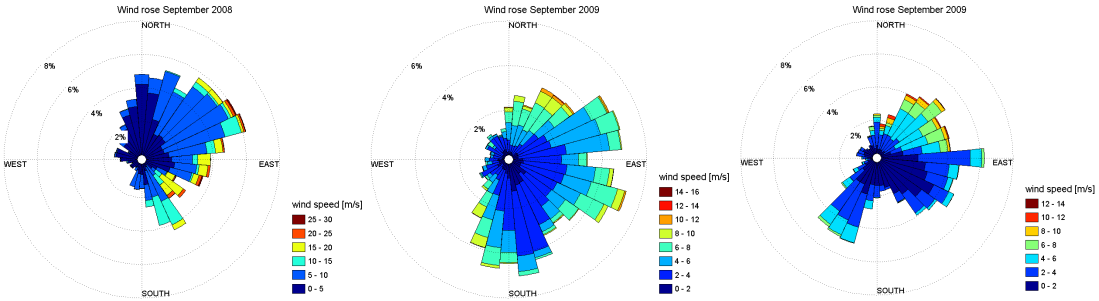

Figure 9.9 Wind rose September 2008 Shell Beach (left), 2009 Shell Beach (middle) and 2009 New Canal (right)

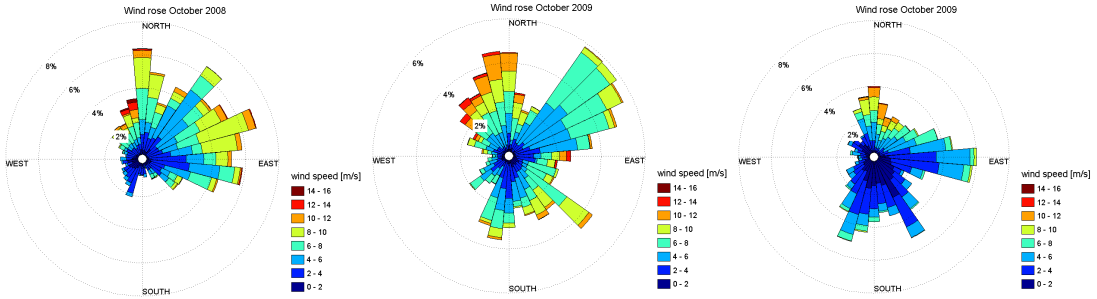

Figure 9.10 Wind rose October 2008 Shell Beach (left), 2009 Shell Beach (middle) and 2009 New Canal (right)

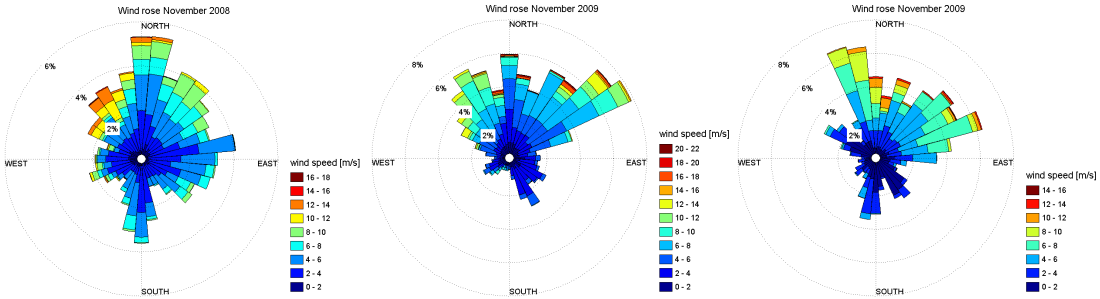

Figure 9.11 Wind rose November 2008 Shell Beach (left), 2009 Shell Beach (middle) and 2009 New Canal (right)

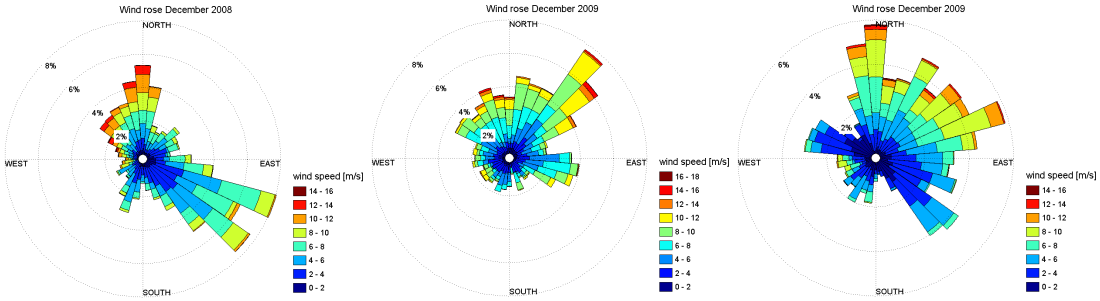

Figure 9.12 Wind rose December 2008 Shell Beach (left), 2009 Shell Beach (middle) and 2009 New Canal (right)